FINITE ELEMENT ANALYSIS OF PIPES BURIED IN LINEAR AND NONLINEAR ELASTIC MEDIA

A Thesis Submitted
in Partial Fulfilment of the Requirements
for the Degree of
MASTER OF TECHNOLOGY

By
K. RAMAKRISHNAN

to the
DEPARTMENT OF CIVIL ENGINEERING
INDIAN INSTITUTE OF TECHNOLOGY KANPUR

DECEMBER, 1979

CE-1979-M-RAM-FIN

20-12-7

CERTIFICATE

Certified that this work on 'FINITE ELEMENT ANALYSIS OF PIPES BURIED IN LINEAR AND NON-LINEAR ELASTIC MEDIA' has been carried out under my supervision and this has not been submitted elsewhere for a degree.

8/12/77

(N.S.V. KAMESWARA RAO)
Professor & Head
Department of Civil Engineering
Indian Institute of Technology, Kanpur

ACKNOWLEDGEMENT

The author wishes to record his deep sense of gratitude and indebtedness to Dr. N.S.V. Kameswara Rao, for his valuable guidance and constant encouragement.

The help rendered by his friends during different phases of this work is also gratefully acknowledged.

The author thanks Sri G.S. Trivedi for his neat typing and Sri J.C. Verma for his tracing work.

K. RAMAKRISHNAN

CONTENTS

LIST OF TABLES

LIST OF SYMBOLS

A	-	Area of bar element per unit length
A_e	-	Area of the continuum element
a	-	Y intercept at the origin in the plot ε_1 versus $\varepsilon_1/(\sigma_1-\sigma_3)$
$[B]$, $[B]_e$	-	Strain-displacement matrix
b	-	Semi-load width
b_1	-	Slope of the straightline plot ε_1 versus $\varepsilon_1/\sigma_1-\sigma_3$
$[C]$, $[C]_e$	-	Constitutive matrix
D	-	Diameter of pipe
$E(z)$	-	Modulus of elasticity of soil at any depth
E_c	-	Modulus of elasticity of pipe material
E_i	-	Initial tangent modulus of soil
E_s	-	Modulus of elasticity of soil
E_t	-	Modulus of elasticity of soft trench material
E_{ta}	-	Tangent modulus of soil at any stress level
$\{f\}$	-	Body force vector
H	-	Cover depth of pipe
HT	-	Height of the soft trench material above the crown
h_e	-	Depth of the centroid of the quadilateral element from the surface
I	-	Moment of inertia of pipe per unit length
$[K]$	-	Global stiffness matrix of the total system

$[K]_i$	-	Global stiffness matrix of the interface system
K_I	-	Stiffness number
$[K]_p$	-	Global stiffness matrix of the pipe system
$[K]_s$	-	Global stiffness matrix of the soil system
K_{st}	-	Tangent shear stiffness at any stress level
$\bar{k}$	-	a diagonal matrix properly expressing the joint stiffness per unit length in the normal and tangential direction
$[k]_e$	-	Element stiffness matrix
k_s	-	Shear stiffness of interface per unit length
k_n	-	Normal stiffness of interface per unit length
L	-	Length of interface element
ℓ	-	Length of bar element
M_s	-	Confined soil modulus
N	-	Springline thrust
n	-	Stiffness exponent
$\{P\}$	-	Vector force per unit length of the interface
P_n	-	Force per unit length of the interface in the normal direction
P_s	-	Force per unit length of the interface in the tangential direction
p	-	Intensity of surface pressure
p_a	-	Atmospheric pressure
p_{cr}	-	Crown pressure

p_{rm} – Maximum radial pressure

$\{Q\}$ – Surface traction vector

R – Radius of pipe

$\{R\}$ – Vector of nodal loads-global

$\{r\}_e$ – Vector of nodal loads-element

R_f – Failure ratio

RRB – Rough Rigid Boundary

S – Surface area of body

SRB – Smooth Rigid Boundary

T_m – Maximum tangential pressure

t – Thickness of pipe

$\{u\}, \{U\}$ – Displacement vector

V – Volume of body

W – Width of soft trench material above the crown

$\{w\}$ – Relative displacement vector of interface

w_s^{top} – Tangential displacement of the interface at top

w_n^{top} – Normal displacement of the interface at top

w_s^{bottom} – Tangential displacement of the interface at bottom

w_n^{bottom} – Normal displacement of the interface at bottom

z – Depth at any point from surface

α – Slope angle of linearly increasing modulus of soil with depth

γ_s – Unit weight of soil

δ – Friction angle in degrees

ΔX – Springline deflection

ΔY_c	-	Crown deflection
$\{\varepsilon\}$	-	Strain vector
ε_1	-	Axial strain
ν_o	-	Poisson's ratio of pipe material
ν_s	-	Poisson's ratio of soil
ν_t	-	Poisson's ratio of trench material
	-	Stress Vector
σ_n	-	Normal stress on the interface
σ_1	-	Major principle stress
σ_3	-	Minor principle stress
$(\sigma_1-\sigma_3)_f$	-	Deviatoric stress-failure
$(\sigma_1-\sigma_3)_{ult}$	-	Deviatoric stress-ultimate
τ	-	Interfacial shear stress
$\emptyset$	-	Strain energy stored in the interface

ABSTRACT

Finite element analysis of pipes buried in linear and non-linear elastic media has been carried out in the present work.

Pipe-soil system is analysed as a soil-structure interaction problem. The pipe-interface-soil is taken as a single unit, where, the pipe is simulated by bar elements, interface by interface elements and soil by 4-CST quadrilateral elements. Small deflection theory is used. Non-linear analysis has been carried out simulating stress-strain behaviour by hyperbolic law. To incorporate this in finite element analysis, incremental procedure has been adopted.

The responses like springline thrust, crown pressure, crown deflection, springline deflection, maximum radial pressure and maximum tangential pressure have been studied for various values of parameters, such as radius-to-thickness of pipe ratio, modular ratio, depth of cover-to-radius ratio and semi-load width-to-radius ratio for surface pressure. The responses have also been studied for the provision of soft trench material above the crown of pipe and non-homogeneity characterised by a linearly increasing modulus with depth for surface pressures. The responses of pipe have been studied for the variation of radius-to-thickness ratio, modular ratio

and depth of cover-to-radius ratio for gravity loads. The results obtained for surface pressure and gravity loads are compared with Burns elasticity solution.

CHAPTER 1

INTRODUCTION

1.1 General

Buried pipes are used for water supply as well as for drainage purposes under highways, embankments and railroads besides other applications. These are manufactured from a variety of materials in a variety of shapes and sizes, the most commonly used ones being corrugated metal and concrete pipe. They are subject to superimposed surface loads and loads due to the weight of the medium in which they are buried. It has been observed that traditional methods used, generally overestimate the loads transmitted to the conduit. The methods assume the load distribution a priori on pipe through semi-empirical methods and hence do not properly represent the pipe-soil interaction.

In a proper soil-structure interaction analysis it is recognised that the pipe and soil system act as a synergistic unit and the load distribution is determined in the course of solution. Development of powerful numerical techniques and high speed computers enable realistic modelling of interaction problems. The finite element method has proven to be a powerful tool in realistically modelling the soil-structure interaction behaviour and can account for non-linear

material properties, complex geometries etc.

1.2 Problem Definition

The object of this work is to develop and apply the finite element method to the analysis of interaction of a shallow buried circular pipe subjected to static superimposed loads and gravity loads. A plane-strain formulation of the interaction problem is attempted, simulating the pipe by bar elements, the medium by four noded quadrilateral elements and the interface behaviour by interface elements. Linear elastic and non-linear elastic material models for soil behaviour are used and special cases of nonhomogeneity and effect of soft trench material on pipe responses are considered.

1.3 Previous Studies

Traditional empirical methods for design of flexible and rigid conduits are documented in Spangler(20), Watkins(22).

Most of the analytical and numerical methods available so far represent the soil system as a continuum and the pipe as a shell or a continuum. Solution techniques for the problem of soil-conduit system can be classified either as analytical methods (using classical elasticity theory and shell theory to obtain 'exact' solutions) or numerical methods (using approximate techniques such as finite difference and finite element).

Some of the earlier analytical solutions have been reported by Burns (5), Hoeg (12) and Luscher (18). Luscher (18) assumed the soil surrounding the pipe to be a thick walled cylinder subjected to a uniform soil pressure around the soil cylinder. In his work theoretical expressions for the buckling resistance of the tube-soil system were developed based on the elastic theory and experimental work was carried out to provide the necessary correlation.

Burns (5) and Hoeg (12) obtained closed form solution of the problem of medium-cylinder interaction analytically by developing static solution for an elastic thin cylinder embedded in a homogeneous, isotropic and elastic medium with surface loading. The no-slip condition and full-slip condition at cylinder-medium interface is considered. In the solutions for no-slip case, the radial and tangential displacements of the cylinder were equated to the corresponding displacements of the cylinder at the medium-cylinder interface. In the solutions for the full-slip case, the radial displacements of the cylinder and medium were equated, but the tangential shear stress was set to zero at the medium-cylinder interface. A uniform surface pressure 'p' was applied on two horizontal boundaries of the medium and a uniform pressure of 'Kp' was applied on the vertical boundaries of the medium (Fig.1.1).

Burns (5) and Hoeg (12) used about the same approach to develop their solutions. However, the resulting equations from Burns solution contain expressions for thrusts and moments in the pipe in addition to expressions for displacements and stresses in the medium and hence are more useful to the designer.

Several investigators, including Kay and Krizek (14), Dar and Bates (7), and Lew (17) have examined Burns solution and proposed design methods based on this theory.

Brown (3) used the finite element method to analyse the forces on rigid culverts under high fills. He used the incremental fill sequence technique for the analysis, but the soil medium was assumed to be elastic. Moreover, the interface boundary condition was treated only approximately by using triangular elements which were assigned very high stiffnesses compared to the fill. Brown et al (4) improved the representation of the culvert by using three overlapping triangular elements. Both rigid and flexible culverts were investigated to study the effects of slippage and no slippage.

Anand (2) studied the stress distribution around shallow buried rigid pipes using finite element method. The study was limited to elastic analysis and depth of embedment equal to one diameter of the pipe. The effect of width of imposed load, relative modulus ratio etc. on responses are

analysed and compared with closed form solutions.

Abel et al (1) have studied the effect of pipe stiffness, depth of cover and effect of slippage at the interface for an elliptical pipe for surcharge loading. It was found that the effect of Poisson's ratio of pipe material and the soil is negligible and the slip at the interface is beneficial for establishing arching action, particularly for deeply buried pipes.

Prakash et al (19) investigated the buried pipe under embankment using finite element method. The validity of assumptions in the Marston-Spangler Theory was studied. The parametric studies for height of fill-to-diameter ratio, diameter-to-thickness ratio and backfill properties were carried out. The effect of sequential construction by assuming linear and non-linear soil behaviour was also carried out. The effect of non-linear behaviour on responses was studied.

Valliappan et al (21) analysed the buried pipe under surface pressure by assuming the medium to be elasto-plastic, limited tension material. Conditions of slippage and no-slippage cases are studied by using interface elements. Two different yield criteria,namely, Von Mises and Drucker's modified Von Mises,have been adopted for the elasto plastic idealisation of the medium.

Duncan (10) studied the behaviour of long span metal culverts by considering soil as a non-linear elastic material. He analysed metal arch culverts with and without curved stiffening ribs. Full bond between soil and pipe was assumed.

Katona et al (13) presented a unified computer methodology for the evaluation of buried culverts made of corrugated steel, aluminium and reinforced concrete and a class of plastic materials. The program uses Burns solution as level 1 and finite element method as level 2 and 3 of analyses. Analytical modelling features incremental construction and non-linear behaviour.

1.4 Objective and Scope of the Present Study

In the present work, soil-structure interaction of shallow buried circular pipes subjected to static surface pressures and gravity loads has been investigated using finite element method. The variability and non-linearity of soil medium properties, complex geometries and interface conditions and simulation of construction sequence encountered in the solution of the above geotechnical problem warrant the use of a powerful and versatile numerical technique such as finite element method.

The traditional methods of design of buried pipes are based on experience and tests and rely mainly on field

experience and test results. They generally overestimate the design loads due to surface pressures and gravity loads. Burns (5) analytical solution offers an accurate assessment of soil-structure interaction of circular buried pipes but contains several simplifying assumptions. The medium is assumed to be elastic, homogeneous, isotropic and weightless and the pipe is assumed to be at infinite depth. As a result of the loading condition, the response of the cylinder is symmetrical about the vertical and horizontal diameters. Hence, the use of this theory to predict the response parameters for limited burial depth is to be verified. Moreover, the surface static pressure is assumed to be acting upto infinity on horizontal planes. The gravity loads can again be taken only as an approximate equivalent overburden pressure equal to the weight of column of depth of burial. The interface behaviour can be either full -slip or no-slip.

The finite element method can model the interaction problem without any of the above limitations of Burns theory. Any realistic material model can be incorporated in the analysis. The weight of the medium, the limited depth of burial and the limited width of load or concentrated load can be incorporated within the framework of the method. Any arbitrary shape of the pipe can also be studied.

The parameters of interest in the study are spring-

line thrust, radial pressure, tangential pressure, crown deflection and springline deflection. The effect of ratios of modulii of pipe-to-soil and radius-to-thickness of pipe on the above responses for different values of depth of burial-to-diameter (H/D = 1, H/D=2) ratios are studied, for static surface pressure of full width. The effect of the interface behaviour on response parameters are also studied. The response of pipe by finite element theory and Burns theory are compared. The material non-linearity characterised by a simple non-linear curve is used. The interface nonlinearity characterised by a non-linear bond-slip relation is also used to model the interface behaviour realistically.

The variations of response parameters due to the self weight of the materials for various ratios of modulii of pipe-to-soil and radius of pipe-to-thickness are studied for two depths of burial (H/D=1, H/D=2). The approximation involved in the use of Burns solution for estimating the stresses due to self weight is brought out.

The Boussinesq theory is used for estimation of vertical crown stress due to loads at surface in traditional methods. A finite element analysis where the inclusion is present can give more realistic value of vertical stress because the interaction effects can be considered. The vertical stresses are analysed for various load widths and are compared with the Boussinesq's values.

The non-homogeneity of soil characterised by a linearly increasing modulus of elasticity with depth is analysed. It is a common construction practice to use a soft trench material above the pipe to reduce the load transferred to the pipe. Few relevant parameters like height of trench-to-radius of pipe, width of trentch-to- radius of pipe and modulus of trench material-to-modulus of soil are studied for one surface pressure case to see the effect on response parameters.

Chapter 2 describes the general principles used for the analysis in the present work. The closed form solution developed by Burns are tabulated for the response parameters. The elements used for the discretization of the pipe, continuum and interface are described briefly. The technique used in simulating non-linear elastic material behaviour of medium and non-linear bond-slip characteristics of the interface are also described.

In Chapter 3, the results obtained by Burns solution and finite element technique for the solution of pipe-soil interaction problem are discussed. The effect of modular ratio E_c/E_s, radius-to-thickness ratio (R/t) and effect of load width on the response parameters are given. The effect of material non-linearity on responses is also given. The variation of response parameters due to gravity loads for various modular

ratios and radius-to-thickness ratios is analysed. The effect of non-homogeneity of medium and presence of soft trench material on the relevant parameters are studied.

Conclusions are summarized in Chapter 4 with suggestions for further research.

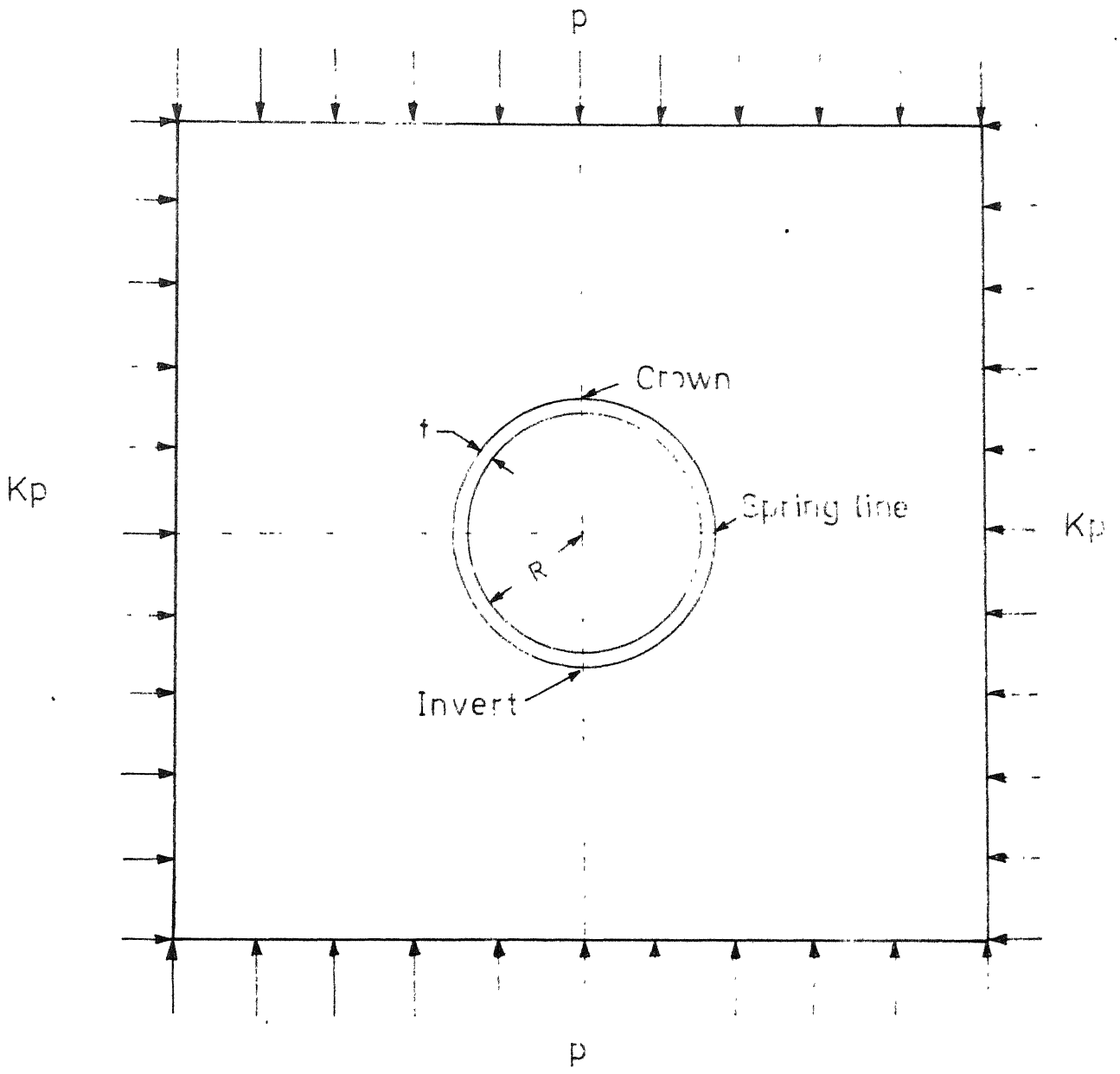

Fig. 1-1 Idealized elasticity boundary value problem of a buried pipe

CHAPTER 2

METHODS OF SOLUTION

2.1 General

In this chapter, Burns closed form elasticity solution and the finite element method of solution are briefly presented. Basic assumptions common to all solutions are: plane-strain geometry and loading, small displacement theory. The elastic theory is more restrictive than the finite element method with regard to the scope of the boundaries, bonding between pipe and soil medium, non-linear material behaviour, non-homogeneities etc.

2.2 Burns Solution

This provides an exact solution for an elastic circular cylindrical shell embedded in an isotropic, homogeneous and infinite elastic medium with a surface pressure (Fig. 1.1). Shell theory is used for the conduit and continuum elastic theory is used for the surrounding infinite medium. The conduit-medium interface is modelled only for two extreme boundary conditions: bonded interface, where both tangential and normal stresses are transmitted across the interface and frictionless interface, where only normal forces are transmitted across the pipe.

Table 2.1 gives the elastic responses of the pipe such as radial and tangential soil pressure on pipe, radial and tangential displacements on pipe and thrust on the pipe. The responses are given for both bonded interface and frictionless interface.

2.3 Finite Element Solution

A static formulation of finite element method can be equivalently derived from virtual work principle or from variational principle. This is well documented in references 8, 23.

The virtual work in any structural system can be expressed as:

$$\int_V \delta\{\varepsilon\}^T\{\sigma\}dV = \int_S \delta\{u\}^T\{Q\}\,dS + \int_V \delta\{u\}^T\{f\}dV \qquad (2.1)$$

where $\{\sigma\}$ = stress vector

$\{\varepsilon\}$ = strain vector

$\{u\}$ = displacement vector

$\{Q\}$ = surface traction vector

$\{f\}$ = body force vector

$\{\ \}^T$ = transpose of vector

$\delta\{\ \}$ = virtual vector

S = surface of body

V = volume of body

Strain energy term in virtual work statement (Equation(2.1))

is written in terms of displacements by use of the consitutive relationships and strain-displacement relationships; i.e.,

$$\{\sigma\} = [C]\ \{\varepsilon\} \qquad (2.2)$$

$$\{\varepsilon\} = [B]\ \{u\} \qquad (2.3)$$

where $[C]$ = Constitutive matrix

$[B]$ = Strain-displacement matrix

Using the above relationships, virtual energy can be written as

$$\int_V \delta\{\varepsilon\}^T \{\sigma\}\, dV = \int_V [B]\ \delta\ \{u\}^T\ [C]\ [B]\ \{u\}\ \ dV \qquad (2.4)$$

The actual form of $[C]$ and $[B]$ is dependent on material and kinematic assumptions and will differ between pipe and soil models. Here, the finite element approximation is introduced by sub-dividing the domain V into a discrete set of elements interconnected at common nodal points such that continuity is maintained at all points on the boundary of the elements. The assemblage of elements and nodes is termed the finite element mesh.

By inserting Equation (2.3) into Equation (2.4) and allowing the integration over the entire domain V (to be represented by a summation of element integrations), the virtual work equation yields the global equilibrium equation:

$$[K]\ \{u\} = [R] \qquad (2.5)$$

where $[K] = \Sigma\{k\}_e$

$[R] = \Sigma\{r\}_e$

Global stiffness matrix $[K]$ and load vector $\{R\}$ are the summation of the element stiffness matrix and load vector respectively, given by:

$$[k]_e = \int_{v_e} [B]_e^T [C]_e [B]_e \, dv_e \qquad (2.6)$$

$$\{r\}_e = \int_{s_e} [B]_e^T \{Q\} \, ds_e + \int_{v_e} [B]_e^T \{f\} \, dv_e \qquad (2.7)$$

The element stiffness matrix, $[k]_e$, is the heart of the finite element formulation and provides versatility for modelling complex boundary value problems by assigning any group of elements, special material characteristics, loadings, and/or boundary condition.

2.3.1 Discretization

Continuum: The continuum with boundaries is given in Fig. 2.1. Because of symmetry one half has been taken for analysis in this study. The lateral boundary which is smooth rigid is fixed at a distance of 4D from the centre of pipe, beyond which the stresses are assumed to be free field. The bottom boundary which is rough rigid is fixed at one diameter below the bottom of the pipe (Reference 2).

The continuum is discretized by 4-CST quadrilateral elements (Fig. 2.1). A quadrilateral element consisting of four constant strain triangles with each node having two degrees of freedom is shown in Fig. 2.2 . Internal degrees

of freedom for 4-CST elements are eliminated using static condensation technique. The details of the stiffness matrix derivation are available in standard text books(8,23).

Pipe: The circular pipe is discretized by one dimensional axial force elements as shown in Fig. 2.3. The stiffness matrix is be given by

$$[k] = \begin{bmatrix} \frac{AE_c}{\ell} & -\frac{AE_c}{\ell} \\ -\frac{AE_c}{\ell} & \frac{AE_c}{\ell} \end{bmatrix} \qquad (2.8)$$

This local stiffness matrix can be transformed to global stiffness matrix.

Interface: The interface of soil and pipe is simulated by one dimensional interface elements developed by Goodman, R.E., et al (11). Interface elements allow consideration of two subassemblies meeting at a common interface (Fig.2.4), such that under loading the subassemblies may slip relative to each other with Coulomb friction; or separate or rebond.

The application of these interface elements in the present problem is in the treatment of the pipe-soil interface. The behaviour of the interface will be seldom linear, and so non-linear bond slip relation has been used. The theory is given in section 2.4.2. The general stiffness matrix

derivation can be given as follows.

The interface element as shown in Fig. 2.4 has length L, but zero width as the nodal pairs (1,4) and (2,3) initially have identical coordinates. It is shown in local coordinate system with the X axis along the length and origin at the centre. Each node has two degrees of freedom. The stored energy, ϕ , in such an element is due to the applied force per unit length acting through the displacements and must be summed through the element

$$\phi = \frac{1}{2} \int_{-L/2}^{+L/2} w_i \, P_i \, dx \qquad (2.9)$$

In matrix notation,

$$\phi = \frac{1}{2} \int_{-L/2}^{+L/2} \{w\}^T \{P\} \, dx \qquad (2.10)$$

where $\{w\}$ = relative displacement vector

can be expressed as

$$\{w\} = \begin{Bmatrix} w_s^{top} - w_s^{bottom} \\ w_n^{top} - w_n^{bottom} \end{Bmatrix} \qquad (2.11)$$

and $\{P\}$ = the vector force per unit length is

$$\{P\} = \begin{Bmatrix} P_s \\ P_n \end{Bmatrix} \qquad (2.12)$$

The vector $\{P\}$may be expressedin terms of product of unit joint stiffness and displacement as

$$\underset{\sim}{P} = \underset{\sim}{k}\,\underset{\sim}{w} \qquad (2.13)$$

where $\underset{\sim}{k}$ = a diagonal matrix property expressing the joint stiffness per unit length in the normal and tangential direction and can be written as

$$\underset{\sim}{k} = \begin{bmatrix} k_s & 0 \\ 0 & k_n \end{bmatrix}$$

Substituting Equation (2.13) in Equation (2.10)

$$\phi = 1/2 \int_{-L/2}^{+L/2} \{w\}^T \, [\underset{\sim}{k}] \, \{w\} \, dx \qquad (2.14)$$

The displacement, $\{w\}$, may be expressed in terms of nodal point displacements through a linear interpolation formula. If u_i and v_i are the displacements in the tangential and normal directions respectively at any nodal point along the bottom of the joint element as shown in Fig. 2.4, then

$$\begin{Bmatrix} w_s^{bottom} \\ w_n^{bottom} \end{Bmatrix} = \frac{1}{2} \begin{bmatrix} 1-\frac{2x}{L} & 0 & 1+2x/L & 0 \\ 0 & 1-\frac{2x}{L} & 0 & 1+\frac{2x}{L} \end{bmatrix} \begin{Bmatrix} u_1 \\ v_1 \\ u_2 \\ v_2 \end{Bmatrix}$$

and along the top of the joint element

$$\begin{Bmatrix} w^{top} \\ w_n^{top} \end{Bmatrix} = \frac{1}{2} \begin{bmatrix} 1+\frac{2x}{L} & 0 & 1-\frac{2x}{L} & 0 \\ 0 & 1+\frac{2x}{L} & 0 & 1-\frac{2x}{L} \end{bmatrix} \begin{Bmatrix} u_3 \\ v_3 \\ u_4 \\ v_4 \end{Bmatrix}$$

Thus Equation (2.11) becomes

$$w = \frac{1}{2} \begin{bmatrix} -A & 0 & -B & 0 & B & 0 & A & 0 \\ 0 & -A & 0 & -B & 0 & B & 0 & A \end{bmatrix} \begin{Bmatrix} u_1 \\ v_1 \\ u_2 \\ v_2 \\ u_3 \\ v_3 \\ u_4 \\ v_4 \end{Bmatrix}$$

in which $A = 1 - \frac{2x}{L}$ and $B = 1 + \frac{2x}{L}$

Symbolically, $\{w\} = \frac{1}{2} [D] \{u\}$ (2.15)

Substituting Equation (2.15) in Equation (2.14) yields

$$\phi = \frac{1}{2} \int_{-L/2}^{+L/2} 1/4 \{u\}^T [D]^T [k] [D] \{u\} \, dx \quad (2.16)$$

By evaluating the integral,

$$\bar{k} = \frac{1}{6} \begin{bmatrix} 2k_s & 0 & 1k_s & 0 & -1k_s & 0 & -2k_s & 0 \\ & 2k_n & 0 & 1k_n & 0 & -1k_n & 0 & -2k_n \\ & & 2k_s & 0 & -2k_s & 0 & -1k_s & 0 \\ & & & 2k_n & 0 & -2k_n & 0 & -1k_n \\ & & & & 2k_s & 0 & 1k_s & 0 \\ & & & & & 2k_n & 0 & 1k_n \\ & & & & & & 2k_s & 0 \\ & & & & & & & 2k_n \end{bmatrix} \quad (2.17)$$

This local stiffness matrix is transformed to global stiffness matrix for further analysis.

2.4 Non-Linear Analysis

A constitutive law defines the relation between stress and strain on phenomenological observations. In order to represent this in finite element analysis the stress-strain matrix should be defined properly.

2.4.1 Soil Non-linearity

Most soils seldom behave linearly. The widely used function for simulation of stress-strain curves in finite element formulation is by Duncan et al (9) using Kondner's (15,16) findings that the plot of stress vs strain in a triaxial compression test is very nearly a hyperbola. Fig. 2.5 illustrates such a relation, which can, be stated in equation form as

$$\sigma_1 - \sigma_3 = \frac{\varepsilon_1}{a + b_1 \varepsilon_1} \qquad (2.18)$$

or

$$\frac{\varepsilon_1}{(\sigma_1 - \sigma_3)} = a + b_1 \varepsilon_1 \qquad (2.19)$$

It has been found by Kondner et al (15,16) that the values of 'a' and 'b_1' can be readily obtained if plot is made according to Equation (2.19) which is shown in Fig. 2.6. Since the compressive strength reaches its peak before the curve becomes asymptotic, failure stress difference $(\sigma_1 - \sigma_3)_f$ can be related to $(\sigma_1 - \sigma_3)_{ult}$ by a factor R_f; i.e.

$$(\sigma_1 - \sigma_3)_f = R_f \, (\sigma_1 - \sigma_3)_{ult} \qquad (2.20)$$

The tangent modulus at any level of stress can be expressed as

$$E_{t_a} = \frac{\partial \sigma}{\partial \varepsilon_1}$$

$$= \frac{b_1}{(b_1 + a\varepsilon_1)^2}$$

$$= E_i \left(1 - \frac{R_f (\sigma_1 - \sigma_3)}{(\sigma_1 - \sigma_3)_f}\right)^2 \qquad (2.21)$$

where E_i = Initial tangent modulus

Equation 2.21 shows that E_{ta} is a function of stress level.

Incremental procedure is applied to study non-linear analysis. Load is applied in increments and at the begining of each new increment of loading an appropriate tangent modulus value is selected (Equation (2.21)) for each element on the basis of stress levels in the element.

2.4.2 Interface Non-linearity

Most analyses have been performed using one of the two limiting assumptions concerning the characteristics of the soil-structure interface: (1) the interface is perfectly rough; or (2) the interface is perfectly smooth. But, the stress-strain behaviour of interface is seldom linear. This non-linearity of interface is simulated by assigning non-linear stress dependent properties of the soil and interface behaviour. The stress-strain curve is simulated by hyperbola as given by Clough et al (6). The shear stiffness value can be given as

$$K_{st} = K_I \gamma_w \left(\frac{\sigma_n}{p_a}\right)^n \left(1 - \frac{R_f \tau}{\sigma_n \tan \delta}\right)^2 \qquad (2.22)$$

where K_I = stiffness number

δ = friction angle in degrees

n = stiffness exponent

R_f = failure ratio

σ_n = normal stress

τ = interfacial shear stress and P_a=atmospheric pressure.

K_I, n, R_f are to be found from experimental direct shear test curves. The procedure to incorporate this non-linearity is same as the one given in section 2.4.1.

2.5 Soil-Pipe-Interface Stiffness Matrix

The stiffness matrices of the sub-systems have been described. For the complete system, the formation of the stiffness matrix will be the simple addition of the pipe stiffness, interface stiffness and soil stiffness. Using strain energy principle,

Strain Energy of the total system = Strain energy of the pipe system + Strain energy of the interface system + Strain energy of the soil system

So, the stiffness matrix of the total system can be expressed as

$$[K] = [K]_s + [K]_i + [K]_p \qquad (2.23)$$

where $[K]$ = stiffness matrix of the total system

$[K]_s$ = stiffness matrix of the soil system

$[K]_i$ = stiffness matrix of the interface system

$[K]_p$ = stiffness matrix of the pipe system

The final equilibrium equation can be written as

$$[K] \{U\} = \{R\} \qquad (2.24)$$

where, $\{U\}$ is the vector of unknown displacements

$\{R\}$ is the vector of nodal loads

Substituting the boundary conditions in Equation (2.24) unknown displacements of the entire system are found out using Gauss elimination solution technique. Knowing the displacements of the entire system, forces in bar elements and stresses in the continuum are found out. The stresses in the continuum are calculated at the centroids of the quadrilaterals.

2.6 Soil Medium with Linearly Varying Modulus of Elasticity, E

Soil, particularly sands, have linearly increasing modulus with depth. To meet this requirements, a laterally homogeneous and depth dependent elastic medium is presented here. The variation in E is assumed as (Figure 2.7)

$$E(z) = E_o (1 + \alpha z) \qquad (2.25)$$

in which E at $z = 0$ is E_o, α is a constant and the poisson's ratio ν_s, and the density of the medium are taken to be same throughout for computation pruposes. Accordingly, the element stiffness matrices (Equation (2.6)) are given as follows, which is now a function of depth z.

$$[k]_e = A_e h_e [B]_e^T [C_o]_e [B]_e E_o (1+\alpha z) \qquad (2.26)$$

in which, E is taken out of matrix [C] (now it is $[C_0]$, say) z is the depth of the centroid of the quadrilateral element from the surface, h is the thickness of the quadrilateral element. If the new $[k]_e$ is found out at the element level, assemblage of the elements can be carried out in the usual manner described earlier.

2.7 Computer Programs

The following four programshave been developed to analyse the plane-strain buried conduits subjected to plane strain static loading. In all the programs, if nodes fall on straight line and are equidistant, data for only the first and the last point of this group are needed, intermediate nodal point data are automatically generated.

2.7.1 LEFBP

This is a Linear Elastic Finite element program for the analysis of Buried Pipes. The applied finite element procedure is based on constant-strain-elements. The use of triangular and quadrilateral elements is permitted for continuum, although the latter is used in this study. The program has been developed using the bar elements for the pipe. The program requires an user-defined mesh. The program can take no slip condition between pipe and soil. The flow chart is given in Fig. 2.8.

Program Details

MAIN	Calls subroutine DATAIN, ASEMBL, BANSOL and STRESS
DATAIN	Reads number of nodes, number of elements, number of materials, number of surface tractions, material properties, nodal point data, boundary condition code, element data, material type, surface tractions.
ASEMBL	Calls subroutine QUAD and assembles the quadrilateral stiffness matrices and loads in the global system, modifies the system equilibrium equation by introducing the boundary conditions.
BAREL	Calculates the stiffness matrices of bar elements and puts in the global system.
QUAD	Divides quadrilateral into four triangular elements, calls subroutine CST to compute the quadrilateral stiffness matrix.
CST	Calculates the triangular element stiffness matrix and adds the corresponding four matrices upto quadilateral stiffness matrix.
STRESS	Calls the subroutine BARSTR, calculates the continuum stresses and strains, calculates the radial pressures and tangential pressures.
BARSTR	Calculates the axial displacements and axial forces in the pipe.
BANSOL	Solves the modified system equilibrium equations for displacements by using Gauss elimination technique.

2.7.2 LEFBPI

This is a Linear Elastic Finite element program for the analysis of Buried Pipes with Interface simulation. The same elements, used in LEFBP, are used in the program for pipe and soil. Interface is simulated by interface elements. This program requires an user-defined mesh. The program can take no-slip and full-slip condition between pipe and soil.

Program Details

MAIN	Calls subroutine DATAIN, ASEMBL, BANSOL and STRESS
DATAIN	Reads number of cards, number of elements, number of materials, number of surface tractions, material properties, nodal point data, boundary condition code, element data, material type, surface tractions.
ASEMBL	Calls subroutine QUAD and assembles the quadrilateral stiffness matrices and loads in the global system, modifies the system equilibrium equations by introducing the boundary conditions.
BAREL	Calculates the stiffness matrices of bar elements and puts them in the global system.
JOINEL	Calculates the stiffness matrices of interface elements and puts them in the global system.
QUAD	Divides quadrilateral into four triangular elements, calls subroutine CST to compute the quadilateral stiffness matrix.

CST	Calculates the triangular stiffness matrix and adds the corresponding four matrices upto quadilateral stiffness matrix.
STRESS	Calls the subroutines BARSTR and INFACS, Calculates the continuum stresses and strains, calculates the radial pressures and tangential pressures.
BARSTR	Calculates the axial displacements and axial forces in the pipe.
INFACS	Calculates the relative displacements and shear and normal stresses.
BANSOL	Solves the modified system equilibrium equations for displacements by using Gauss elimination technique.

2.7.3 NEFBPI

This program is a Non-linear Elastic Finite element program for Buried Pipes with the Interface simulation. The non-linear material properties and non-linear interface behaviour are incorporated in this program. The program requires an user-defined mesh. The program can take no-slip and full-slip condition. The elements used are same as in LEFBPI. The flow chart is shown in Fig.2.9.

Program Details

MAIN — Calls subroutine DATAIN, reads number of increments, calls subroutine INITIA, solves for successive load increments by calling subroutines ASEMBL, BANSOL and STRESS, controls incremental procedure.

DATAIN — Reads number of nodes, number of elements, number of materials, number of surface tractions, material properties, nodal point data, boundary condition code, element data, material type, surface tractions.

INITIA — Initializes all the vectors.

ASEMBL — Calls subroutine QUAD and assembles the quadrilateral stiffness matrices and loads in the global system, modifies the system equilibrium equations by introducing the boundary conditions.

BAREL — Calculates the stiffness matrices of bar elements and puts them in the global system.

JOINEL — Calculates the stiffness matrices of interface elements and puts them in the global system.

BANSOL — Solves the assembled banded stiffness matrix using Gauss elimination technique.

QUAD — Divides quadrilateral into four triangular elements, calls subroutine CST to compute the quadrilateral stiffness matrix.

CST — Calculates the triangular element stiffness matrix and adds the corresponding four matrices upto quadrilateral stiffness matrix.

STRESS	Calls subroutines CSTRES, BARSTR and INFACS, finds the total stresses for continuum.
CSTRES	Calculates the incremental strains and stresses for the continuum and total and incremental radial and tangential pressures.
BARSTR	Calculates the incremental and total axial displacements and axial forces in the pipe.
INFACS	Calculates the incremental and total relative displacements and stresses.

2.7.4 BURNS

This program uses the BURNS elasticity theory equations for the responses of the pipe. The program can take no-slip and full-slip condition.

Table 2.1: Elasticity Solutions for Pressure on Pipe and Pipe Responses for Bonded and Frictionless Interfaces (Burns(5))

Structural response of pipe	Common factor	Bonded Interface $a_o=C(2BU-')/B(1+2CU)$ $d = CV(1+B+2BCU)+CU(1+C/2)+C+1$ $b_2=(CV(B+2BCU)-BCU/2-B)/d$ $a_2=(CV(2BCU-C)+C^2U/2-B)/d$	Frictionless Interface $a_o=C(2BU-1)/B(1+2CU)$ $d = (4BCV+C+2)$ $b_2= (4BCV-B)/d$ $d_2= (4BCV+C)/d$
Radial pressure on pipe: p_r	$p_o x$	$B(1-a_o)-C(1+3a_2-4b_2)\text{Cos } 2\theta$	$B(1-a_o)-C(1+3a_2-4b_2)\text{Cos } 2\theta$
Tangential pressure on pie:T	$p_o x$	$C(1-a_2+2b_2)\text{ Sin } 2\theta$	0.0
Radial displacement of pipe: w	$\frac{p_o R}{M_s} x$	$BU(1-a_o)-CV(1+a_2-2b_2)\text{ Cos } 2\theta$	$BU(1-a_o)-2/3\ CV(1+3a_2-4b_2)\text{Cos}2\theta$
Tangential displacement of pipe:v	$\frac{p_o R}{M_s} x$	$1/2(1+a_2+2b_2\ C/B)\text{Sin } 2\theta$	$1/3CV(1+3a_2-4b_2)\text{Sin } 2\theta$
Thrust on pipe wall: N	$p_c R\ x$	$B(1-a_o)+C(1-a_2)\text{Cos } 2\ \theta$	$B(1-a_o)+1/3C(1+3a_2-4b_2)\text{Cos } 2\theta$

Soil Properties

M_s=confined modulus=$E_s(1-\nu_s)/((1+\nu_s)(1-2\nu_s))$

K =lateral pressure coefficient= $\nu_s/(1-\nu_s)$

p_o=surface normal pressure

Pipe Properties

$\bar{E}$ =effective Youngs Modulus = $E/(1-\nu^2)$

I= moment of inertia per unit length

A=thrust area per unit length

R=average radius

Dimension-less Parameter

B=(1+K)/2

C=(1-K)/2

$U=M_s R/\bar{E}A$

$V=M_s R3/6\bar{E}I$

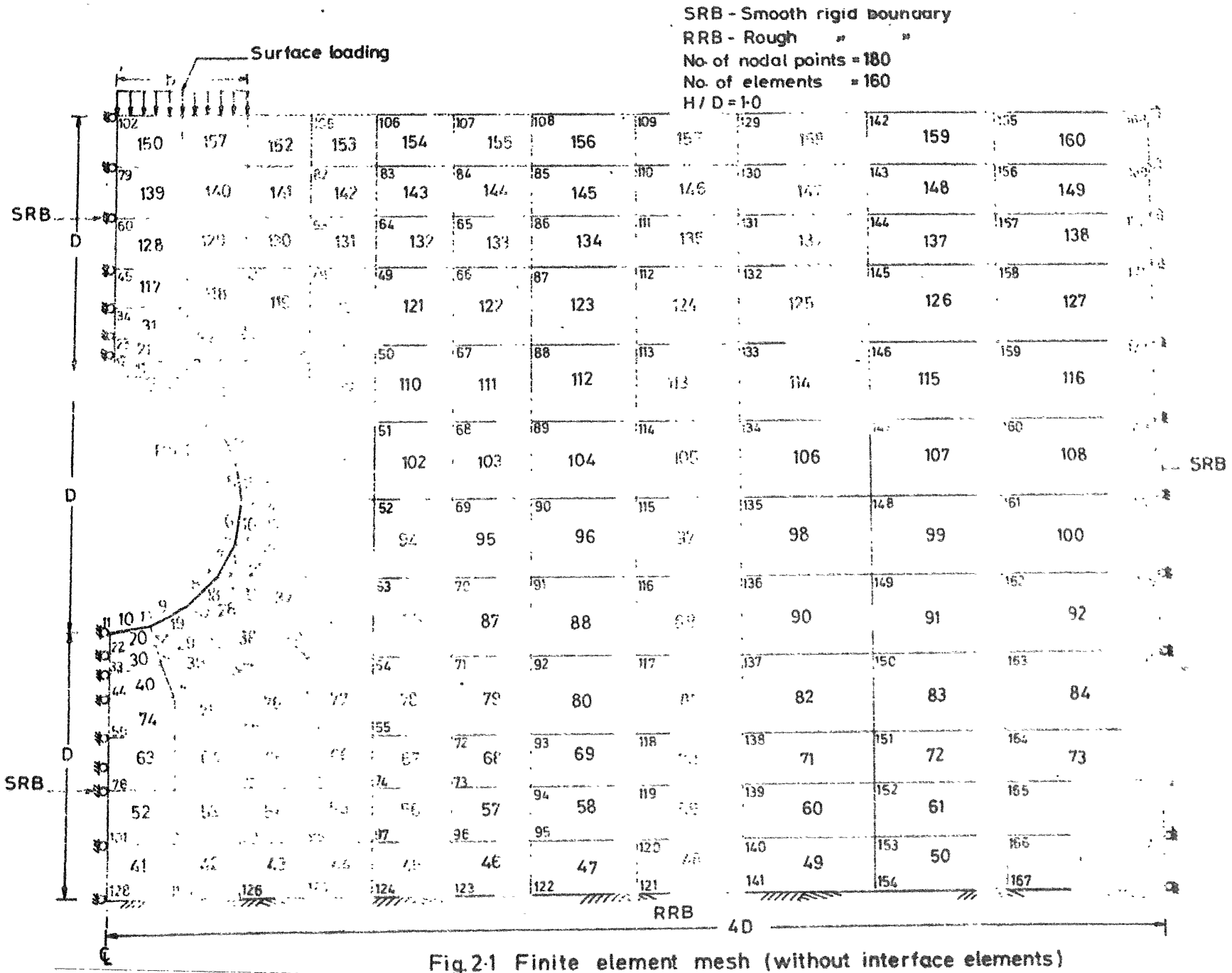

Fig. 2·1 Finite element mesh (without interface elements)

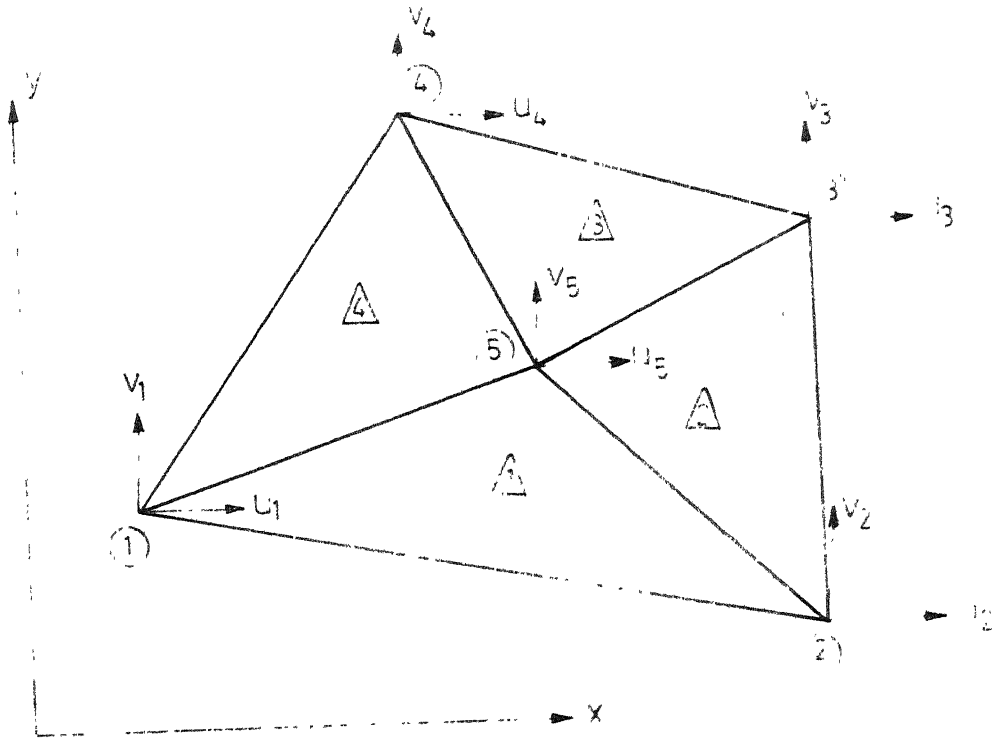

Fig. 2-2 4-CST Quadrilateral element

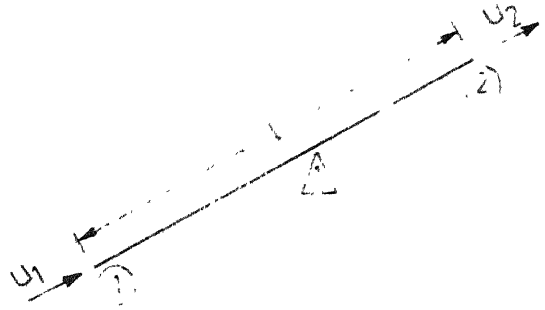

Fig. 2-3 Axial force element

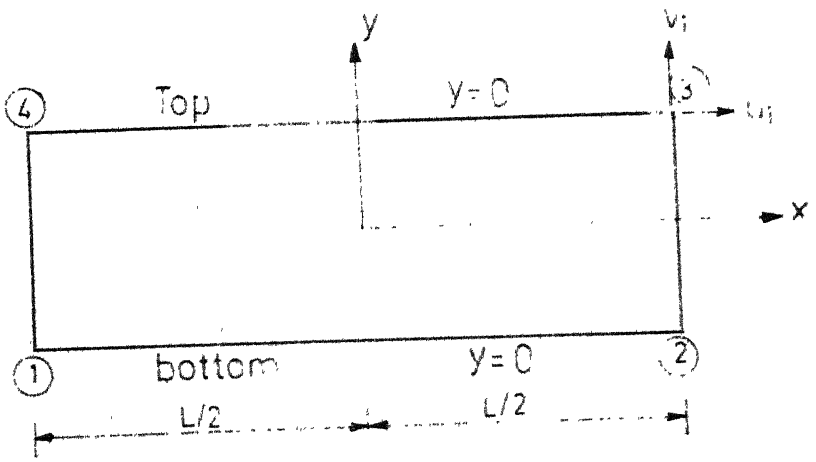

Fig. 2-4 Interface element

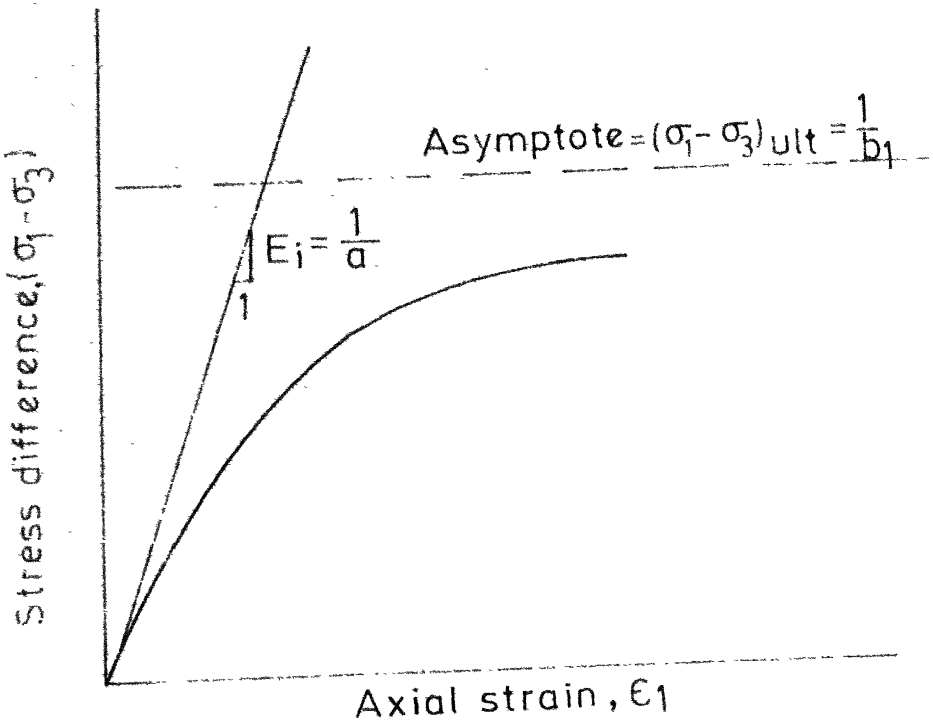

Fig.2-5 Hyperbolic stress strain curve

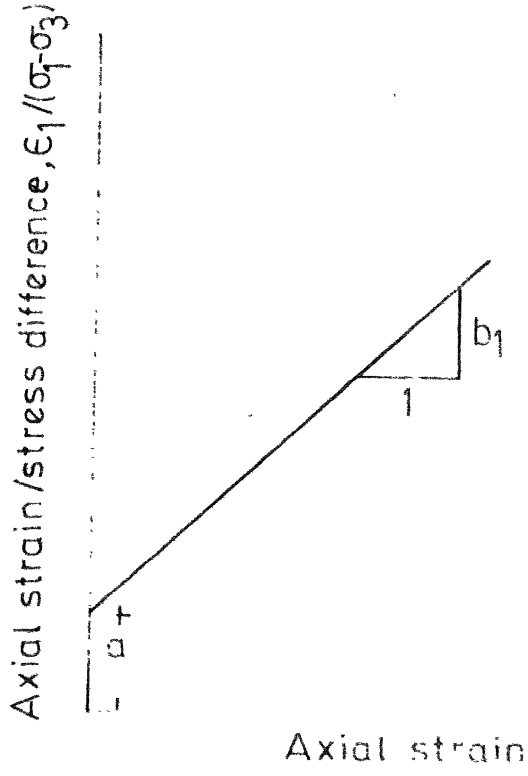

Fig.2-6 Transformed hyperbolic stress-strain curve

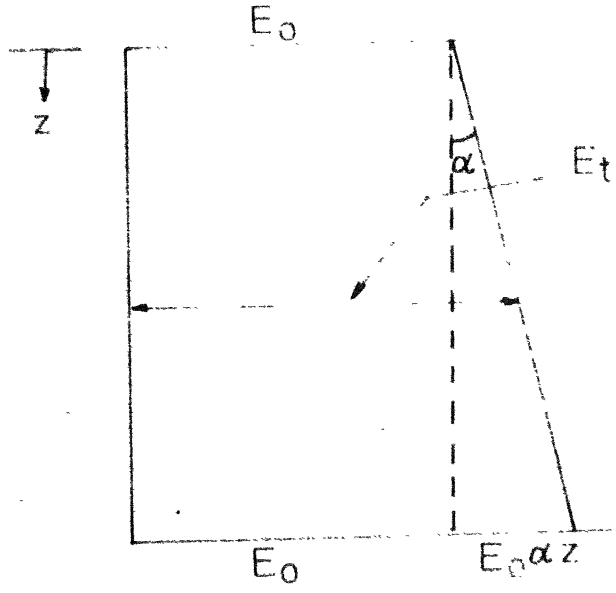

E_o = Tangent modulus at z = 0

α = Slope in radians

Fig.2-7 Non homogeneity - linearly varying modulus of elasticity of soil medium with depth

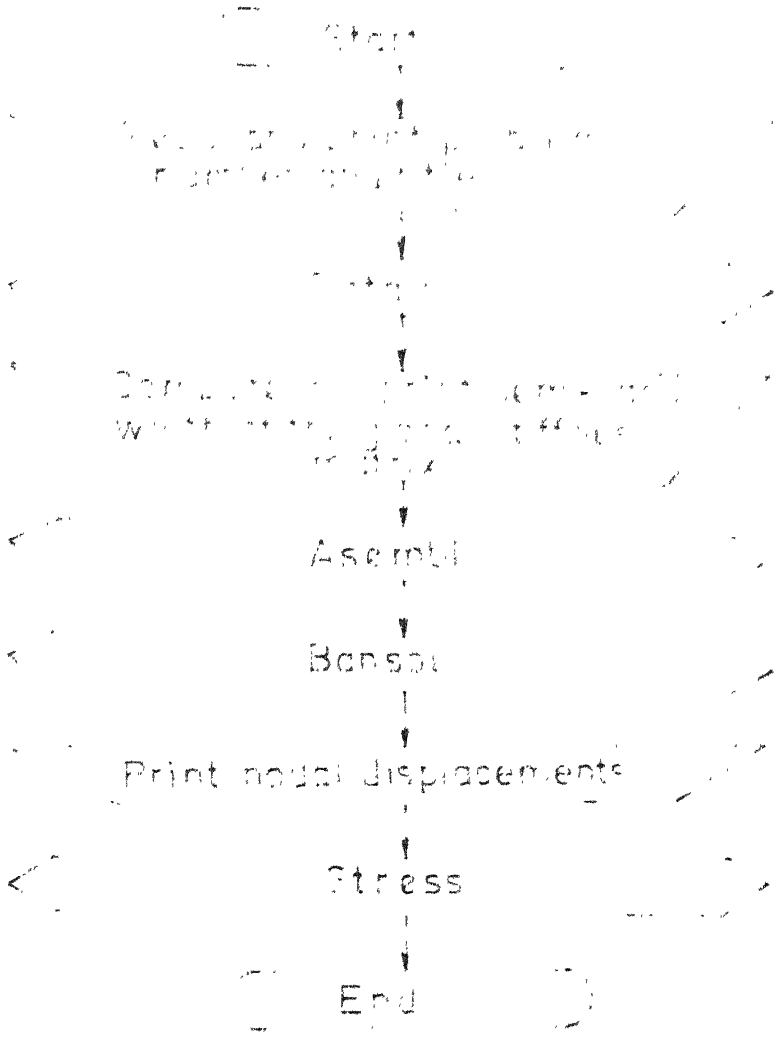

Fig. 2·8 Flow chart for main
(Program Lefbp and Lefbpi)

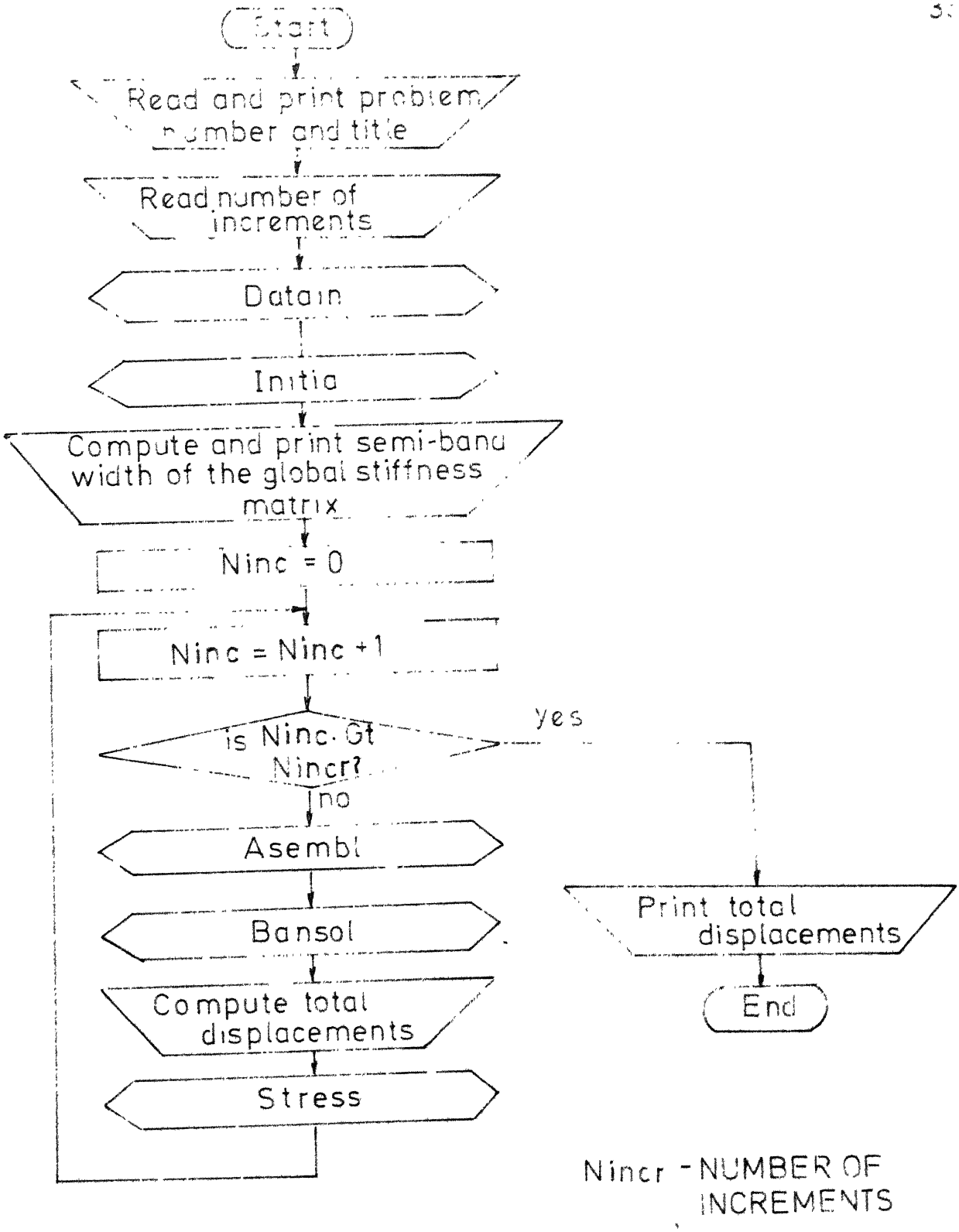

Fig.2·9 Flow chart for main (Program Netbi)

CHAPTER 3

RESULTS AND DISCUSSIONS

3.1 General

The formulation described in the previous chapter is applied to solve the soil structure interaction of buried pipes. Linear analysis results and non-linear analysis with the same initial tangent modulus of linear analysis results, are presented and compared with Burns solution. No-slip and full-slip cases have been analysed. Full-slip condition in elastic analysis is achieved by using interface elements and giving zero shear stiffness value in interface elements. This is achieved in non-linear analysis by giving the following values in interface elements as given by Clough et al (6) on the basis of experimental results for sands;

$$\delta = 0.1^{o}$$

$$K_I = 1.0$$

$$n = 0.0$$

$$R_f = 1.0$$

where δ = friction angle in degrees

K_I = stiffness number

n = stiffness exponent

R_f = failure ratio

These values used in non-linear analysis, give very low

stiffness values.

No-slip condition is achieved in elastic analysis without using interface elements or giving high values of shear stiffness for interface elements. This can be achieved in non-linear analysis by giving the following values suggested by Clough et al (6) on the basis of experimental results for sands;

$\delta = 35^{\circ}$

$K_I = 35000$

$n = 1.0$

$R_f = 0.9$

These values used in non-linear analysis give very high shear stiffness values for interface elements.

Separation between pipe and soil is prevented by giving a very high normal stiffness value in interface elements. The normal stiffness value given is 0.7000×10^{10} KN/M.

Results are non-dimensionlised as follows:

1. The crown deflections and springline deflections are non-dimensionalised by pxR/M_s where p is the intensity of the surface pressure, M_s is confined modulus equal to $E_s(1-\nu_s)/(1+\nu_s)\ (1-2\nu_s)$ and R is the radius of pipe.
2. The springline thrust is non-dimensionalised by pxR.

3. The crown pressure, maximum radial pressure and maximum tangential pressure are non-dimensionalised by p.

In the gravity load analysis, p will be equal to $\gamma_s H$ where

γ_s = unit weight of soil

H = cover depth of pipe.

3.2 Parametric Studies for Surface Pressure

The effect of various parameters on the responses like springline thrust, crown pressure, crown displacement, springline displacement, maximum radial stress and maximum tangential stress are studied. The general variation of crown pressure, tangential pressure and springline thrust are shown in Figs. 3.1 to 3.3. The various parameters studied and responses obtained are given here.

(a) Variation of responses with R/t for no-slip and full-slip condition for full load width.

(b) Variation of responses with E_c/E_s for no-slip and full-slip condition for full load width.

The above studies are mainly concentrated to investigate no-slip to full-slip Factors (F). The responses and Factors(F), for different parameters involved are given in Tables 3.1 and 3.2. Graphically responses are shown around the pipe for a typical case in Figs. 3.4 and 3.5.

These studies reveal that no-slip to full-slip responses differ very little as can be seen from Figs. 3.1 to 3.3 and Tables 3.1 and 3.2. So all other parametric studies are made for no-slip condition.

3.2.1 Effect of Radius-to-Thickness Ratio

The responses have been studied for various radius-to-thickness (R/t) ratios for full load width. The interaction curves are investigated for the commonly used range of R/t=15 to R/t=40. Modular ratio taken for this study is 400. The analyses have been done for H/D ratios 1 and 2. Table 3.3 gives the details of the parametric study as shown at (A).

(i) Crown Deflection : The maximum diametrical deflection occurs at the pipe crown relative to invert. The variation of dimensionless crown deflection with R/t ratios has been plotted in Fig.3.6. The crown deflection increases with increasing R/t in linear elastic, non-linear elastic and Burns solution for both H/D ratios 1 and 2. But the large increase in the cylinder wall thickness changes the crown deflection only by a small amount. The non-linear elastic deflections are around 1.9 times of linear elastic deflections for the same initial tangent modulus. The linear elastic deflections do not differ with increasing H/D ratio for all R/t ratios. But the non-linear elastic deflections decrease with increasing H/D ratio for all R/t values.

(ii) Springline Deflection: The variation of dimensionless springline deflection with R/t is plotted in Fig. 3.7. It can be seen that springline deflection decreases with increasing R/t values. But the large increase in the cylinder wall thickness changes the springline deflection only by a marginal amount. Burns solution agrees with linear elastic finite element solution except in lower values of R/t ratios. Non-linear analysis gives higher springline deflections than linear elastic analysis. The springline deflection decreases with increasing H/D ratio in non-linear analysis but the decrease is not noticeable in linear finite element analysis.

(iii) Crown Pressure: The dimensionless crown pressure variation with R/t is plotted in Fig. 3.8. Crown pressure decreases with increasing R/t ratio. The decrease of crown pressure in Burns solution is steep whereas it is gradual in linear and non-linear analysis. Non-linear analysis predicts higher values than linear elastic analysis. Crown pressure decreases with increasing H/D ratio in non-linear finite element analysis. This decrease is very small in linear finite element analysis.

(iv) Springline Thrust: The variation of dimensionless thrust with R/t values is plotted in Fig. 3.9 (Thrust is maximum at the springline). Thrust decreases with increasing R/t ratio but dimensionless values are more than 1 in all

the analyses. This indicates that the pipe draws load more than pxR. Thrust increases with increasing H/D ratio for all R/t values in non-linear elastic analysis but this is not seen in linear elastic analysis. Burns solution given higher value than finite element solutions.

(v) Maximum Radial Pressure: The maximum dimensionless radial pressure variation with R/t is shown in Fig. 3.10. The maximum radial pressure linearly decreases with increasing R/t. The large decrease in R/t ratio changes the maximum radial pressure only by a small amount. But in Burns solution it increases with increasing R/t ratio upto R/t=20 and beyond this ratio, it does not change. The maximum radial pressure slightly increases with increasing H/D ratio in non-linear analysis but its increase is unnoticeable in linear finite element analysis.

(vi) Maximum Tangential Pressure: The maximum dimensionless tangential pressure variation with R/t is shown in Fig. 3.11. Similar trends of maximum radial pressure are seen for tangential pressure also.

3.2.2 Effect of Modular Ratio

The interaction effects have been studied for various modular ratios (E_c/E_s). The study is carried out for R/t=20. The dimensionless curves have been drawn for linear elastic analysis, non-linear elastic analysis and Burns solution. H/D ratios 1 and 2 have been studied. Table 3.3 gives the details

of the various parameters involved (shown at B).

(i) Crown Deflection: The variation of dimensionless crown deflection with E_c/E_s is shown in Fig. 3.12. The crown deflection decreases with increasing E_c/E_s ratio. Burns solution agrees well with linear elastic solution. But non-linear solution shows a deflection of 1.9 times of linear elastic deflection for H/D =1 for the same initial tangent modulus. The deflections do not change with increasing H/D ratio for all E_c/E_s ratio in linear elastic analysis. But the deflections decrease with increasing H/D ratio for all E_c/E_s ratio in non-linear elastic analysis.

(ii) Springline Deflection: The variation of dimensionless springline deflection with E_c/E_s ratio is shown in Fig. 3.13. The springline deflection increases with increasing E_c/E_s ratio. It decreases with increasing H/D ratio in non-linear elastic analysis but this is not seen in linear elastic analysis Burns solution compares well with linear finite element analysis. Non-linear analysis predicts higher deflections.

(iii) Crown Pressure: The crown pressure variation with E_c/E_s is shown in Fig. 3.14. The crown pressure increases with increasing E_c/E_s ratio. But it remains constant beyond E_c/E_s ratio equal to 600. The crown pressure decreases with increasing H/D ratio for all E_c/E_s ratio in non-linear elastic analysis. But this decrease is not seen in linear

elastic analysis. Burns solution differs approximately by 0.1 p with linear elastic solution in predicting the crown pressure for all E_c/E_s ratio .

(iv) Springline Thrust: The dimensionless springline thrust variation with E_c/E_s is shown in Fig. 3.15. The springline thrust increases with increasing E_c/E_s ratio. The dimensionless thrust lies above 1.0 in all the analyses. Beyond E_c/E_s equal to 600, the increase is nominal. The pipe draws more load with increasing E_c/E_s ratio. Springline thrust also increases with increasing H/D ratio in non-linear analysis but this increase is unnoticeable in linear analysis for all E_c/E_s ratios. Burns solution predicts higher values than the finite element analysis.

(v) Maximum Radial Pressure: The dimensionless maximum radial pressure variation with E_c/E_s is shown in Fig. 3.16. The maximum radial pressure increases will increasing E_c/E_s ratio. It remains almost constant beyond E_c/E_s equal to 600. Maximum radial pressure increases with increasing H/D ratio in non-linear analysis for all E_c/E_s ratio . But this change with H/D ratio in linear analysis is not noticeable. Burns solution gives higher value than finite element solution.

(vi) Maximum Tangential Pressure: The maximum tangential pressure variation with E_c/E_s is shown in Fig. 3.17. The maximum tangential pressure does not change much with increasing

E_c/E_s ratio. It increases with increasing H/D ratio for all E_c/E_s ratio in non-linear elastic analysis but this increase is not seen in linear elastic analysis. Burns solution given higher value than finite element solution.

3.2.3 Effect of Load Width

The responses of pipe for various load widths have been studied. They are studied for a radius- to-thickness ratio of 20 and a modulus ratio of 400. H/D ratios 1 and 2 have been studied. Both linear and non-linear results are given. Table 3.3 gives the various semi-load width-to-radius (b/R) ratios studied (shown at C). The variation of response around the pipe with change in semi-load width-to-radius ratio (b/R) is shown in Figs. 3.18 to 3.20.

(i) Crown Deflection: The dimensionless crown deflection variation with b/R is shown in Fig. 3.21. Crown deflection increases with b/R upto a value of 4 in linear and non-linear elastic analysis and beyond this it starts decreasing for H/D =1. The steepness of the curve decreases with increasing H/D ratio in both the analyses and beyond b/R=4 the crown deflection tends to be constant. Non-linear elastic analysis gives higher value than linear elastic analysis with the same initial tangent modulus.

(ii) Springline Deflection: Similar trends of crown deflection are seen for springline deflection (Fig. 3.22).

(iii) Crown Pressure: The dimensionless crown pressure variation with b/R is shown in Fig. 3.23. The crown pressure increases with b/R. All the curves flatten beyond b/R=7. The crown pressure decreases with increasing H/D ratios for all b/R ratio . The elastic solution for vertical stress on the centre line for strip load on a semi-infinite mass is plotted. It is observed that for all b/R ratios considered the crown pressure obtained from finite element analysis is less than the one obtained by elastic solution for a strip load. The inclusion reduces the crown pressure by interaction.

(iv) Springline Thrust: The springline thrust variation with b/R is shown in Fig. 3.24. Similar trends as that of crown pressure have been seen in the variation of springline thrust also. Beyond b/R=4, the pipe starts drawing load more than pR in all the analyses for both H/D ratios 1 and 2.

(v) Maximum Radial Pressure: The maximum radial pressure variation with b/R is shown in Fig. 3.25. The maximum radial pressure increases with b/R. There is not much of difference between linear elastic and non-linear elastic analyses in the computation of radial pressure distribution.The maximum radial pressure decreases with increasing H/D ratio for all b/R in both the analyses.

(vi) Maximum Tangential Pressure: The maximum tangential pressure increases with increasing b/R and beyond certain

values of b/R, it starts decreasing (Fig. 3.26). It reaches peak at b/R=4 in non-linear analysis and at 3 in linear analysis for H/D =1.

3.2.4 Effect of Soft Trench Material:

It is an usual practice to provide a soft trench material above the crown as shown in Fig. 3.27. The purpose of this material is to develop positive arching. The influence of trench material width, height and material stiffness on the interaction effects have been studied. The responses are nondimensionalised using the responses of a homogeneous system, and so, response ratios less than 1.0 indicate that pipe distress being relieved by the soft material. Table 3.4 gives the various parameters involved in this study. The response ratio can be defined as the response of system with soft trench material to the response of the system with homogeneous material.

(i) Effect of Trench Width: The height of the trench material is taken 0.9 R. The study is made for trench modulus equal to 1/10 E_s and for E_c/E_s ratio equal to 400, H/D equal to 1.

The variations of springline thrust, maximum radial pressure and maximum tangential pressure with increasing trench width are shown in Fig. 3.28. The springline

thrust and maximum radial pressure are reduced with increasing trench material width. They decrease by 12 percent at width 1.1 R. Beyond width equal to 1.1R, the trench material does not help in reducing the stress response. But the maximum tangential pressure increases with increasing width. The tangential pressure distribution cannot be predicted because the distribution has got disturbed.

The variations of crown pressure, crown deflection and springline deflection are shown in Fig. 3.29. These responses decrease gradually upto a width R where the crown pressure, crown deflection and springline deflection get reduced by 25 percent, 15 percent and 14 percent respectively. Beyond this width, they show an increasing trend. The crown deflection will be more than the crowndeflection with homogeneous material for trench material width > 1.3R. The crown pressure and springline deflection approach a constant value beyond a width of 1.4R.

(ii) Effect of Trench Material Height: The responses are studied for the variation of height of the trench material. The above study concludes that responses do not get reduced beyond width 1.0R and so the width for the study is chosen to be equal to 1 R. The same radius-to-thickness ratio, modular ratio and H/D ratio have been studied.

The variations of springline thrust, maximum radial pressure and maximum tangential pressure are given in Fig. 3.30. The response ratios for springline thrust and maximum radial pressure drop down gradually to 0.88 at a height equal to 0.9R. Beyond this height the responses remain horizontal. Maximum tangential pressure does not get distressed with trench material.

The variations of crown deflection, crown pressure and springline deflection with increasing height of trench material are shown in Fig. 3.31 . . The crown pressure, crown deflection and springline deflection drop down by 25 percent, 15 percent and 25 percent respectively at a height of 0.9R. Any further increase in the height of trench material does not give any improvement.

(iii) Effect of Trench Material Modulus: The responses have been studied for various modulii of trench material . Modulus of trench material is taken as a fraction of the modulus of the homogeneous soil. The same radius -to-thickness ratio and modulus ratio with reference the homogeneous soil have been taken. This study has been done for trench width equal to R and height equal to 0.9R.

The variations of springline thrust, maximum radial pressure and maximum tangential pressure are given in Fig. 3.32. The response ratios for springline thrust and

maximum radial pressure drop down to 0.9 at $E_t/E_c = 1/10$. The response ratios increase with increase in the trench modulus beyond this. The variation of tangential pressure does not show any definite trend.

The response ratios of springline deflection, crown deflection and crown pressure reduce by 25 percent, 18 percent and 25 percent respectively at E_t/E_s equal to 1/10 (Fig.3.33). The response ratios start increasing gradually to 1 with increasing trench modulus beyond this value.

3.2.5 Nonhomogeneity Linearly Increasing Modulus of Elasticity of Soil with Depth

Soils, particularly sands, have linearly increasing modulus with depth. The pipe responses are studied by taking this variation into account. The radius-to-thickness ratio, modular ratio and H/D ratio taken for this study are 20, 600 and 1 respectively. The responses are non-dimensionalised with reference to homogeneous soil-pipe responses.

The variation of modulus at any depth is given by Equation (2.25). Three slopes (α) 0.05, 0.10 and 0.25 have been studied. Table 3.5 gives the parameters involved in this study.

(i) Crown Deflection and Springline Deflection: Crown deflection and springline deflection variations with slope

are shown in Figs. 3.34 and 3.35. They decrease with increasing slope. The curves flatten at higher values of α, Crown deflection and springline deflection decrease with increasing H/D ratio for all slope .

(ii) Crown Pressure: As can be seen from Fig. 3.36 the crown pressures do not change much from the ratio 1 with increasing α for both H/D ratios 1 and 2. They are less than 1 at higher α values.

(iii) Springline Thrust, Maximum Radial Pressure and Maximum Tangential Pressure: It is apperent from Fig. 3.37 that thrust decreases linearly with increasing α values for both H/D ratios 1 and 2. It decreases with increasing H/D ratios for all values of α. Similar trend has been found for maximum radial pressure variation(Fig.3.38). But the maximum tangential pressure decreases linearly with α but increases with increasing H/D ratios for all α values (Fig. 3.39).

3.3 Parametric Studies for Gravity Loads

The pipe responses due to gravity loads cannot be neglected, particularly at higher depths. In the present study, the responses due to gravity load have been studied for various modular ratios and radius-to-thickness ratios. As burns solution neglects the soil weight, an equivalent

load of $\gamma_s H$ has been applied as surface pressure for full width. Table 3.6 gives all the parameters involved in this study. H/D ratios 1 and 2 have been analysed.

3.3.1 Effect of Radius-to-Thickness

In this study, the modular ratio has been taken as 400. The responses are studied for various R/t ratio .

(i) Crown Deflection: The dimensionless crown deflection variation with R/t is shown in Fig. 3.40. A value greater than 1.0 implies that the pipe soil system is softer in deflection resistance than a homogeneous soil field. The crown deflection increases with increasing R/t ratio for both H/D ratios 1 and 2. Burns solution gives slightly lower value than linear elastic analysis. The crown deflection decreases with increasing H/D ratios for all R/t ratios.

(ii) Springline Deflection: The dimensionless springline deflection variation with R/t is shown in Fig. 3.41. The springline deflection decreases with increasing R/t ratios. The springline deflection also decreases with increasing H/D ratios for all R/t ratio . The change in crown deflection with larger variation in R/t values in Burns solution appears to be small.

(iii) Crown Pressure: The dimensionless crown pressure variation with increasing R/t ratios is shown in Fig.3.42.

The crown pressure linearly decreases with increasing R/t in linear elastic analysis. It also decreases with increasing H/D ratios for all R/t ratio . The crown pressure decreases steeply with increasing R/t ratio in Burns solution. At R/t = 40, the finite element solution gives 0.8 times of $\gamma_s H$ for H/D=1 whereas Burns solution gives only 0.65 times of $\gamma_s H$.

(iv) Springline Thrust: The dimensionless springline thrust variation with R/t is shown in Fig. 3.43. The variation of thrust is very flat and the dimensionless value is more than 1.0 for both H/D ratios 1 and 2. It reveals that the pipe draws loads more than the soil column weight (negative arching). Thrust decreases with increasing H/D ratio for all R/t ratio . The thrust value given by Burns solution is smaller than finite element solution.

(v) Maximum Radial Pressure and Maximum Tangential Pressure:

Figs. 3.44 and 3.45 show the variations of dimensionless maximum radial pressure and maximum tangential pressure with R/t. They decrease with increasing R/t ratios. They also decrease with increasing H/D ratios for all R/t ratio . In the case of Burns solution, the values remain constant beyond R/t=20.

3.3.2 Effect of Modular Ratio

The responses of pipe have been studied for various

modular ratios. The R/t ratio used in this analysis is 20.

(i) Crown Deflection: The dimensionless variation of crown deflection with increasing E_c/E_s is plotted in Fig.3.46. Crown deflection decreases with increasing E_c/E_s ratios for both H/D ratios 1 and 2. Burns solution gives slightly lower value than finite element solution. It decreases with increasing H/D ratios for all E_c/E_s ratio .

(ii) Springline Deflection: Fig. 3.47 gives the variation of dimensionless spring line deflection with E_c/E_s ratios. The springline deflection increases as E_c/E_s ratio increases. Beyond E_c/E_s=400, the deflection does not change much with increasing E_c/E_s ratio. The springline deflection decreases with increasing H/D ratio for all E_c/E_s ratio . Burns solution differs with the finite element solution.

(iii) Crown Pressure: The crown pressure variation with E_c/E_s is shown in Fig. 3.48. The crown pressure increases gradually with increasing E_c/E_s ratio. Beyond E_c/E_s=600, the crown pressure remains constant. It decreases with increasing H/D ratio for all E_c/E_s ratio . Burns solution gives smaller value than finite element solution.

(iv) Springline Thrust: The springline thrust variation is shown in Fig.3.49. It increases with increasing E_c/E_s ratio. Beyond E_c/E_s ratio equal to 400, it almost remains constant. The springline deflection decreases with

increasing H/D ratio for all E_c/E_s ratio . Burns solution gives smaller values of springline thrust than finite element solution.

(v) Maximum Radial Pressure and Maximum Tangential Pressure:

The maximum radial pressure and tangential pressure variations are shown in Figs. 3.50 and 3.51. They increase with E_c/E_s ratios, and beyond E_c/E_s ratio equal to 400, they remain almost the same. They decrease with increasing H/D ratio for all E_c/E_s ratios. The finite element solution gives higher value than Burns solution in lower depths.

Table 3.1: No Slip to Full Slip Response Factors for the Variation of R/t

No slip to full slip factors (F)

Parametric study R/t ratio for surface pressures
(b/R= 8 → Full load width)
$\nu_s = 0.3$, $\nu_c = 0.2$

		H/D	b/R	E_c/E_s	Factors(F)		
					R/t=15	R/t=20	R/t=30
Crown deflection	LEF	1	8	400	0.9989	0.9980	0.9999
	NLEF	1	8	400	0.9902	0.9967	0.9846
Springline deflection	LEF	1	8	400	0.9979	0.9989	1.0020
	NLEF	1	8	400	0.9852	0.9956	0.9739
Crown pressure	LEF	1	8	400	0.9930	1.0070	1.0010
	NLEF	1	8	400	1.0090	1.0090	1.0120
Springline thrust	LEF	1	8	400	0.9968	0.9989	0.9995
	NLEF	1	8	400	0.9967	0.9980	0.9922

LEF - Linear Elastic Finite Element Analysis

NLEF- Non-linear Elastic Finite Element Analysis

Table 3.2: No Slip to Full Slip Response Factors For the Variation of E_c/E_s

No slip to full slip factors (F)

Parametric study E_c/E_s ratio for surface pressures

(b/R =8 → Full load width)

ν_s =0.3, ν_c=0.2

		H/D	b/R	R/t	Factors(F)		
					$\frac{E_c}{E_s}$=300	$\frac{E_c}{E_s}$=400	$\frac{E_c}{E_s}$=600
Crown deflection	LEF	1	8	20	0.9983	0.9980	0.9932
	NLEF	1	8	20	0.9983	0.9967	0.9986
Springline deflection	LEF	1	8	20	0.9980	0.9989	0.9936
	NLEF	1	8	20	0.9988	0.9956	1.0050
Crown pressure	LEF	1	8	20	1.0050	1.0070	1.0180
	NLEF	1	8	20	1.007 0	1.0090	1.0010
Springline thrust	LEF	1	8	20	0.9920	0.9989	1.003 0
	NLEF	1	8	20	1.0010	0.9980	1.0030

LEF - Linear Elastic Finite Element Analysis

NLEF- Non-linear Elastic Finite Element Analysis

Table 3.3 : Parametric Studies for Surface Pressure

(b/R =8 → Full load width)

	H/D	E_c/E_s ratio	b/R ratio	R/t ratio	ν_c	ν_s	Analysis
R/t ratio study (A)	1,2	400	8	15 20 30 40	.2	.3	LEF, NLEF and Burns solution
E_c/E_s ratio study (B)	1,2	300 400 600 800	8	20	.2	.3	LEF, NLEF and Burns solution
Load width study (C)	1,2	400	1 2 4 8	20	.2	.3	LEF, NLEF and Burns solution

LEF- Linear Elastic Finite Element Analysis

NLEF-Non-linear Elastic Finite Element Analysis

Table 3.4 : Trench Material Parametric Study

	H/D	$\frac{E_c}{E_s}$	R/t	b/R	E_t/E_s	W/R	HT/R	ν_c	ν_s	ν_t
Trench material width study(A)	1	400	20	8	.10 - - -	.50 1.0 1.25 2.00	- - .90 -	.20	.30	.40
Trench material height study(B)	1	400	20	8	.10 - - -	- 1.0 - -	.20 .50 .90 1.30	.20	.30	.40
Trench material modulus study(C)	1	400	20	8	.10 .30 .5 .8	- - 1,0 - -	- - .90 -	.20	.30	.40

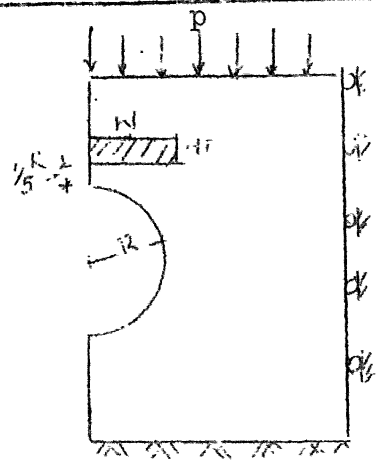

W - Width of trench material
HT- Height of trench material

Fig. 3.27 Soft Trench Material

Table 3.5: Study of Linearly Varying Modulus of Soil with Depth for Various Slope Angles

Non-homogeneous Soil-$E(z) = E_o\ (1+\alpha z)$

H/D	R/t	E_c/E_s	b/R	α
1,2	20	600	8	.05 .10 .25

Table 3.6: Parametric Studies for Gravity Loads

	H/D	E_c/E_s	R/t	ν_c	ν_s
R/t ratio study(A)	1,2	- 400 - -	15 20 30 40	.2	.3
E_c/E_s ratio study(B)	1,2	300 400 600 800	- 20 - -	.2	.3

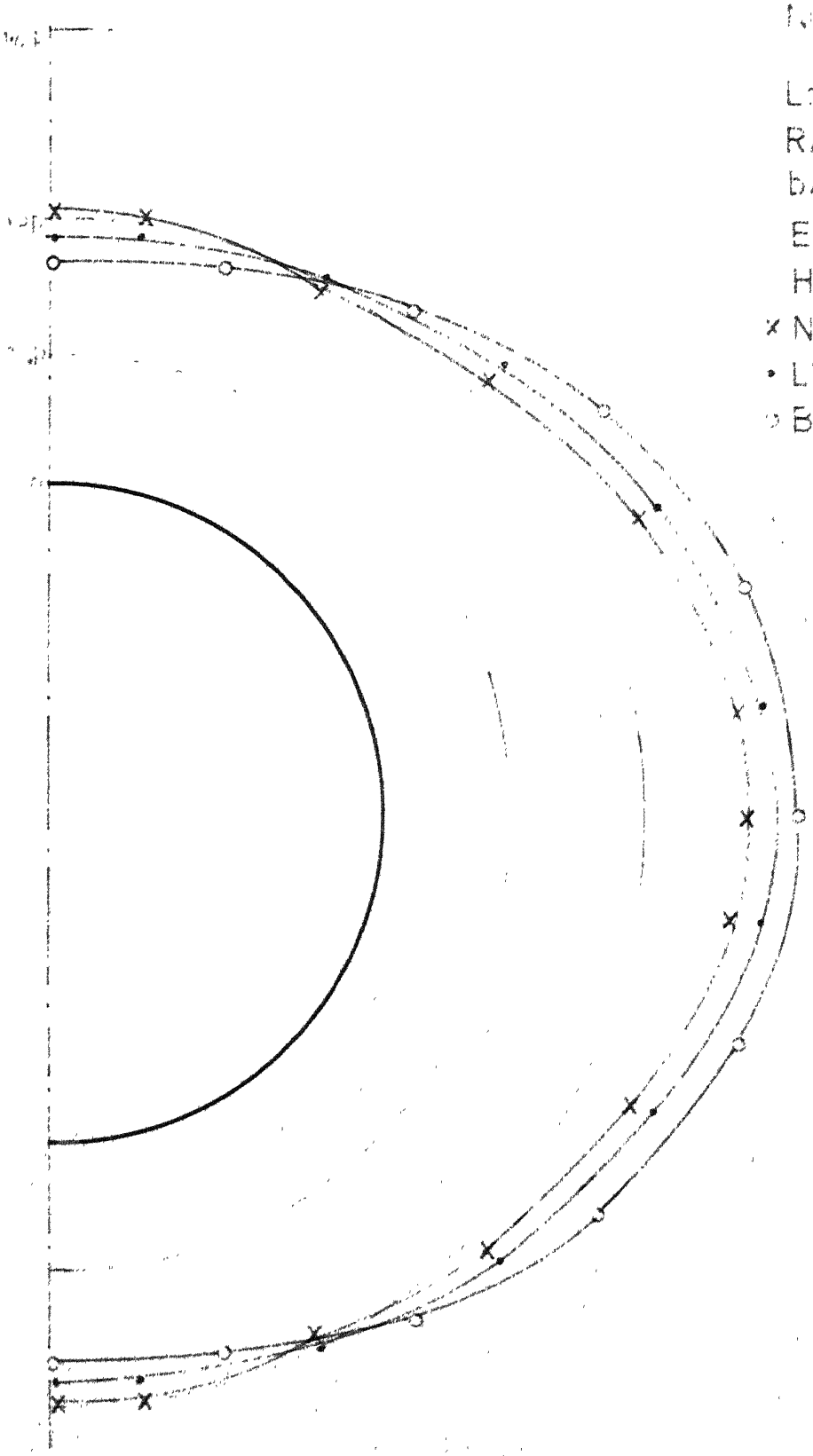

Fig. 3-1 General variation of radial pressur distribution around the pipe for surface loading

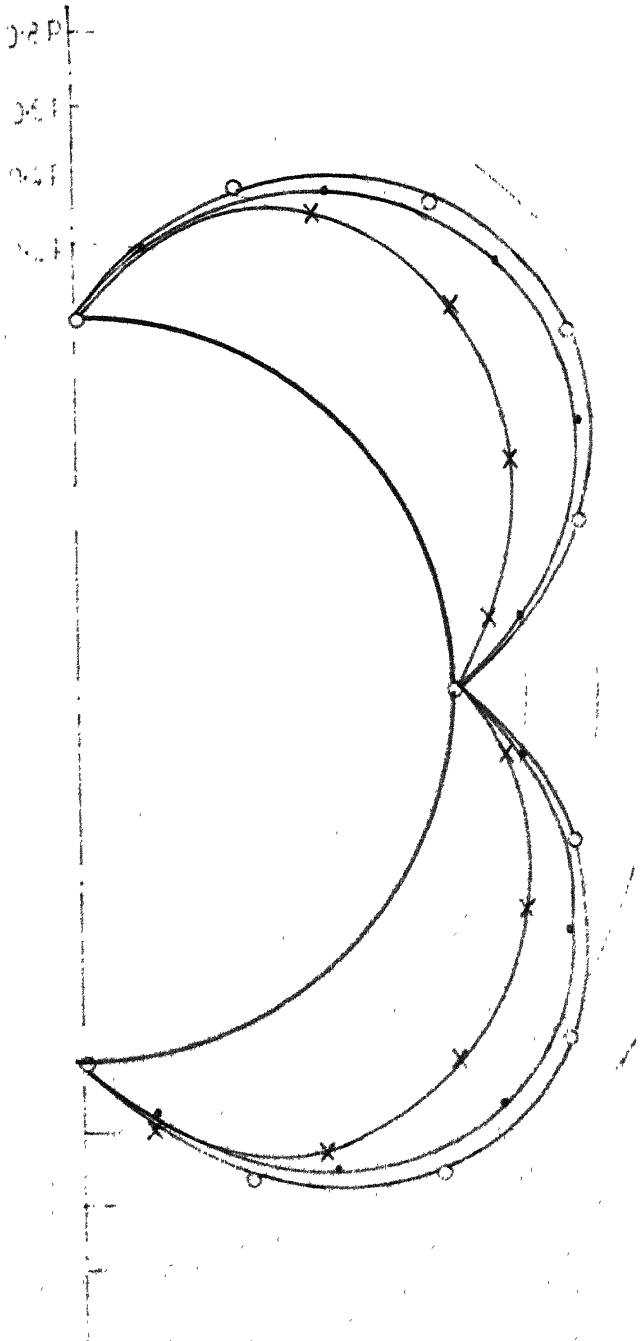

No-slip

Loading-surface pressure

b/R=8

R/t =20

E_c/E_s=300

H/D =1·0

x Non-linear elastic

• Linear elastic

o Burns solution

℄ of pipe

Fig.3-2 General variation of tangential pressure distribution around the pipe for surface loading

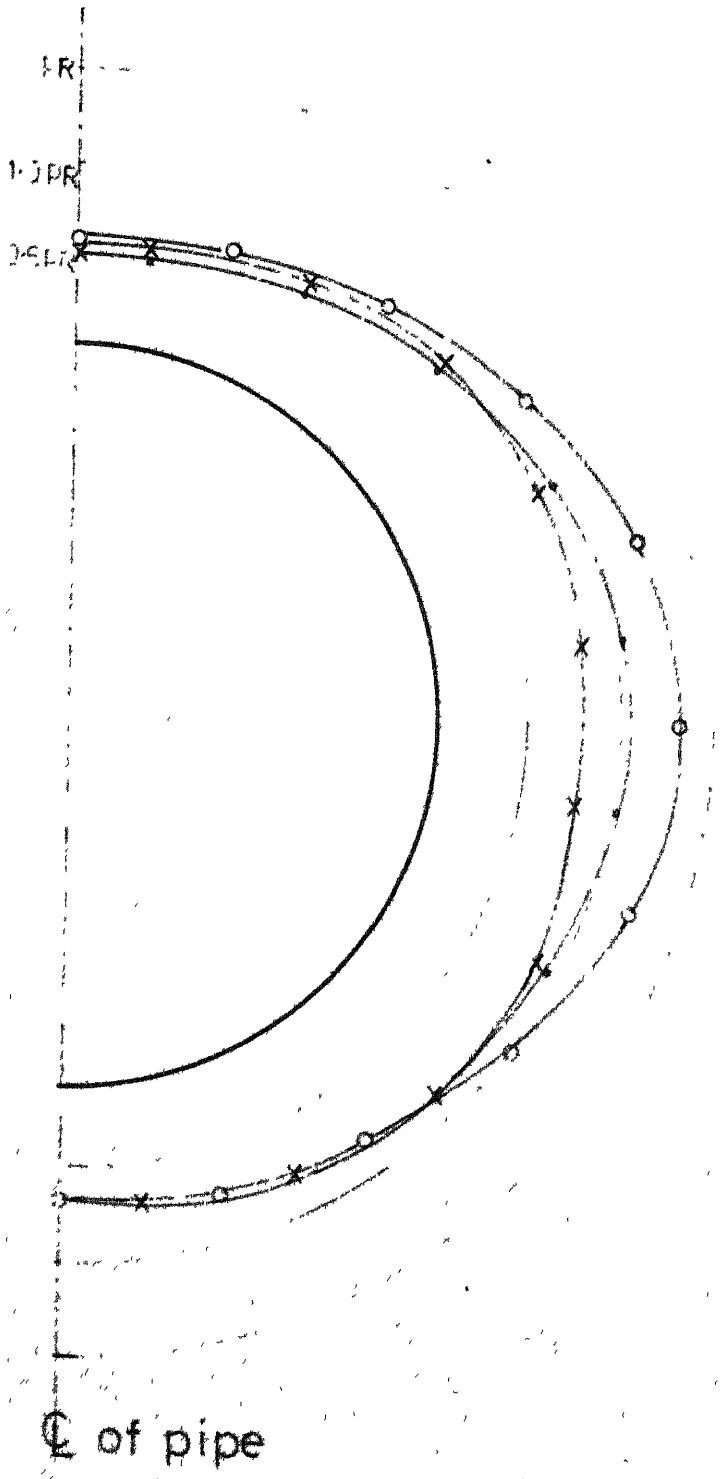

No-slip

Loading-surface pressure
b/R = 8
R/t = 20
E_c/E_s=300
H/D = 1·0
x Non-linear elastic
• Linear elastic
o Burns solution

Fig. 3-3 General variation of axial thrust along the pipe for surface loading

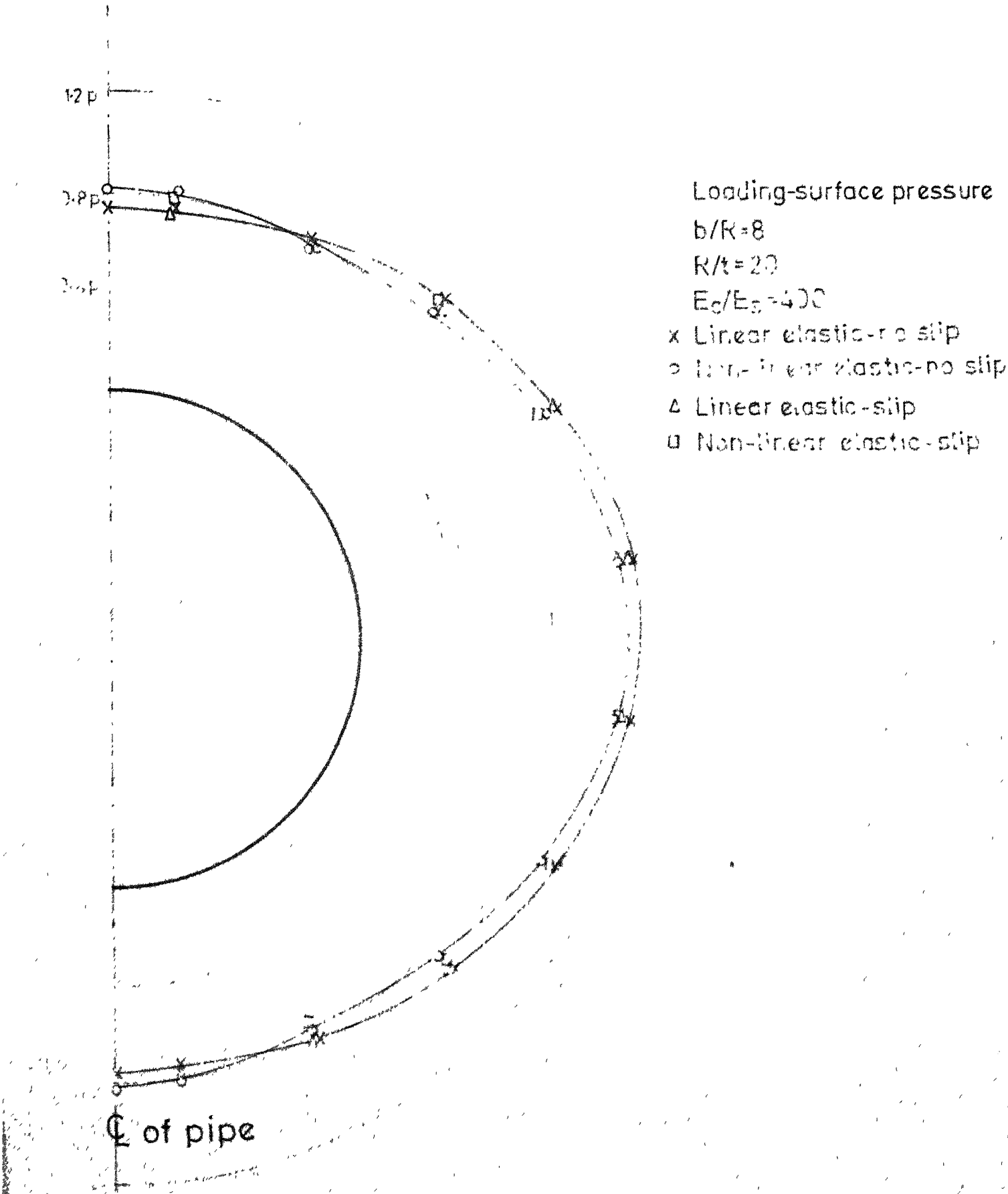

Fig. 3-4 Variation of radial pressure distribution around the pipe for no-slip and full-slip cases for surface loading

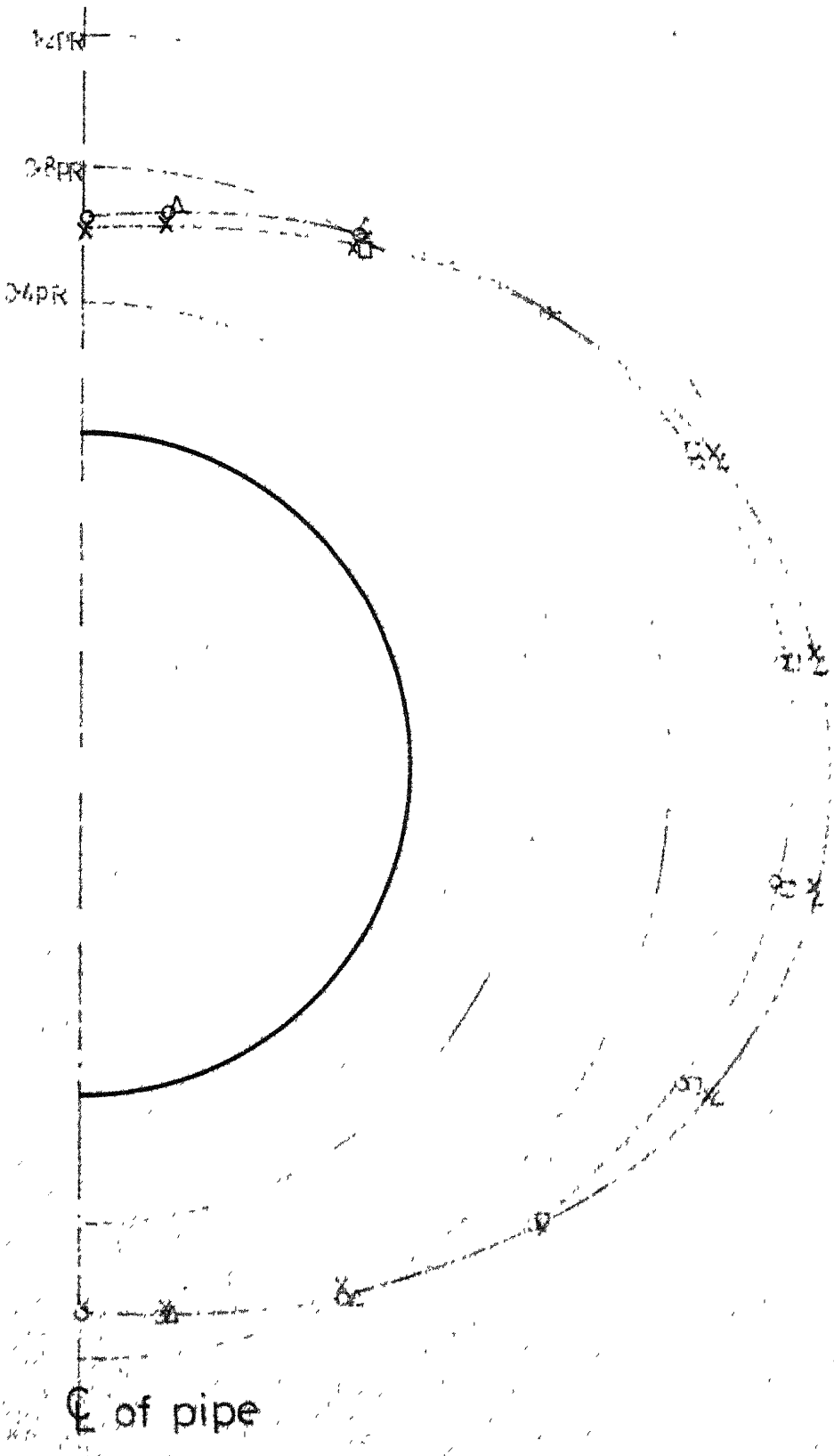

Fig. 3-5 Variation of axial thrust distribution along the pipe for no-slip and full-slip cases for surface loading

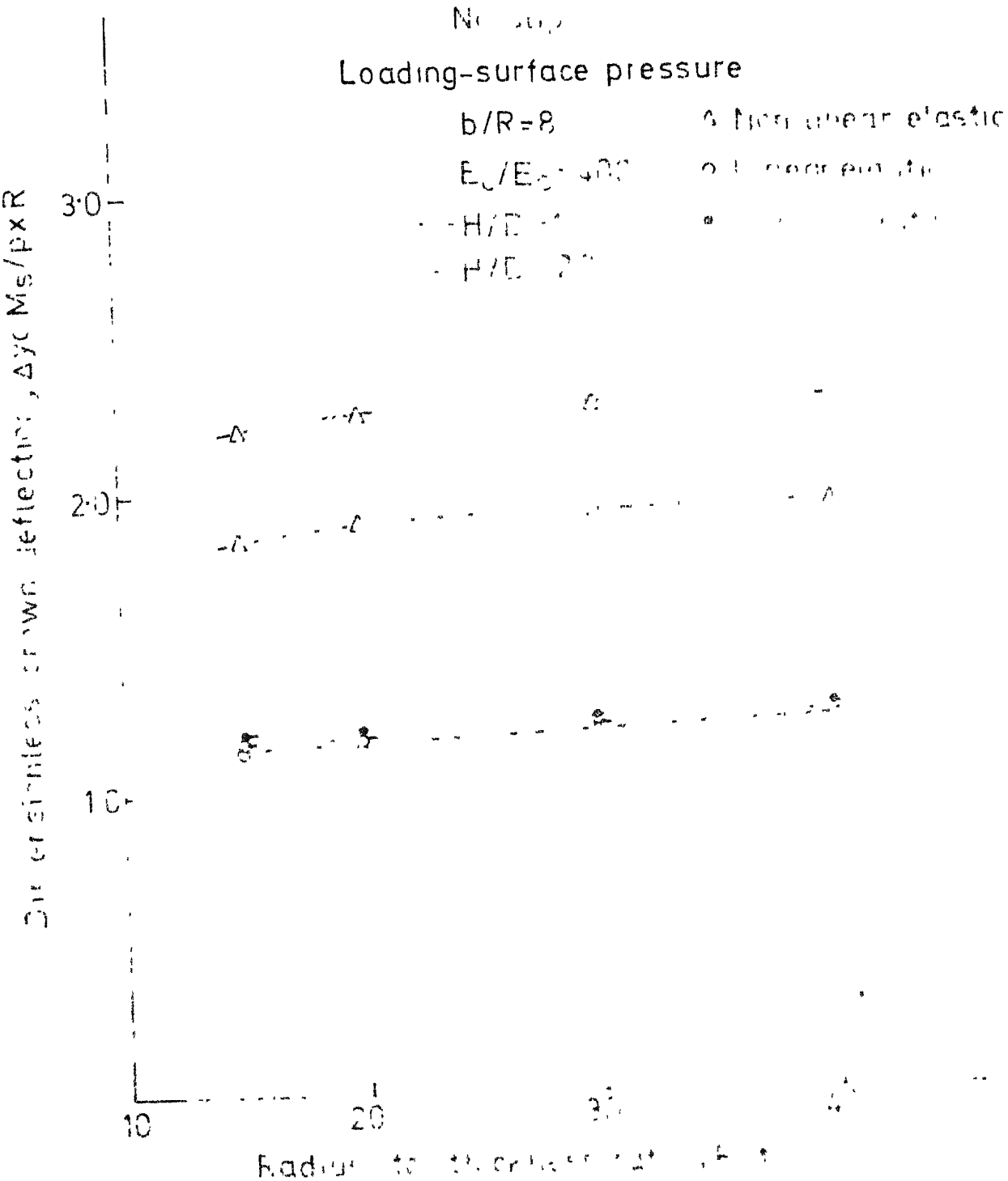

Fig. 3-6 Dimensionless crown deflection versus radius to the boundary for surface loading

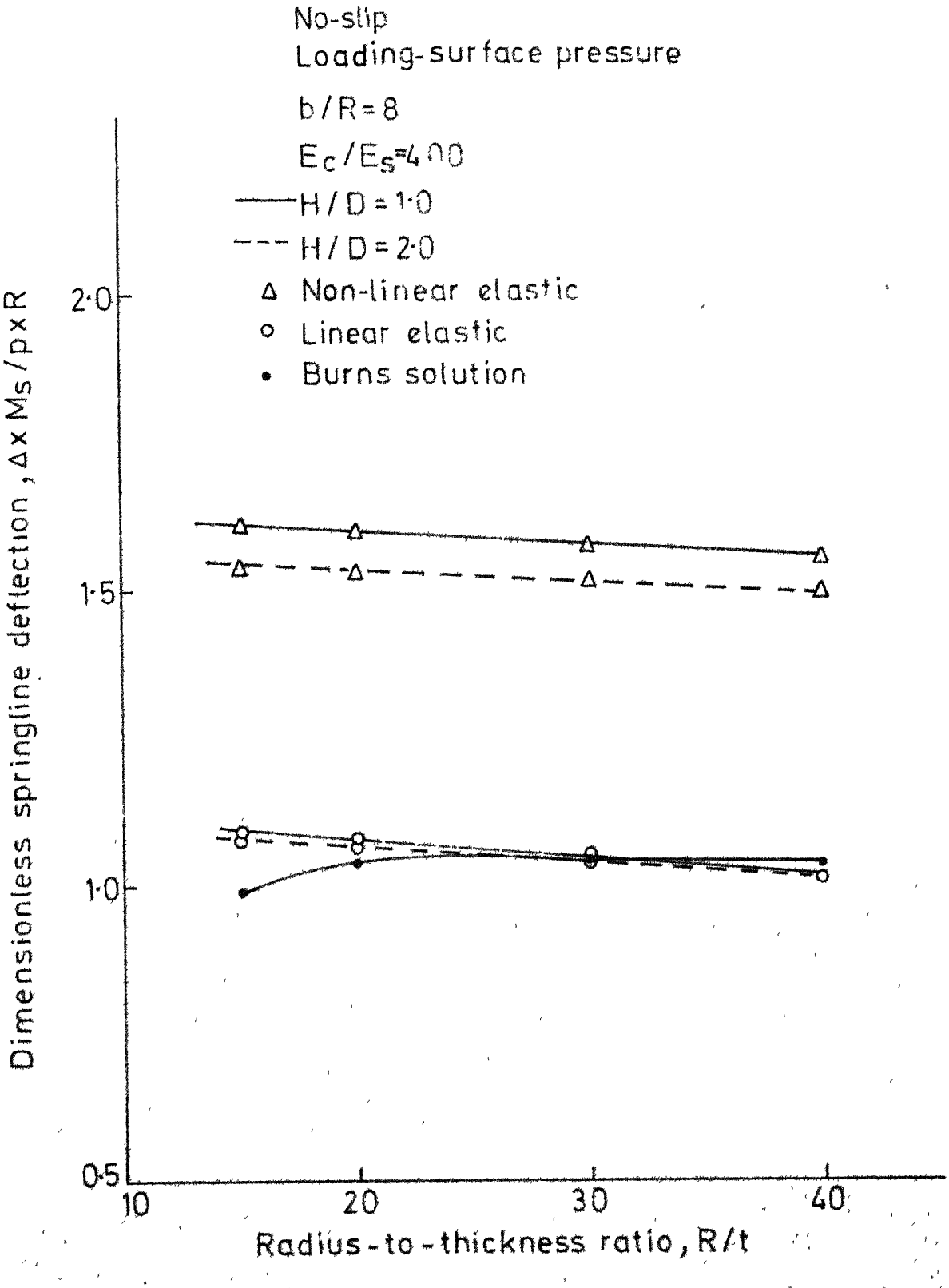

Fig. 3-7 Dimensionless springline deflection versus radius-to-thickness ratio for surface loading

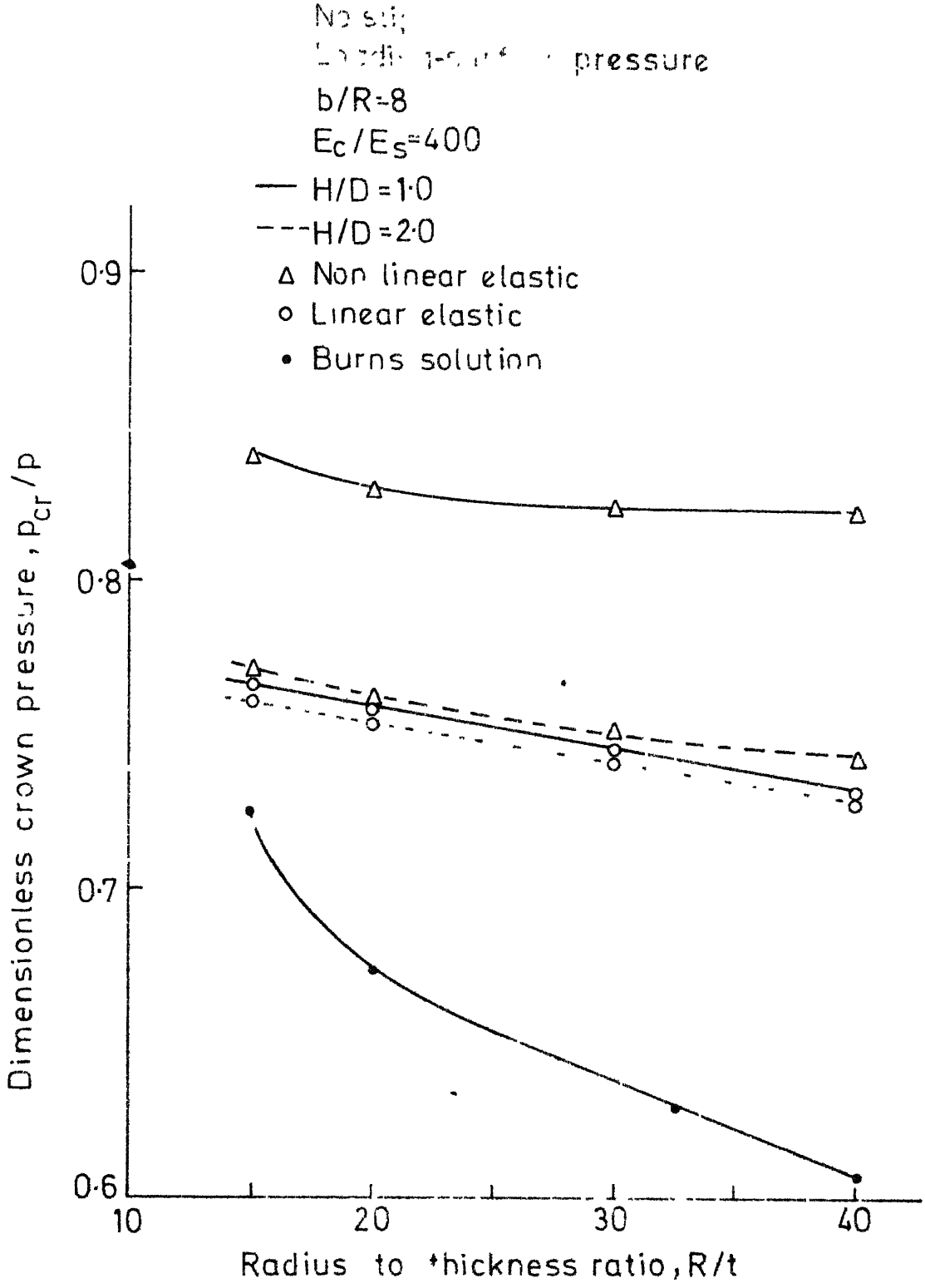

Fig.3-8 Dimensionless pressure versus radius -to- thickness ratio for surface loading

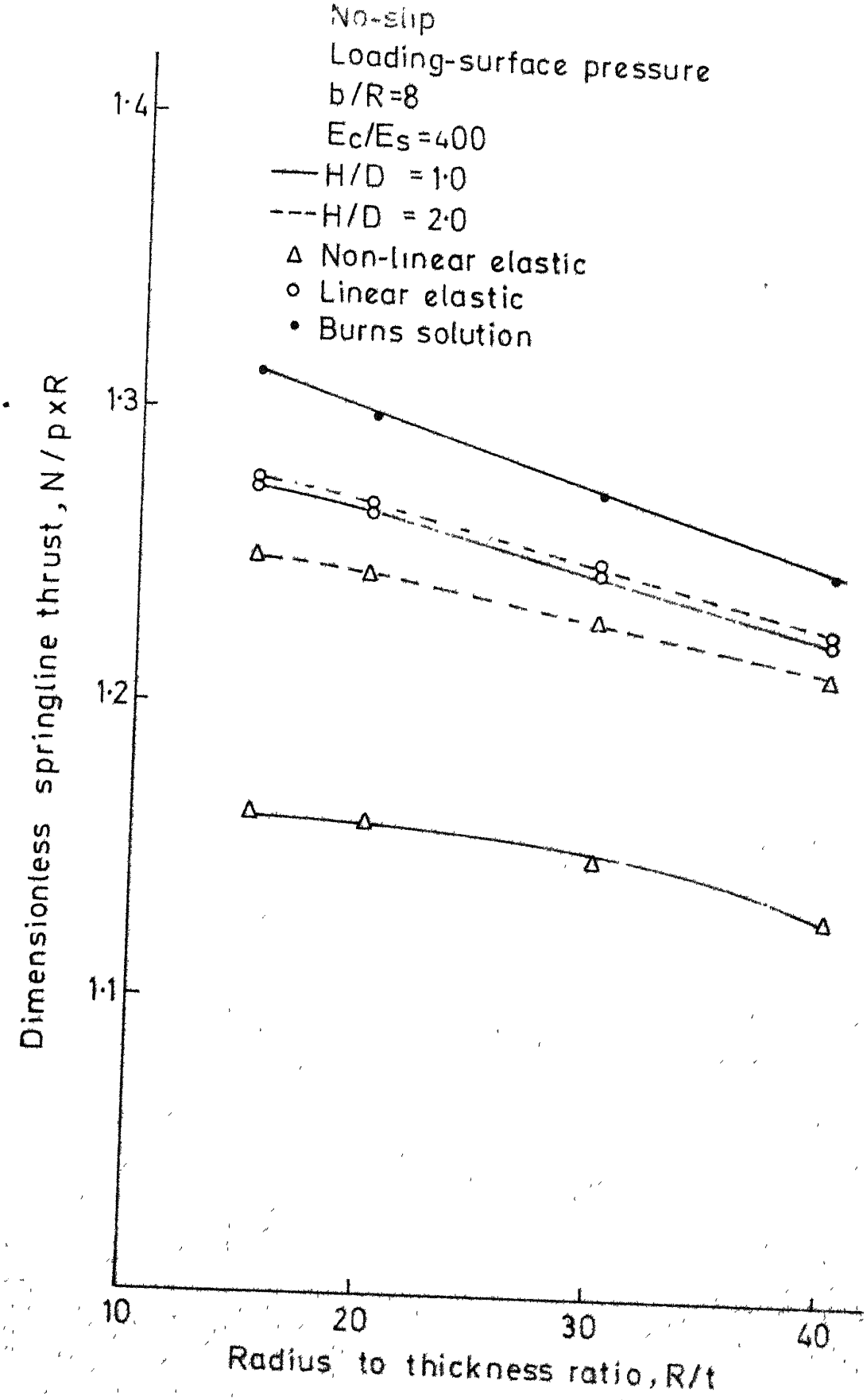

Fig.3-9 Dimensionless springline thrust versus radius-to-thickness ratio for surface loading

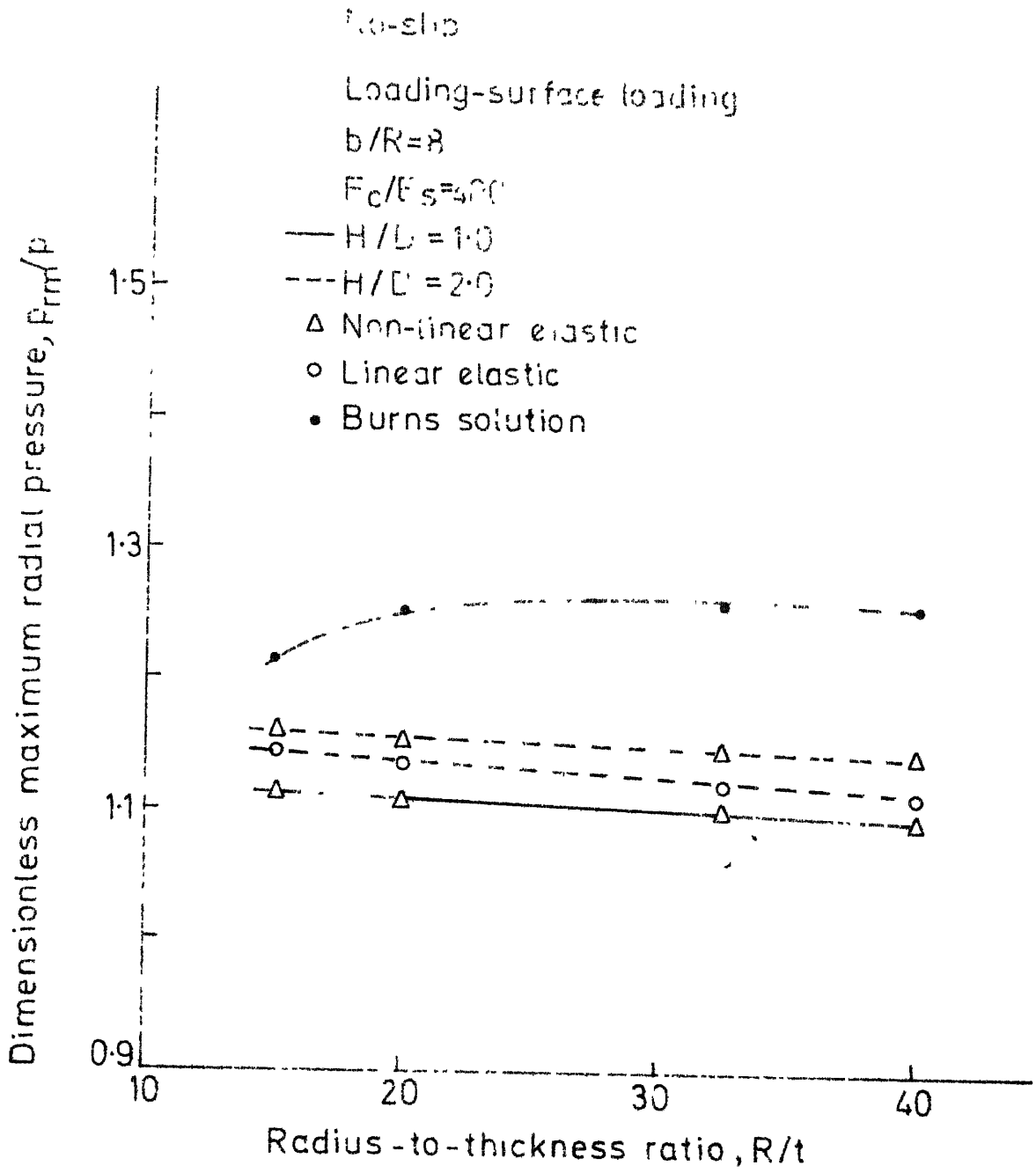

Fig. 3-10 Dimensionless maximum radial pressure versus radius-to-thickness ratio for surface loading

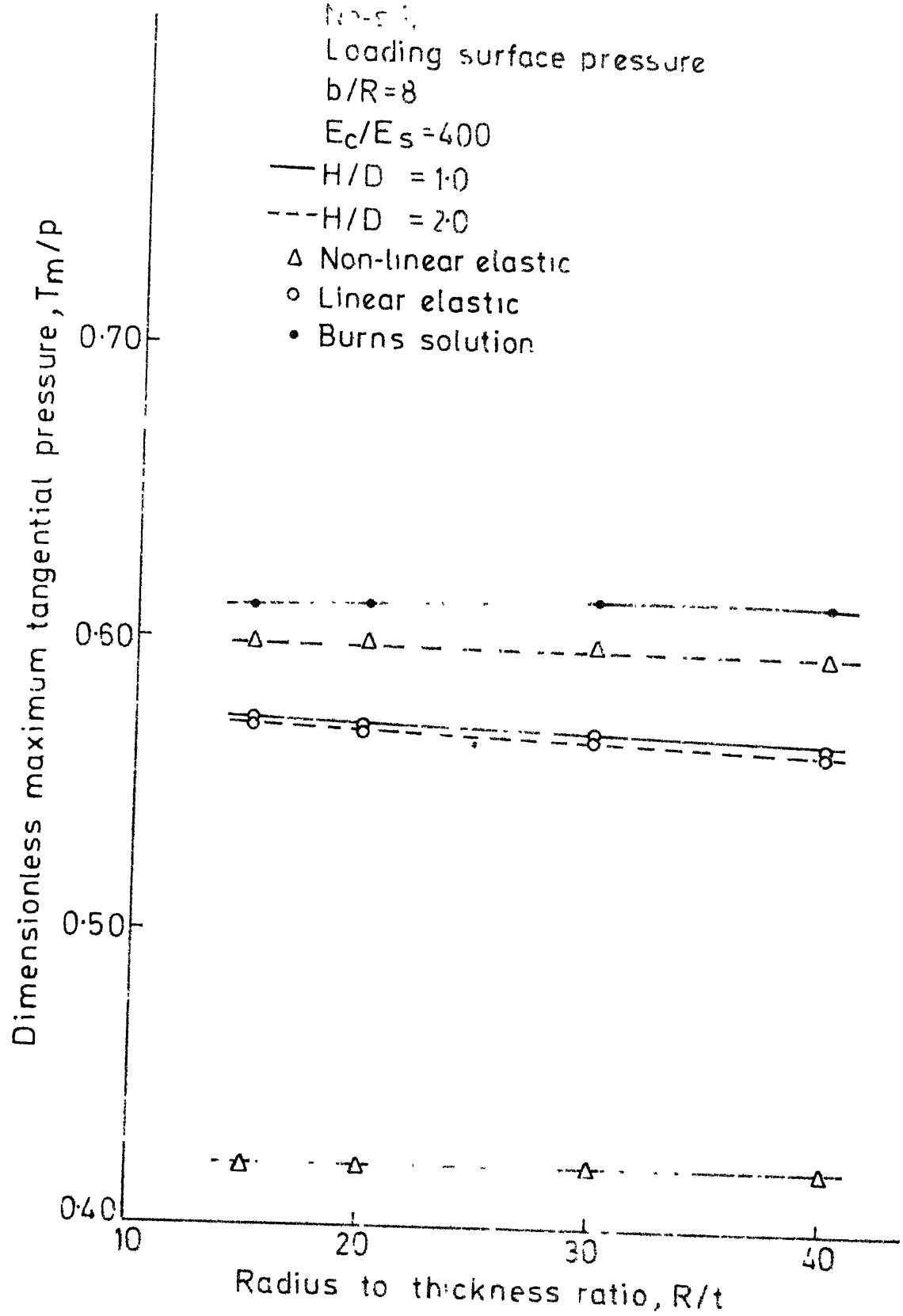

Fig. 3-11 Dimensionless maximum tangential pressure versus radius-to-thickness ratio for surface loading

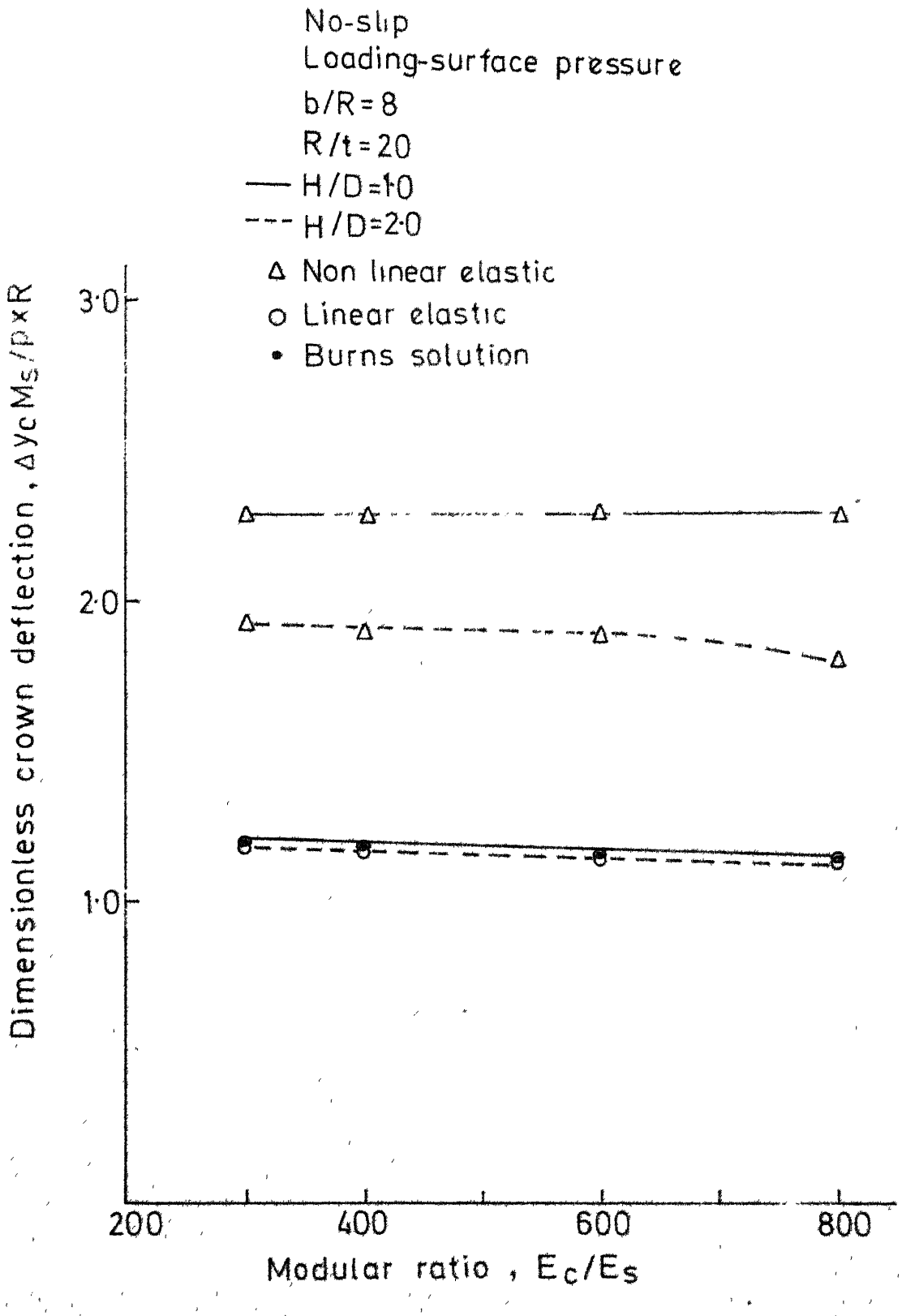

Fig. 3-12 Dimensionless crown deflection versus modular ratio for surface loading

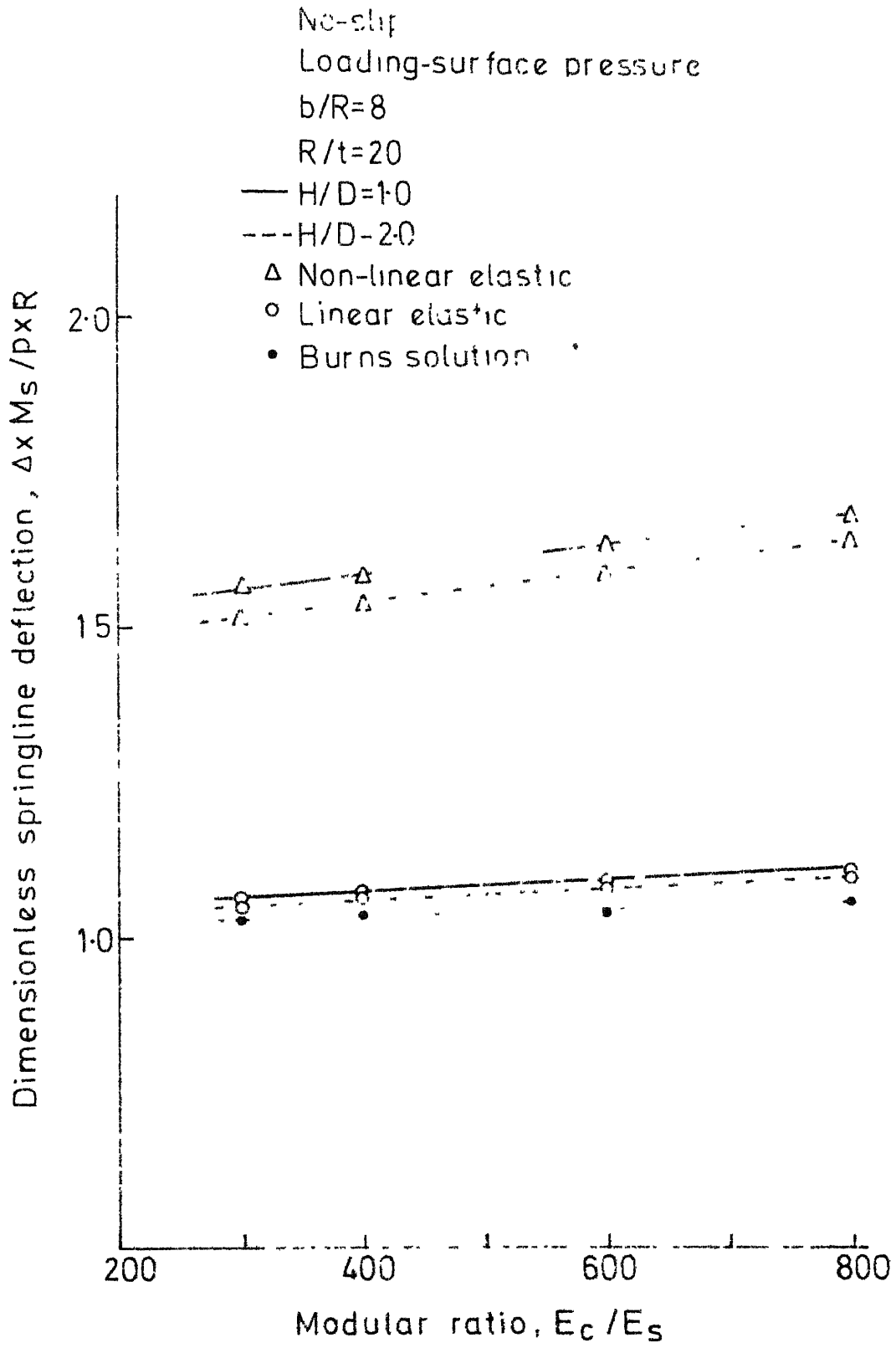

Fig. 3-13 Dimensionless springline deflection versus modular ratio for surface loading

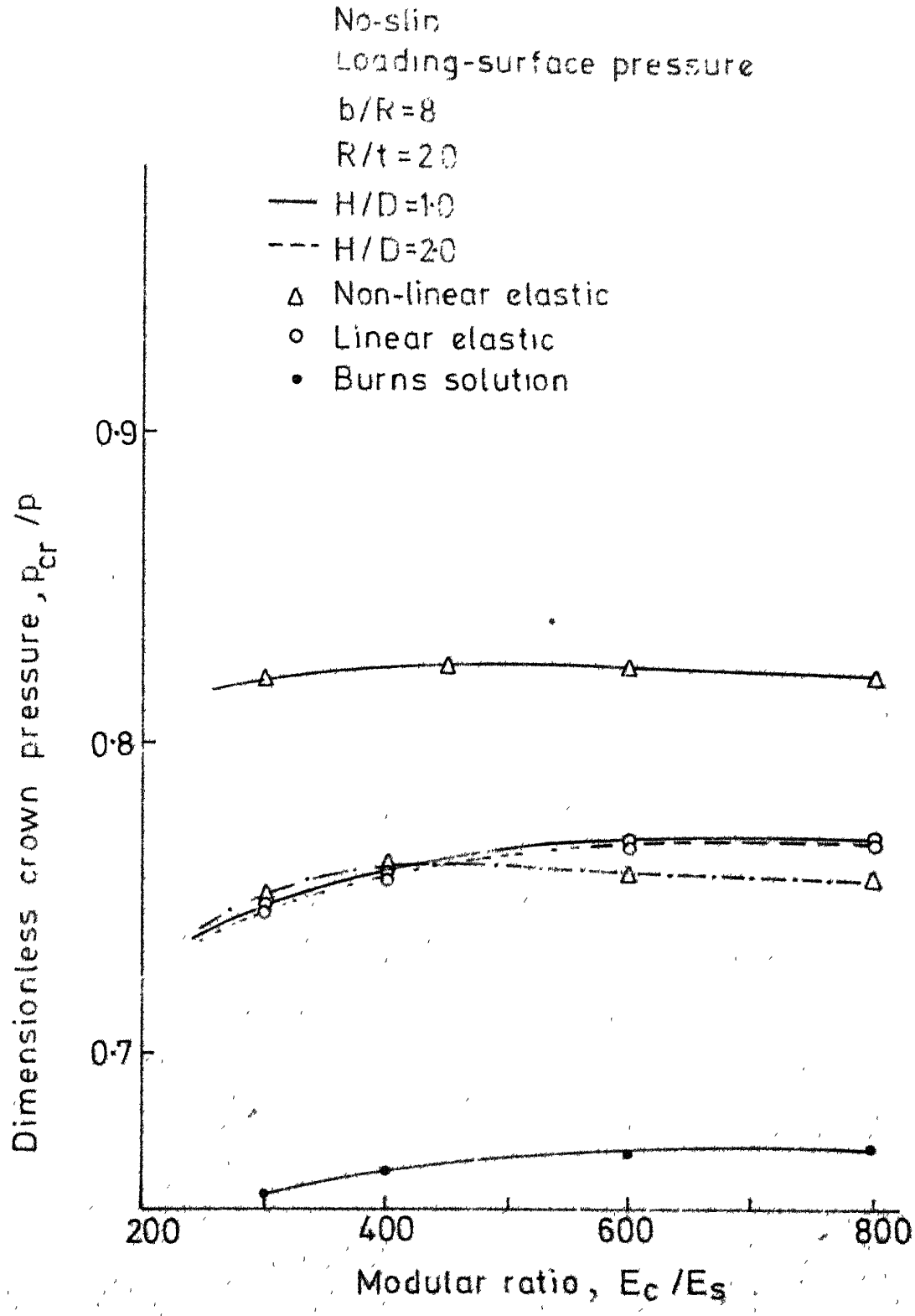

Fig. 3-14 Dimensionless crown pressure versus modular ratio for surface loading

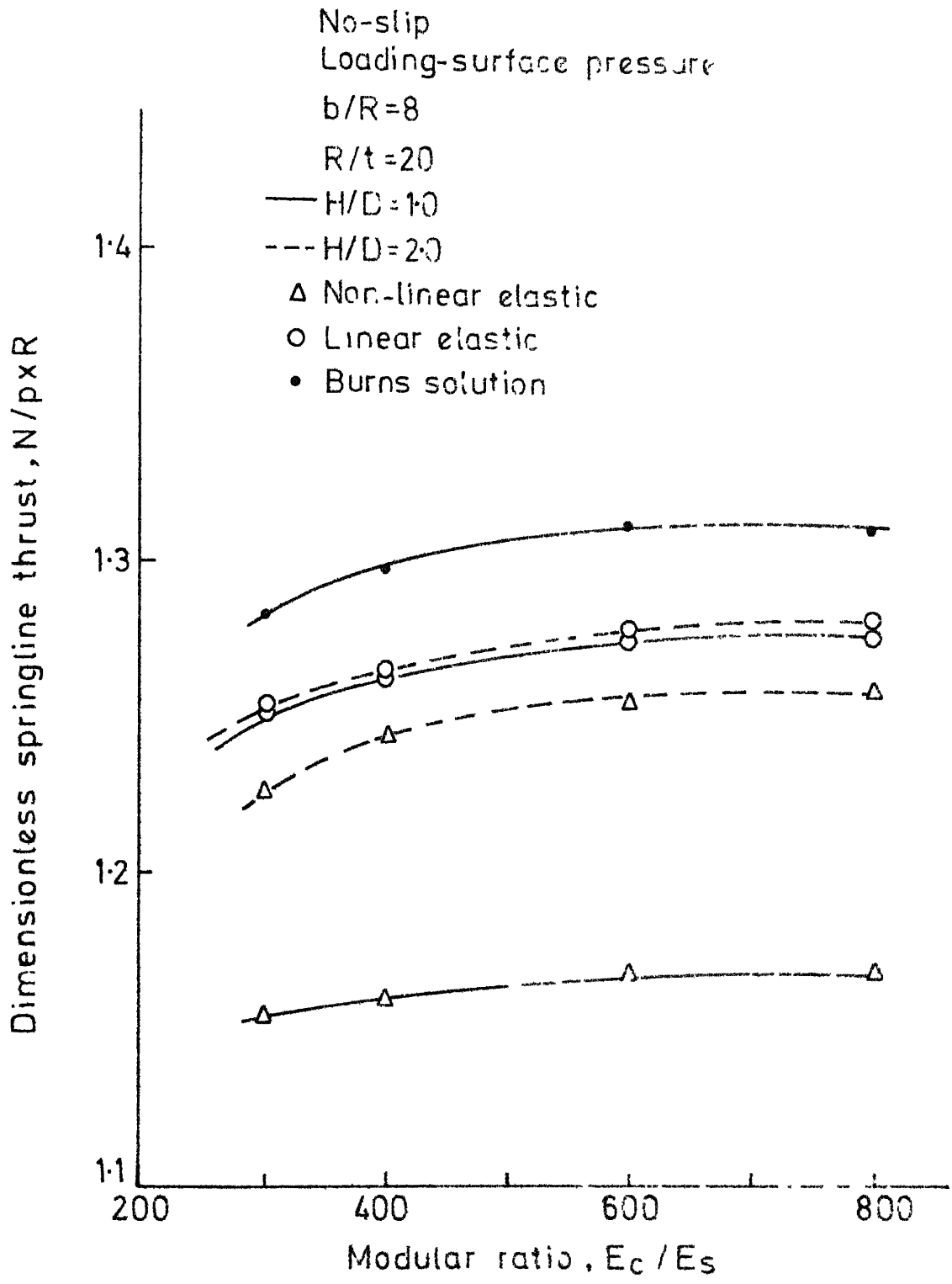

Fig. 3·15 Dimensionless springline thrust versus modular ratio for surface loading

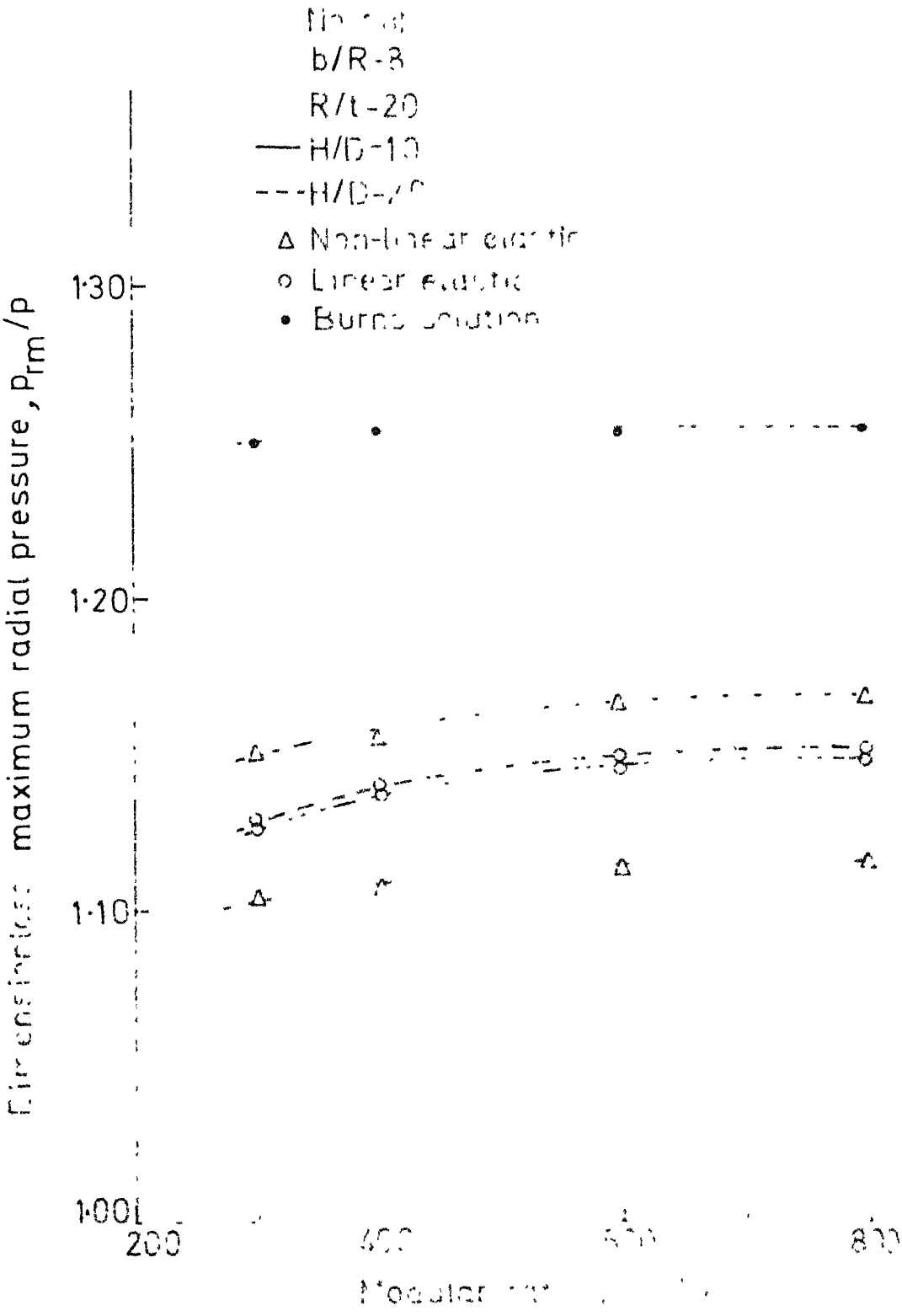

Fig. 3-16 Dimensionless maximum radial pressure versus modular ratio for surface load

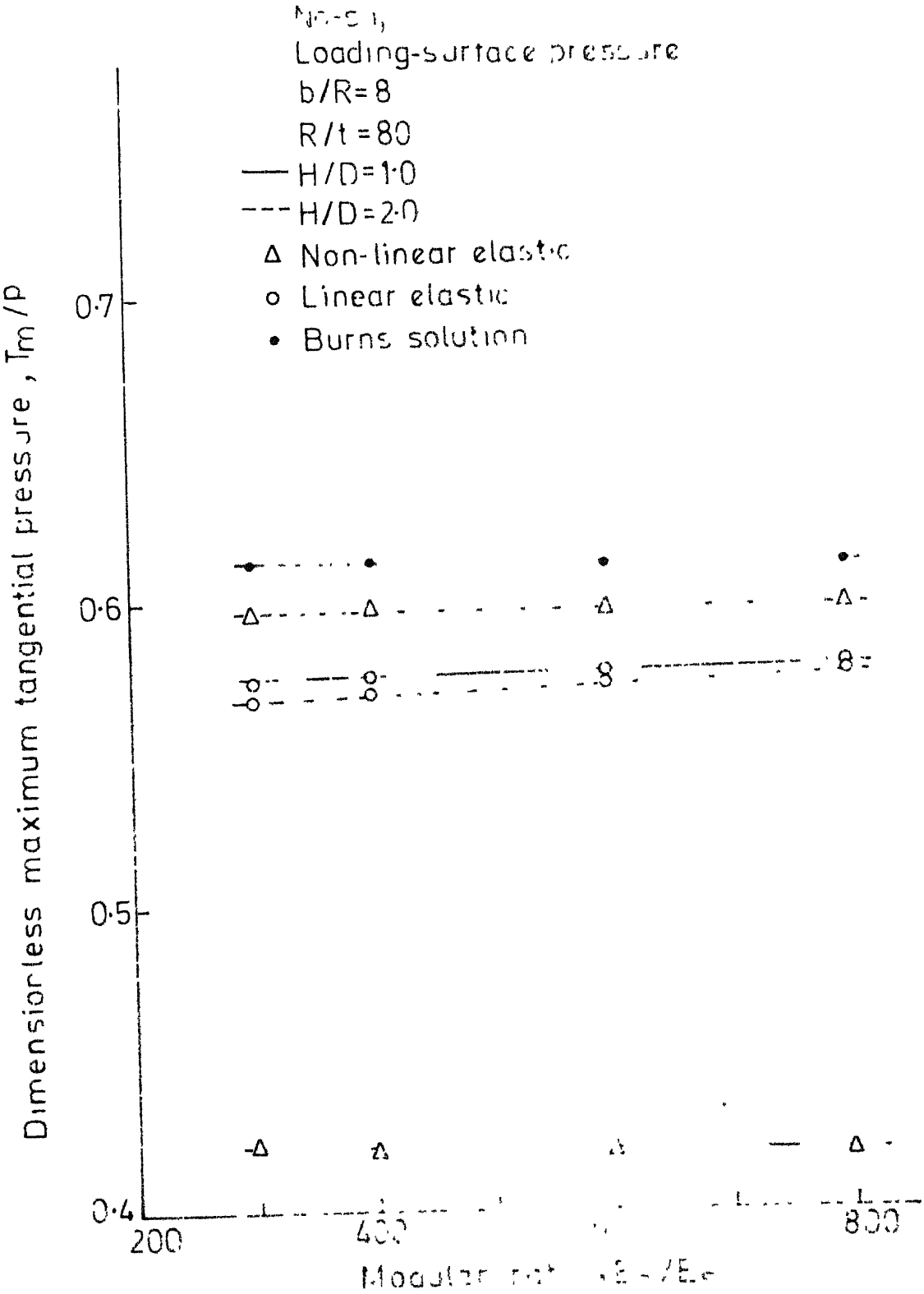

Fig. 3-17 Dimensionless maximum tangential pressure versus modular ratio for surface loading

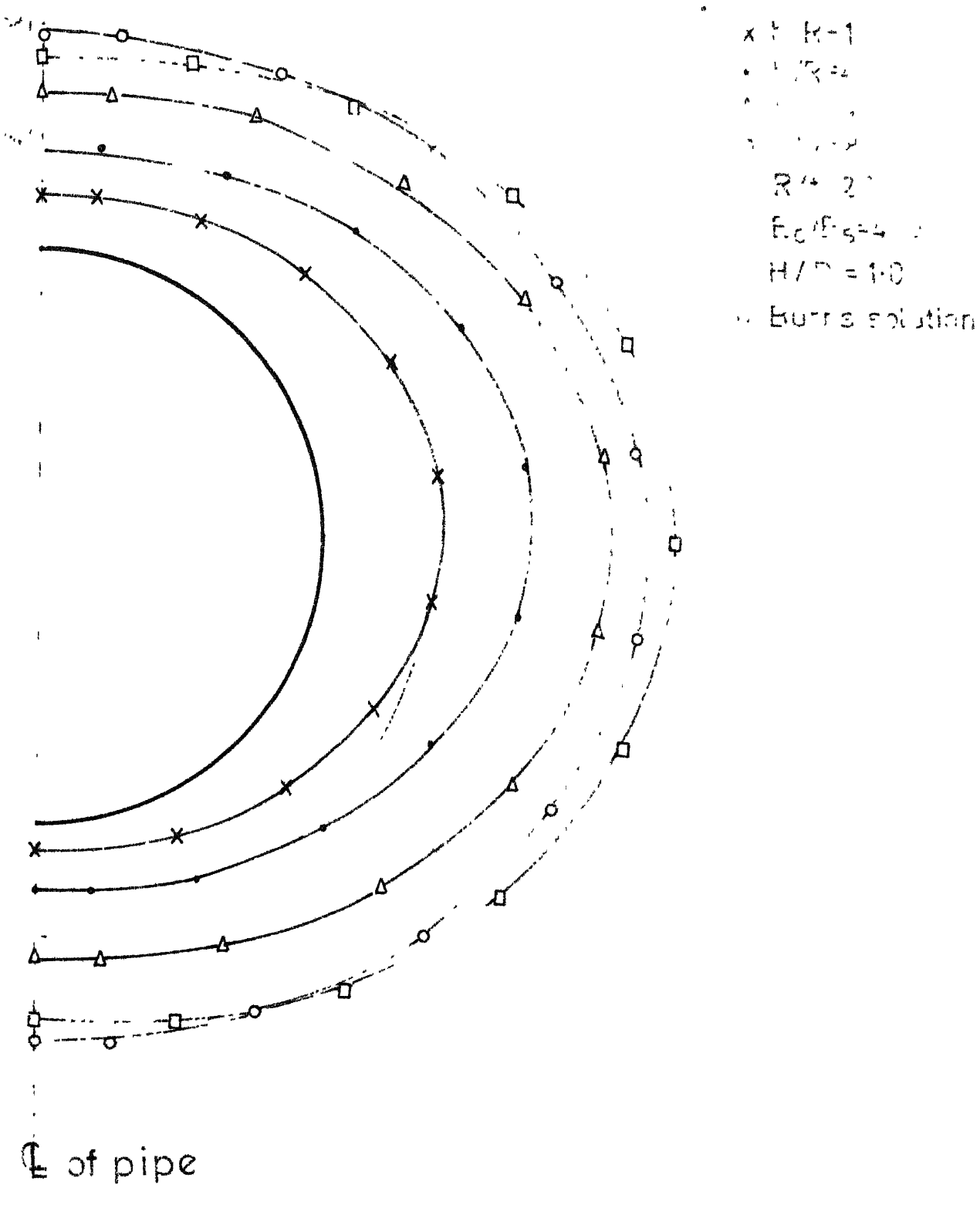

Fig. 3-18 Variation of radial pressure distribution around the pipe for different semi-load width-to-radius ratios for surface loading

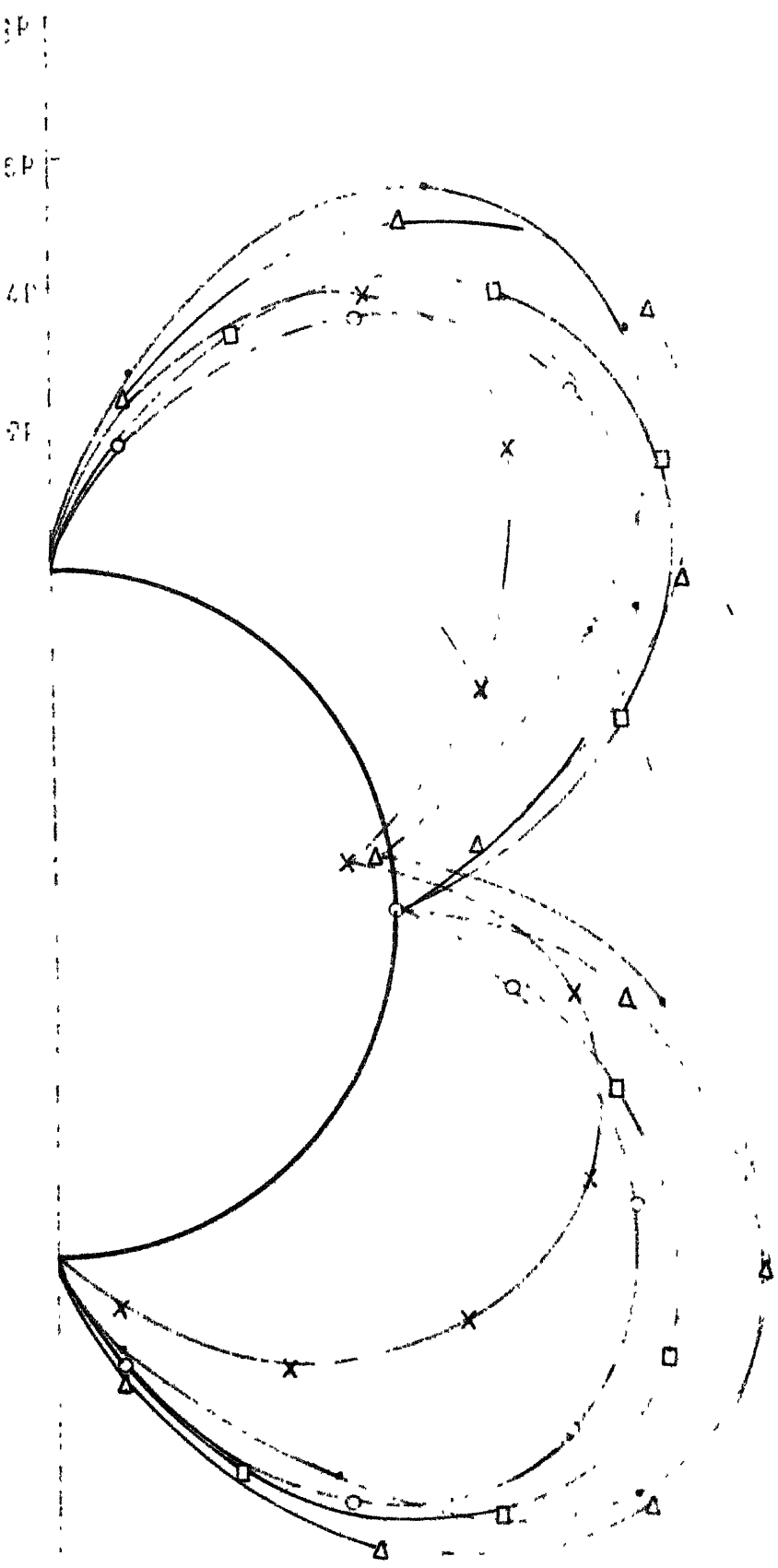

℄ of pipe

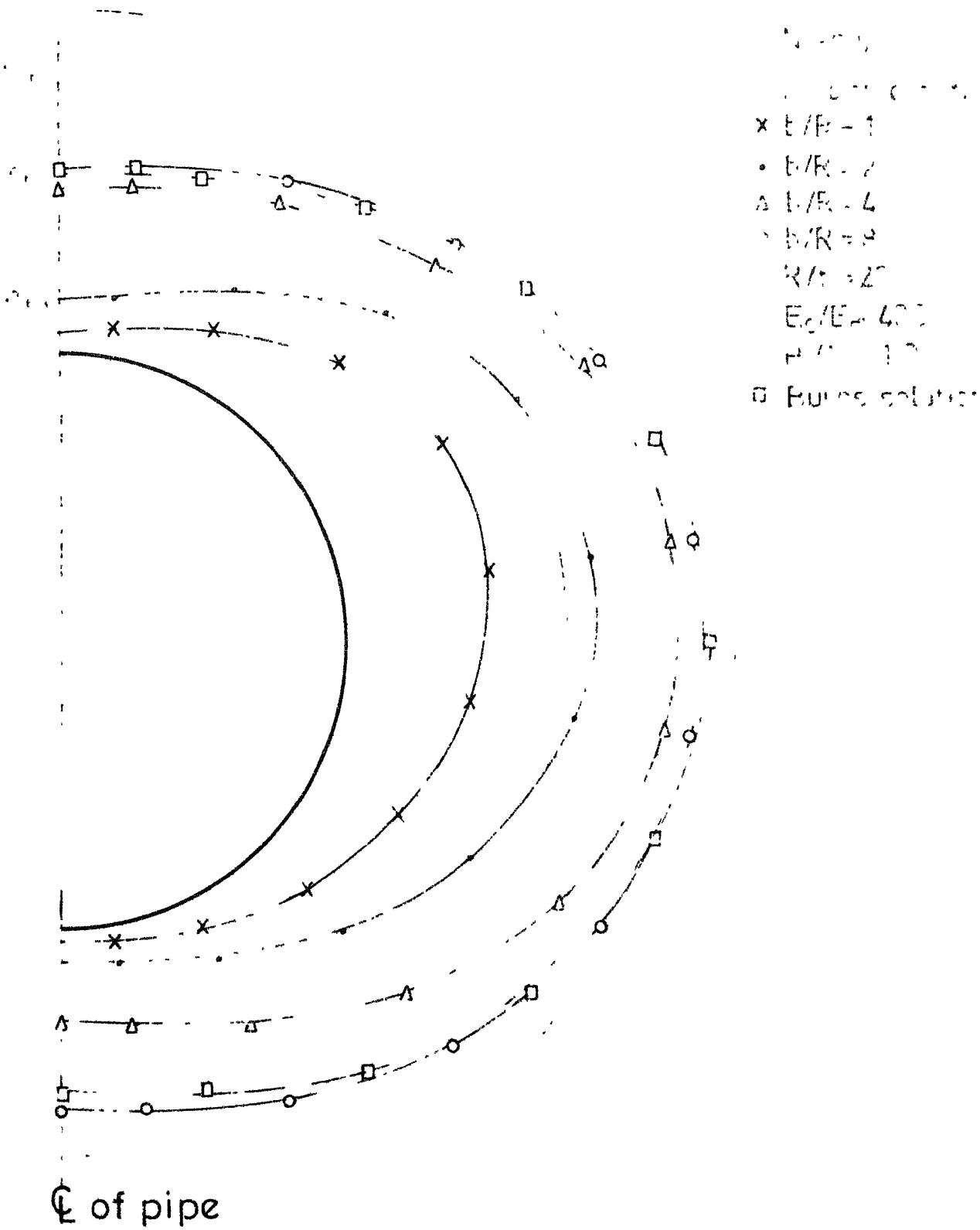

Fig.3-20 Variation of axial thrust distribution along the pipe for different semi-load width-to-radius ratios for suface loading

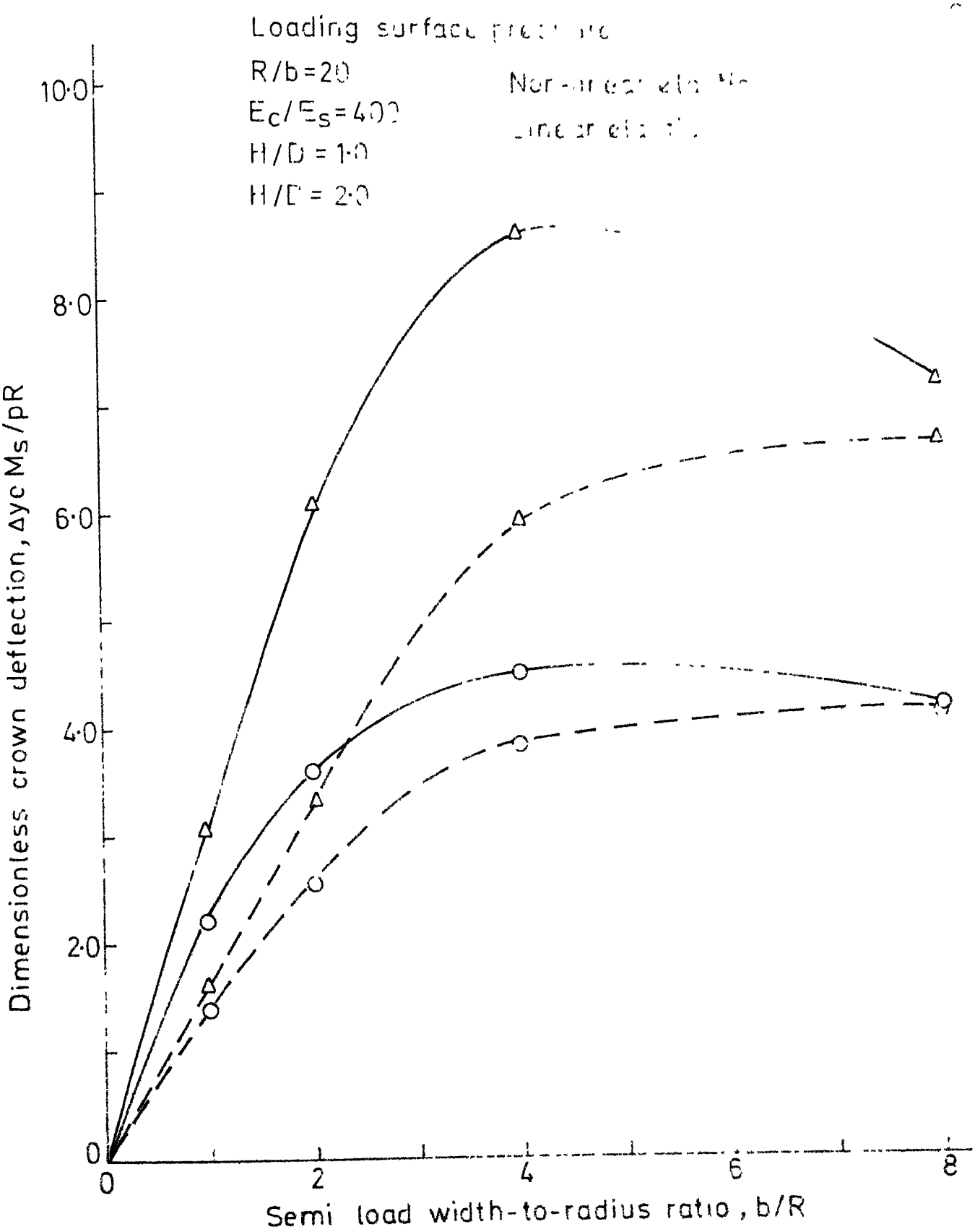

Fig. 3·21 Dimensionless crown deflection versus semi-load width-to-radius ratio

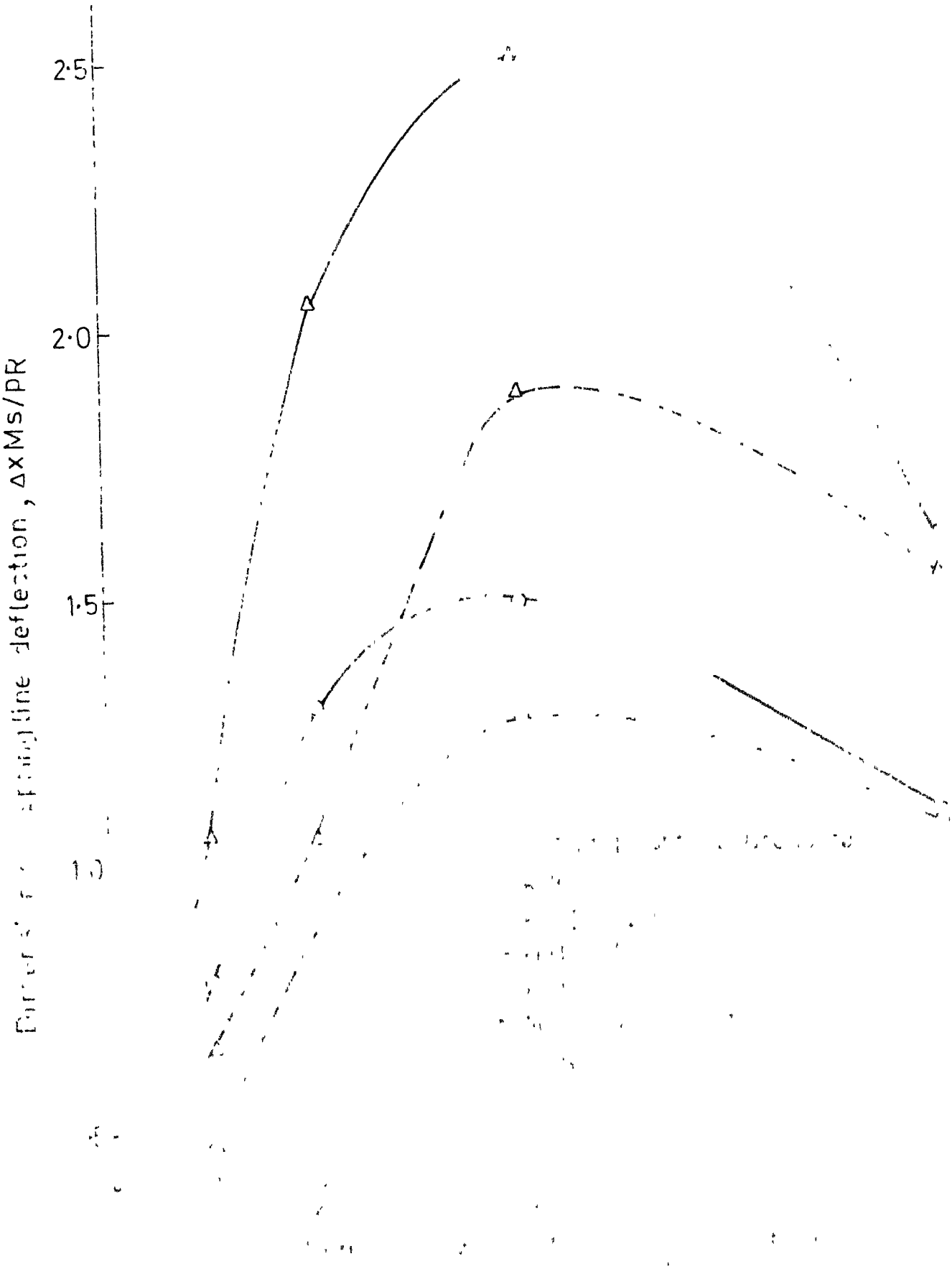

Fig.3-22

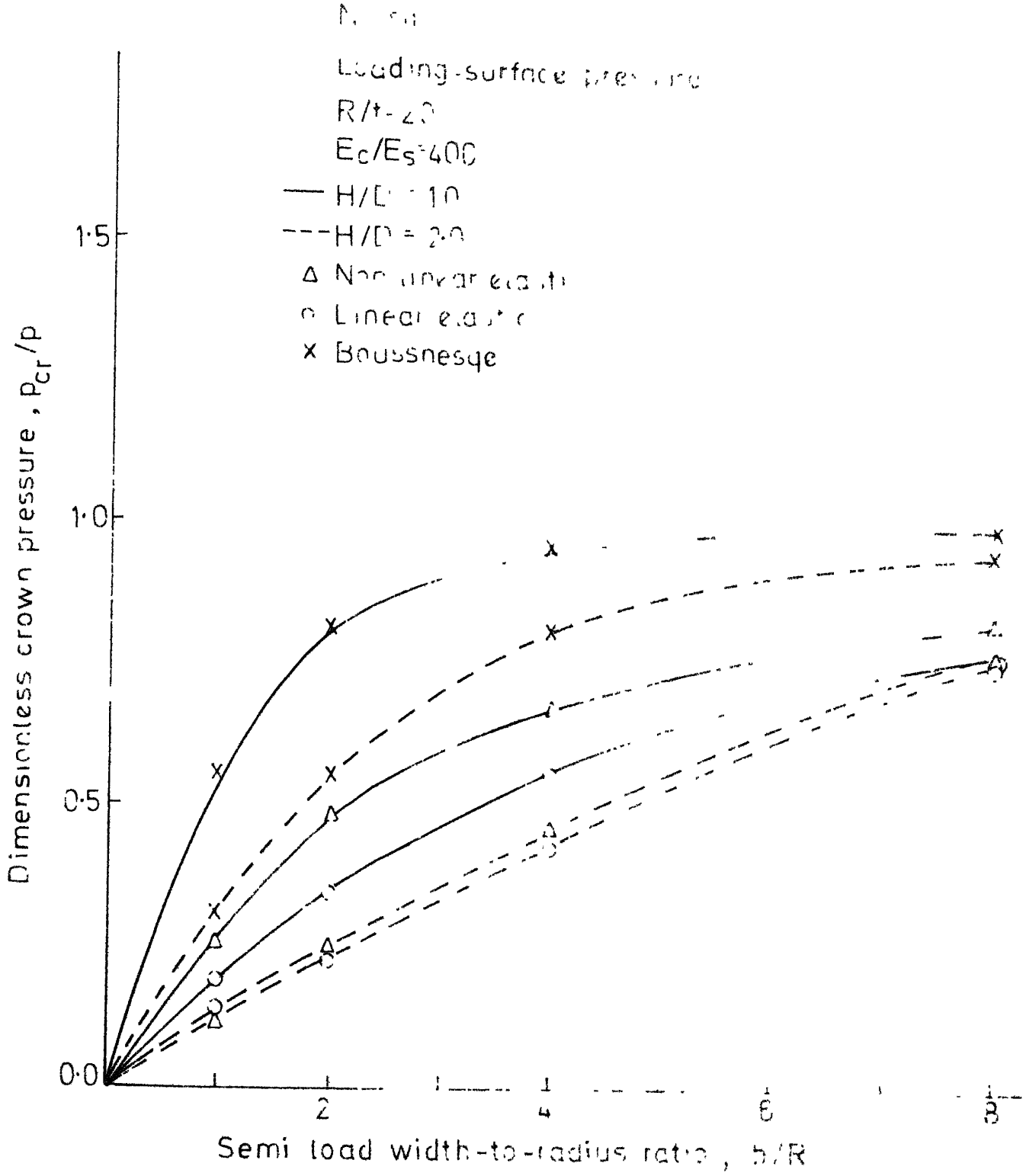

Fig. 3-23 Dimensionless crown pressure versus semi-load width-to-radius ratio

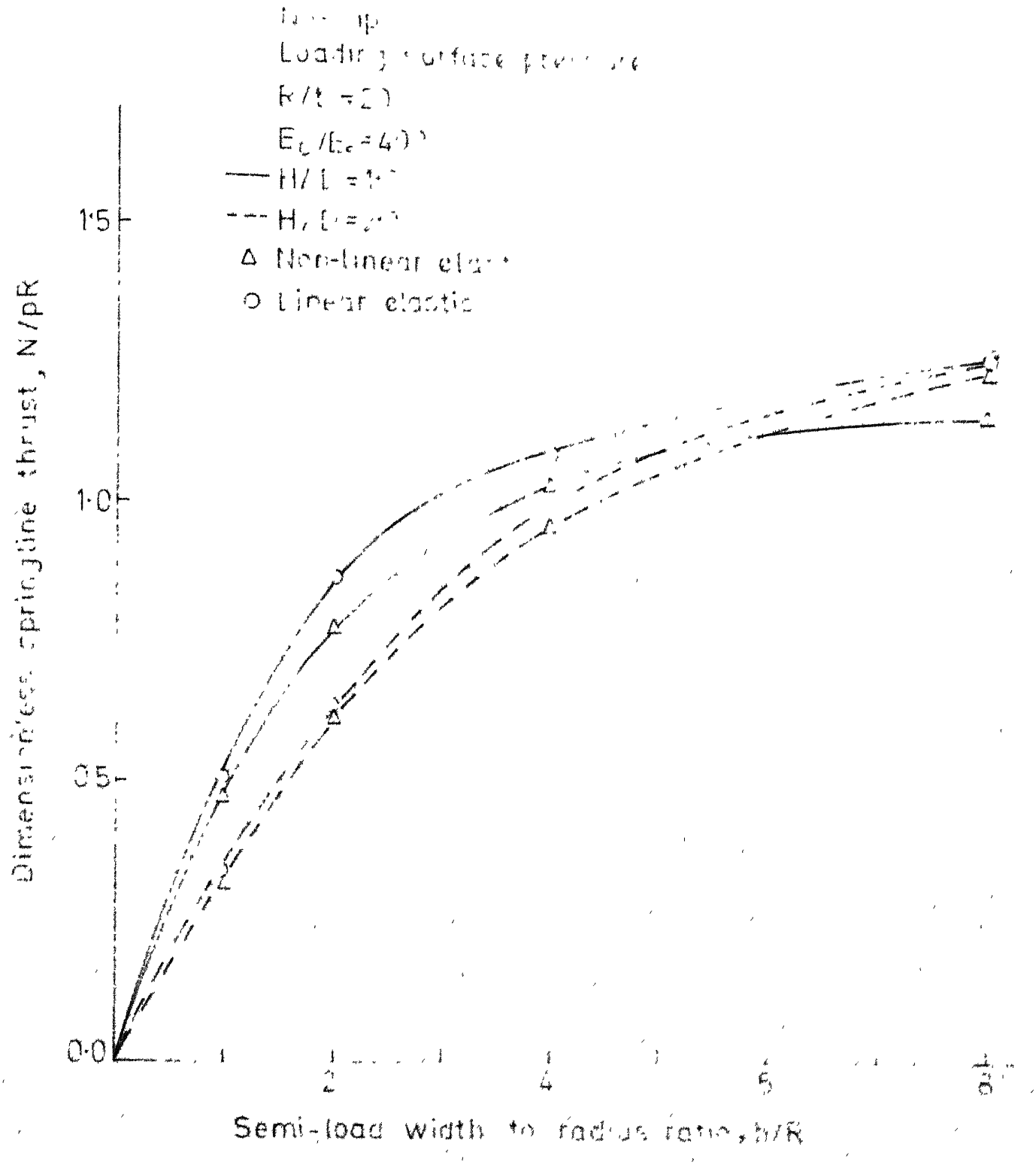

Fig.3-24 Dimensionless springline thrust versus semi-load width-to-radius ratio

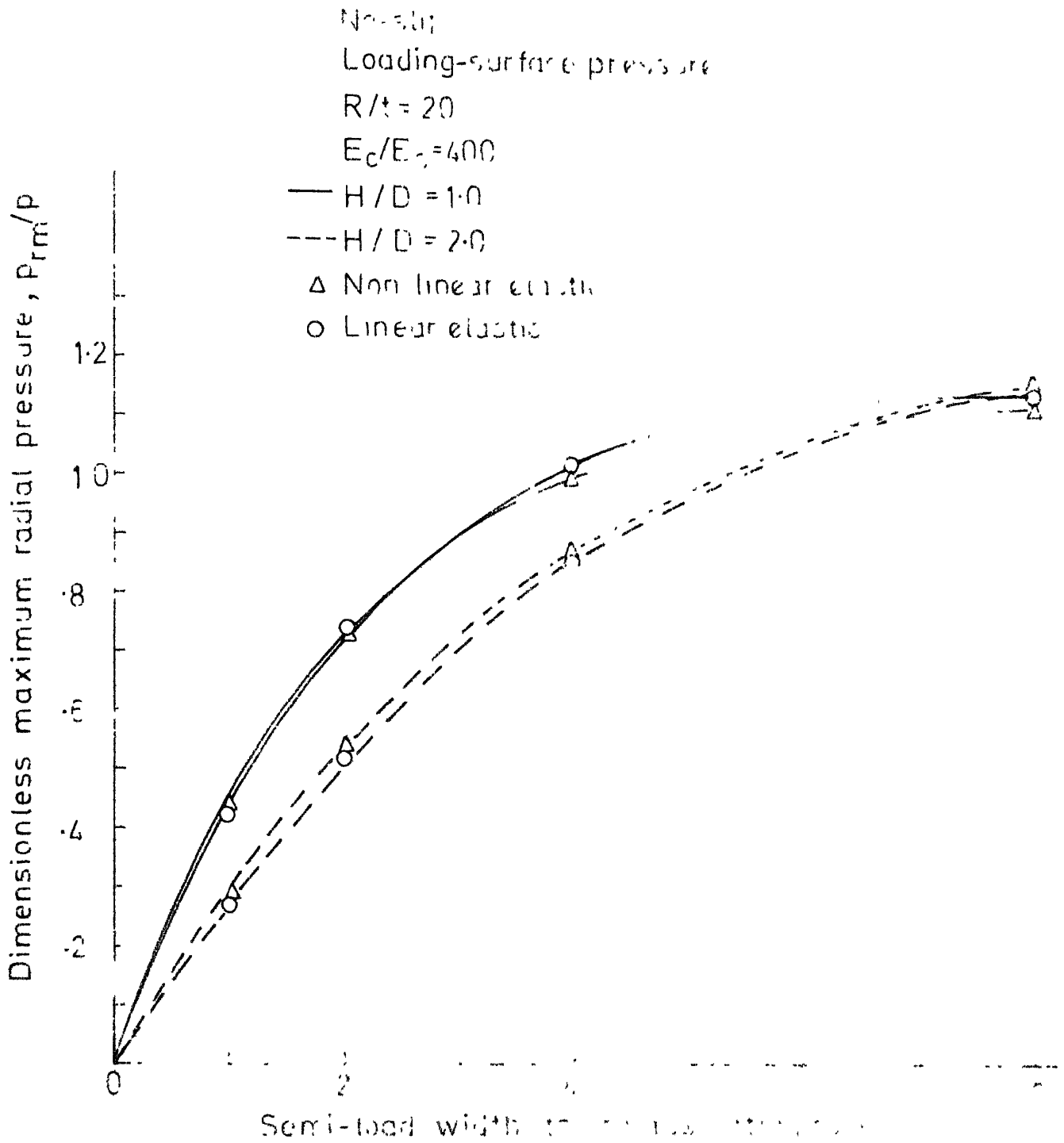

Fig. 3-25 Dimensionless maximum radial pressure versus semi-load width-to-radius ratio

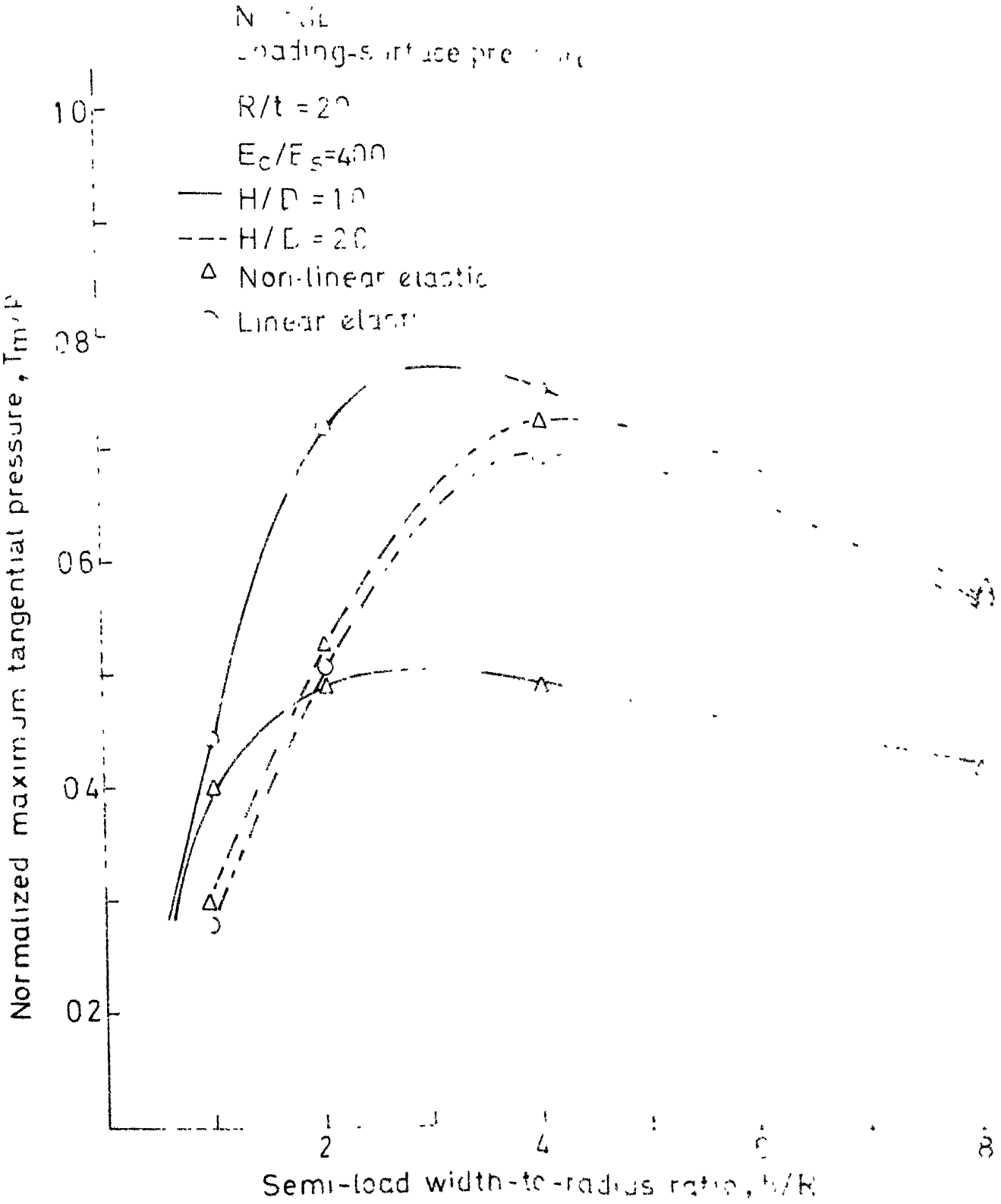

Fig. 3-26 Dimensionless maximum tangential pressure versus semi-load width-to-radius ratio

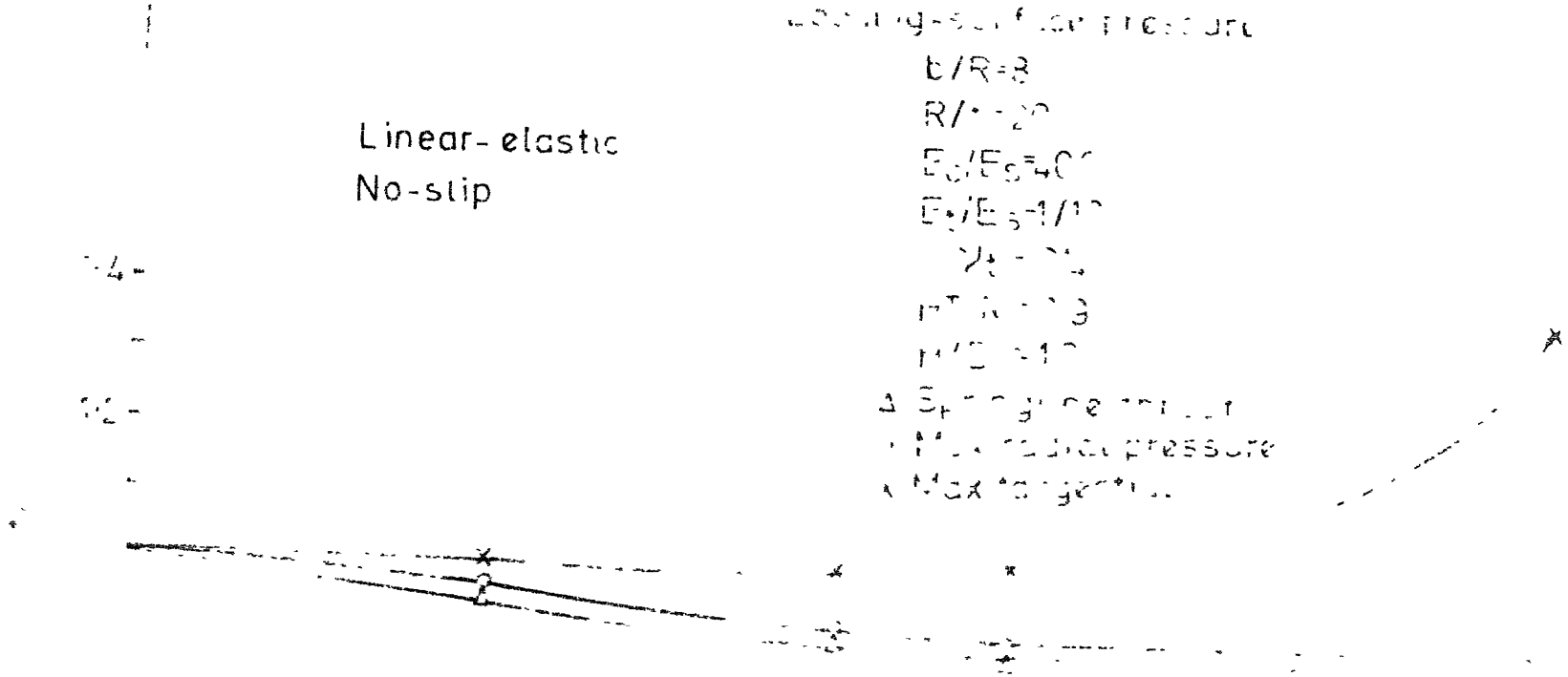

Surface

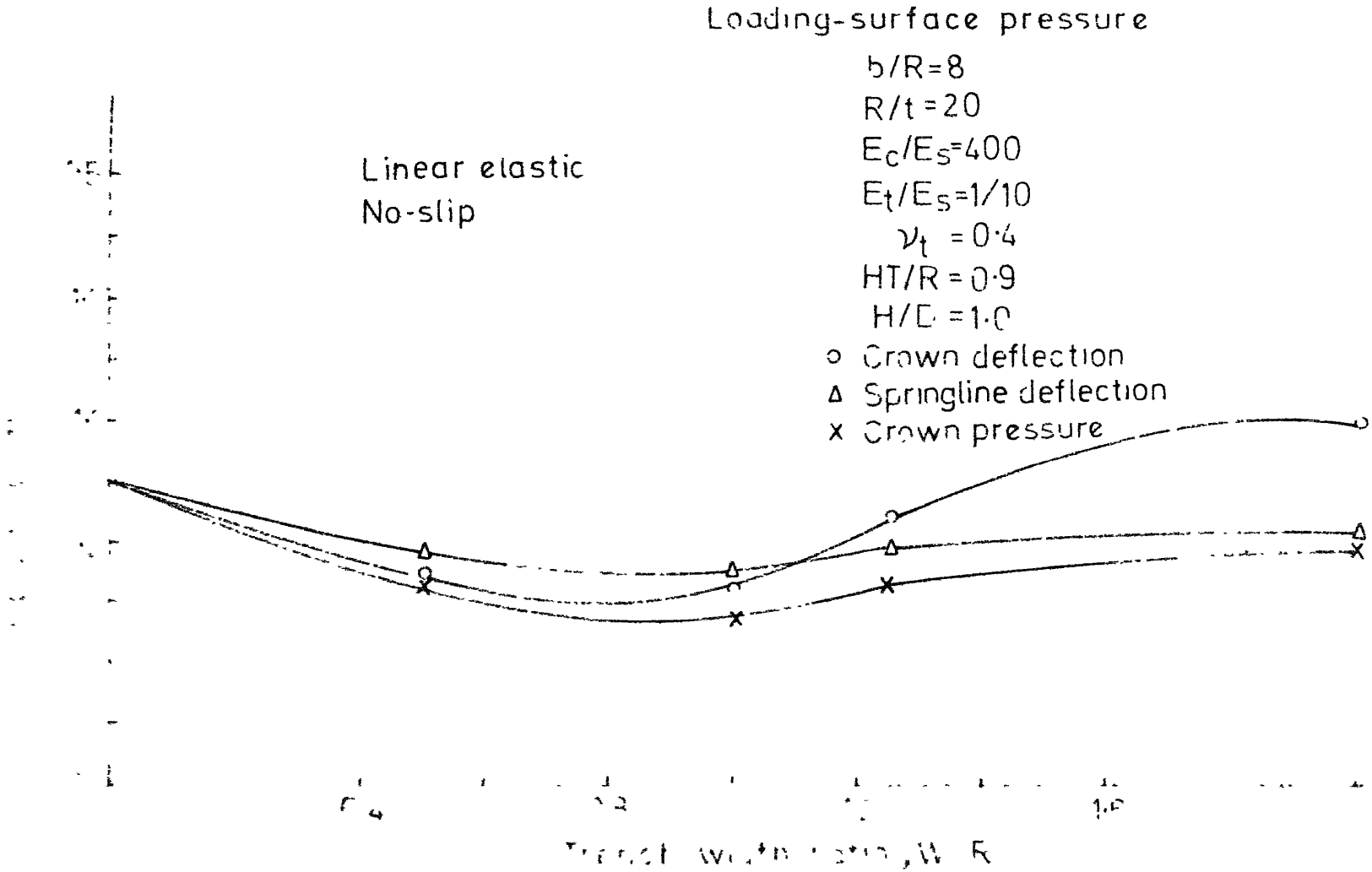

Fig.3-29 Influence of soft trench material on responses for surface loading

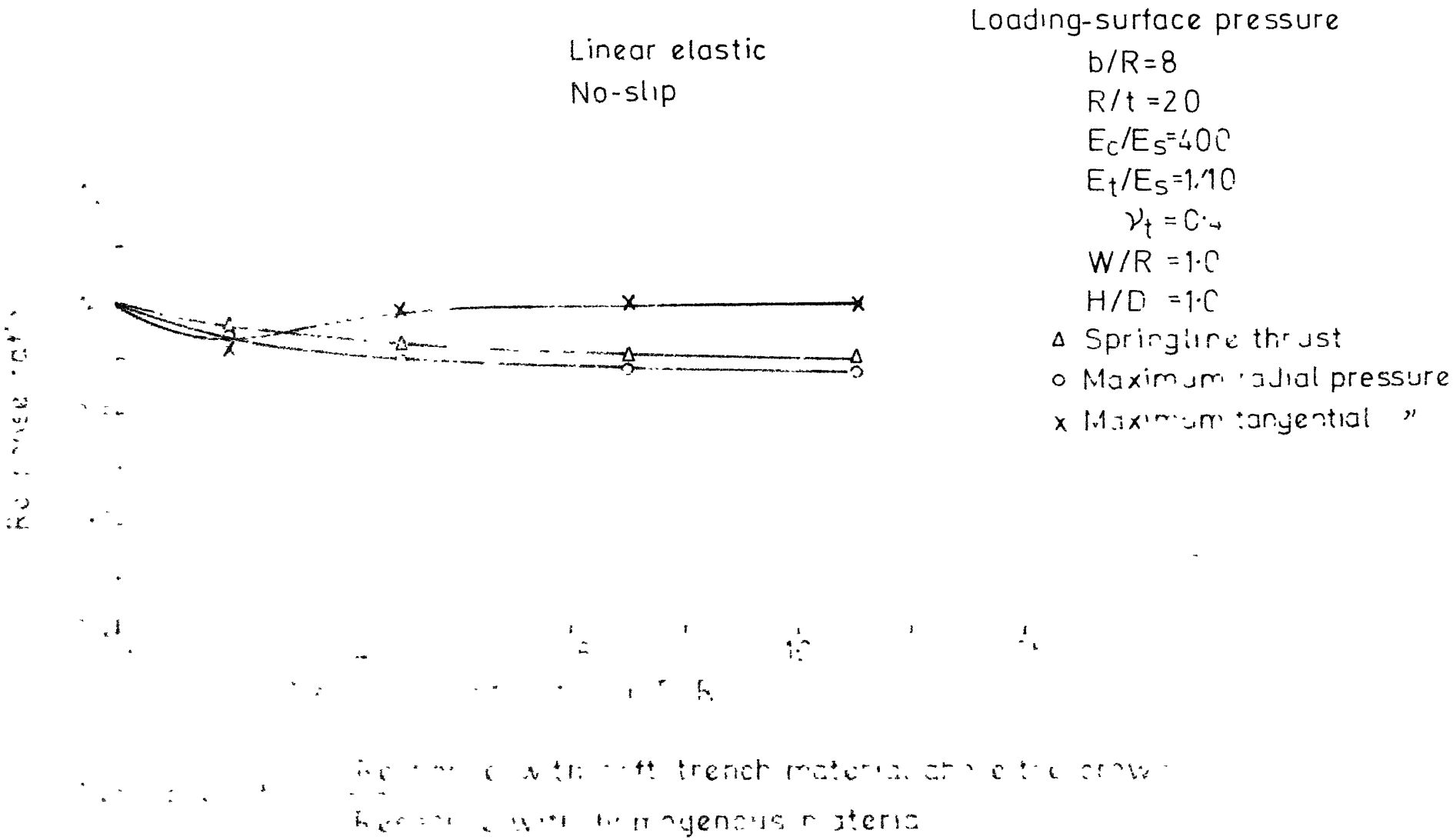

Fig. 3-30 Influence of soft trench material on responses for surface loading

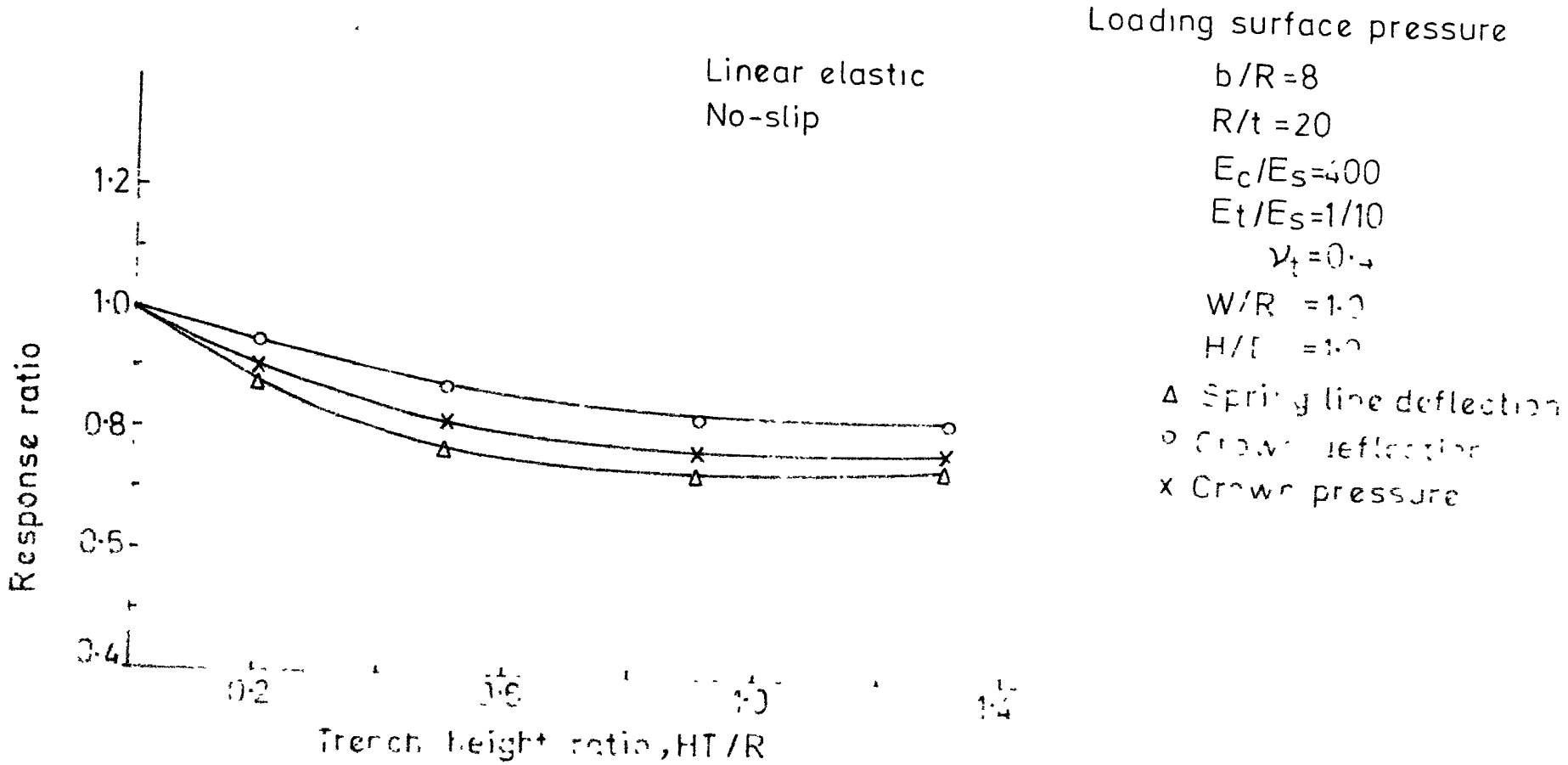

$$\text{Response ratio} = \frac{\text{Response with soft trench material above the crown}}{\text{Response with homogeneous material}}$$

Fig. 3-31 Influence of soft trench material on responses for surface loading

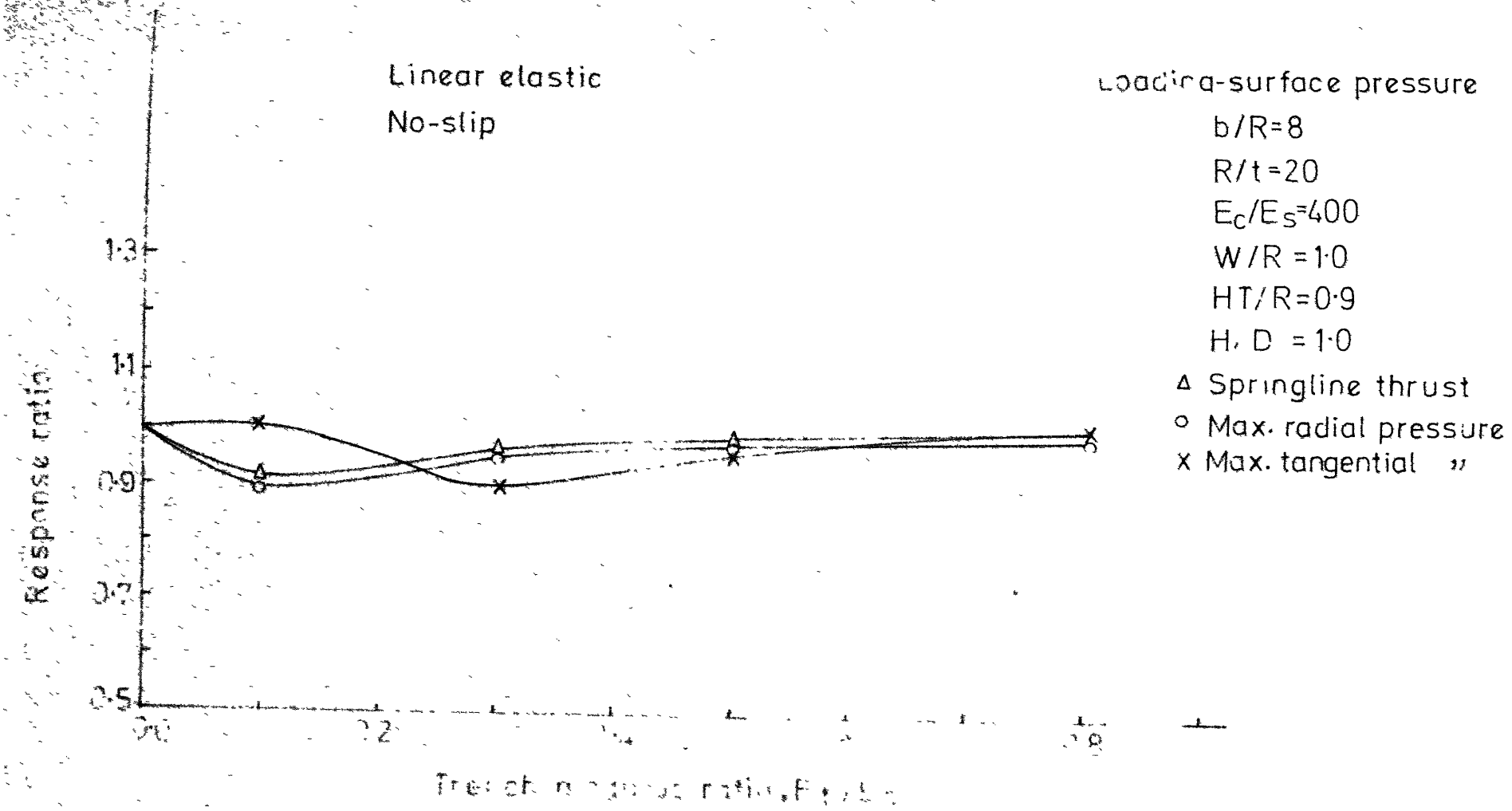

Response ratio = Response with soft trench material / Response with homogeneous material

Fig. 3-32 Influence of soft trench material on responses for surface loading

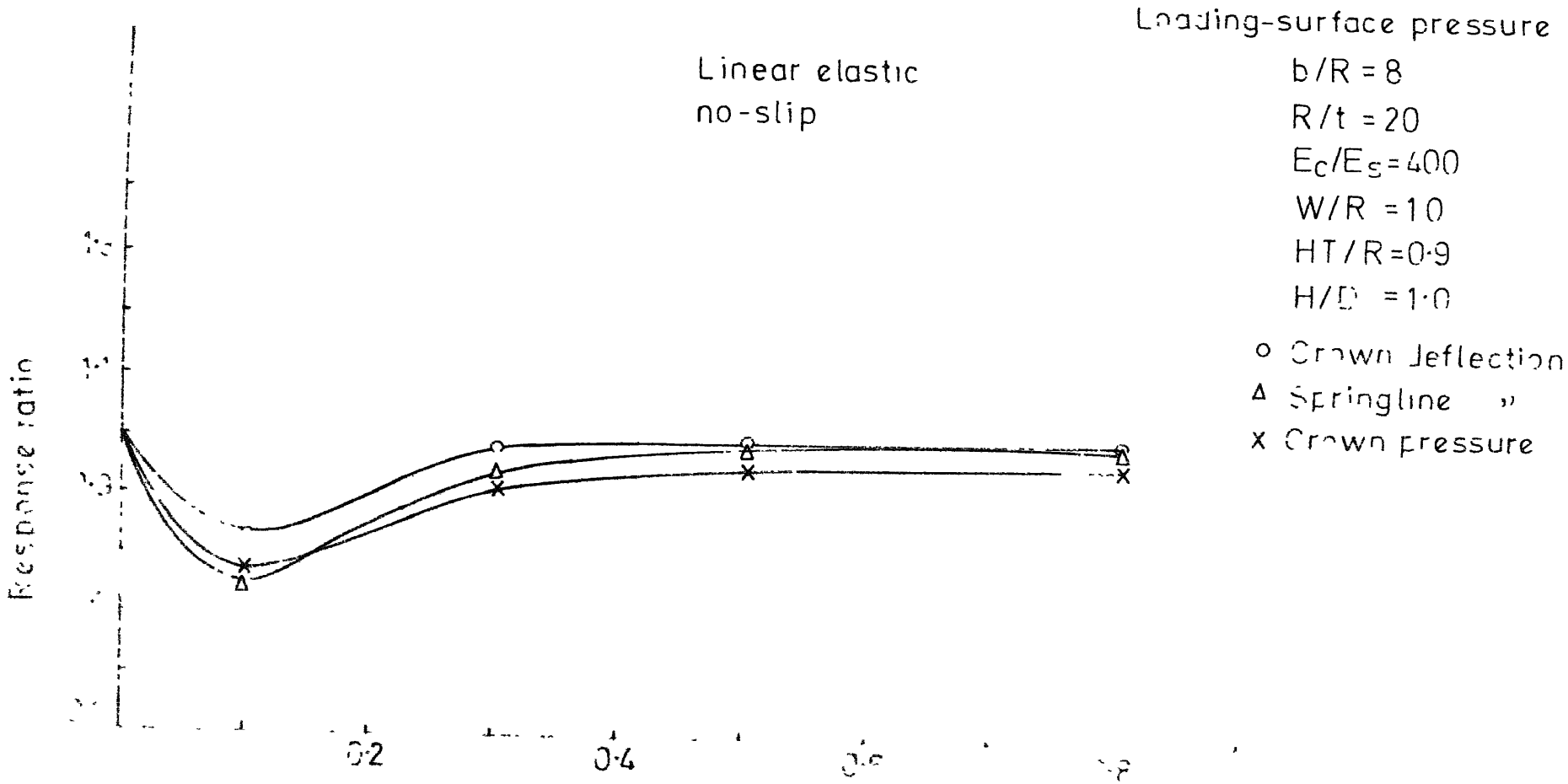

Fig. 3-33 Influence of soft trench on response for surface loading

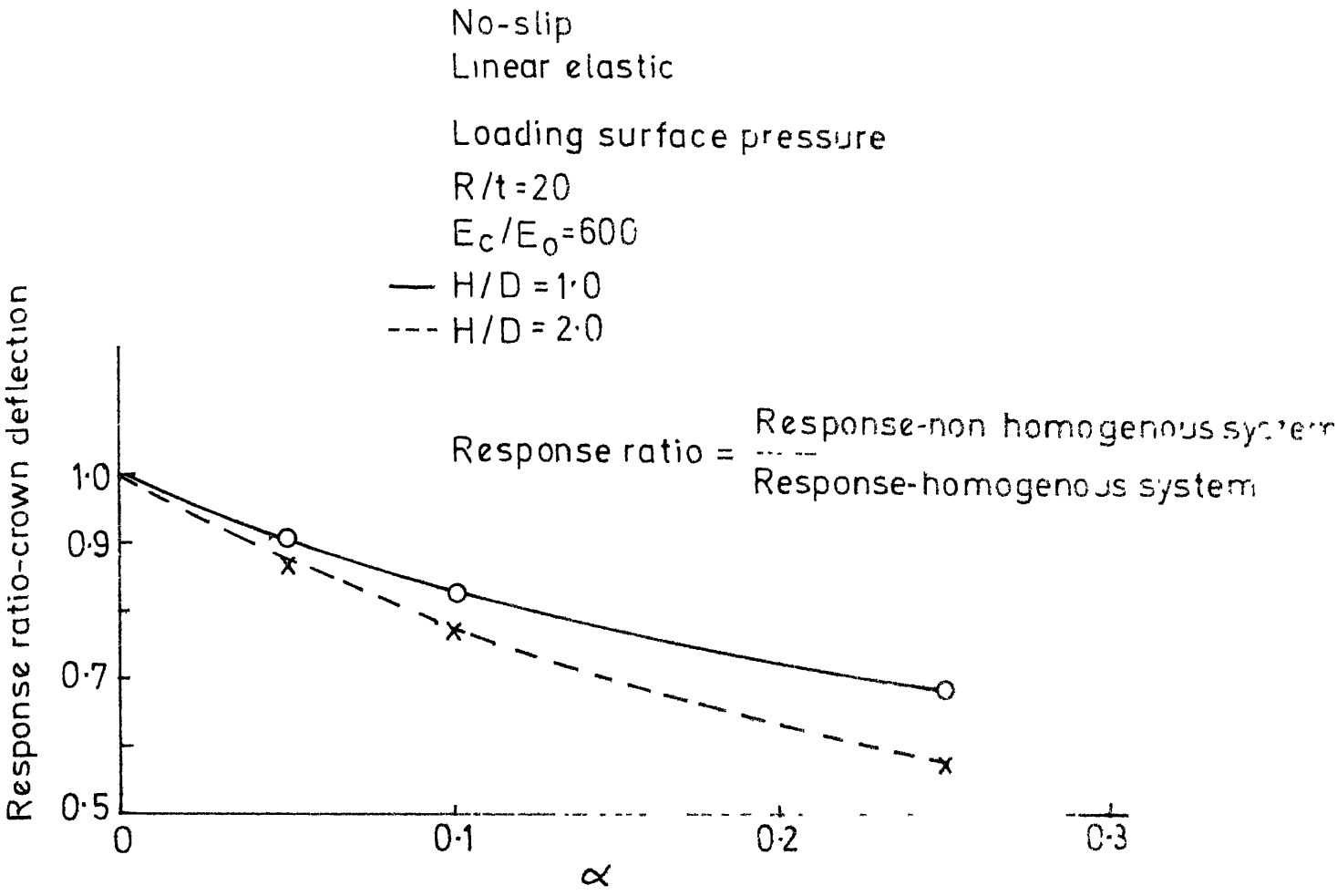

Fig.3-34 Response ratio of crown deflection versus α for surface loading

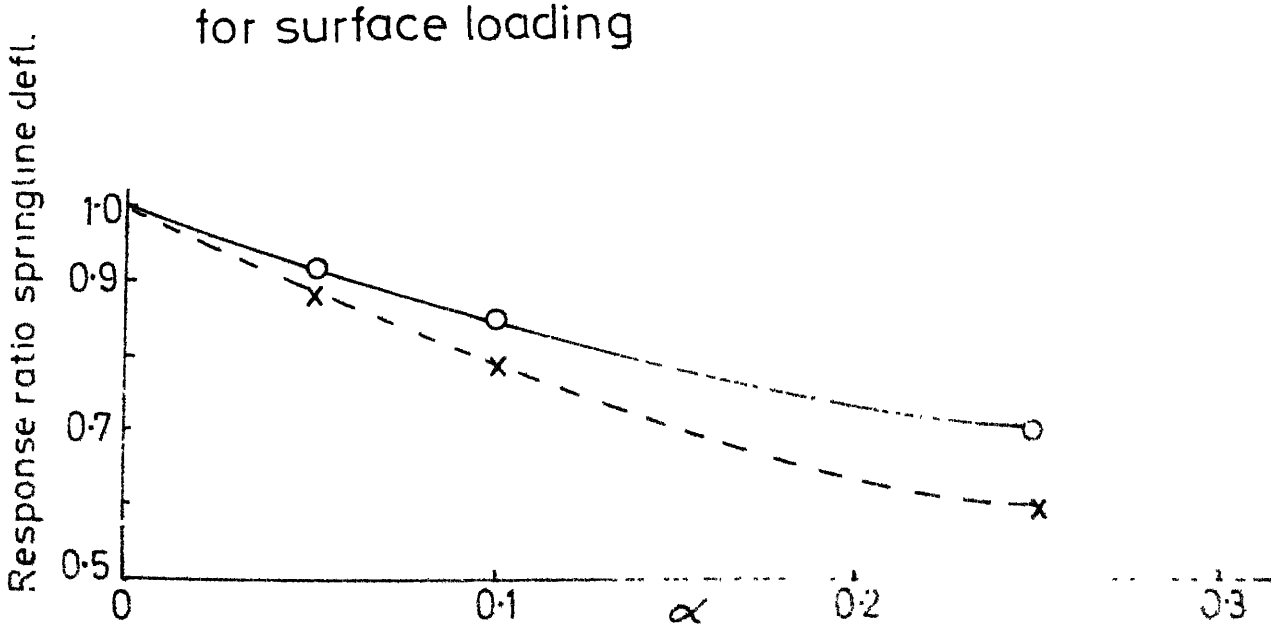

Fig 3-35 Response ratio of springline deflection versus α for surface loading

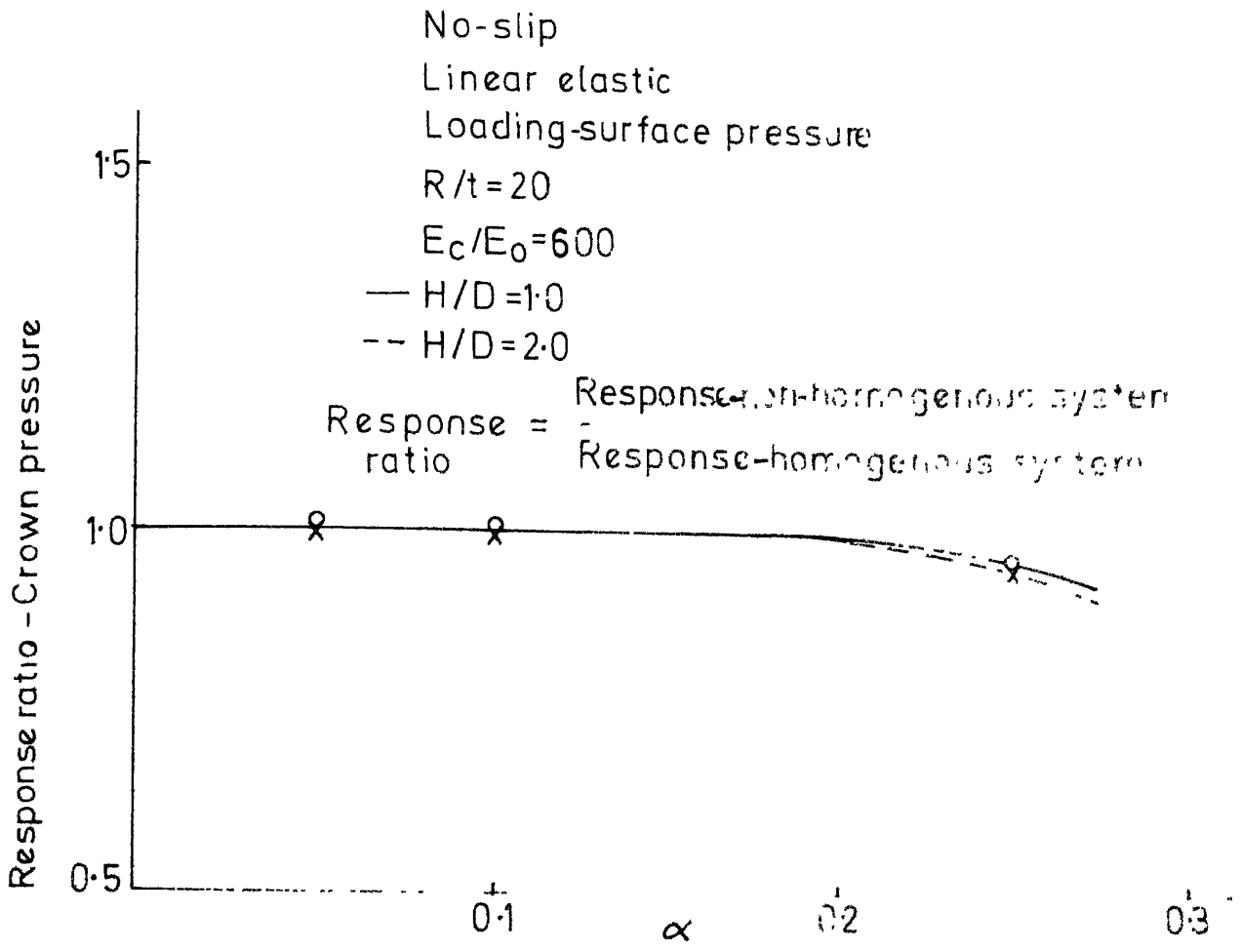

Fig. 3-36 Response ratio of crown pressure versus α for surface loading

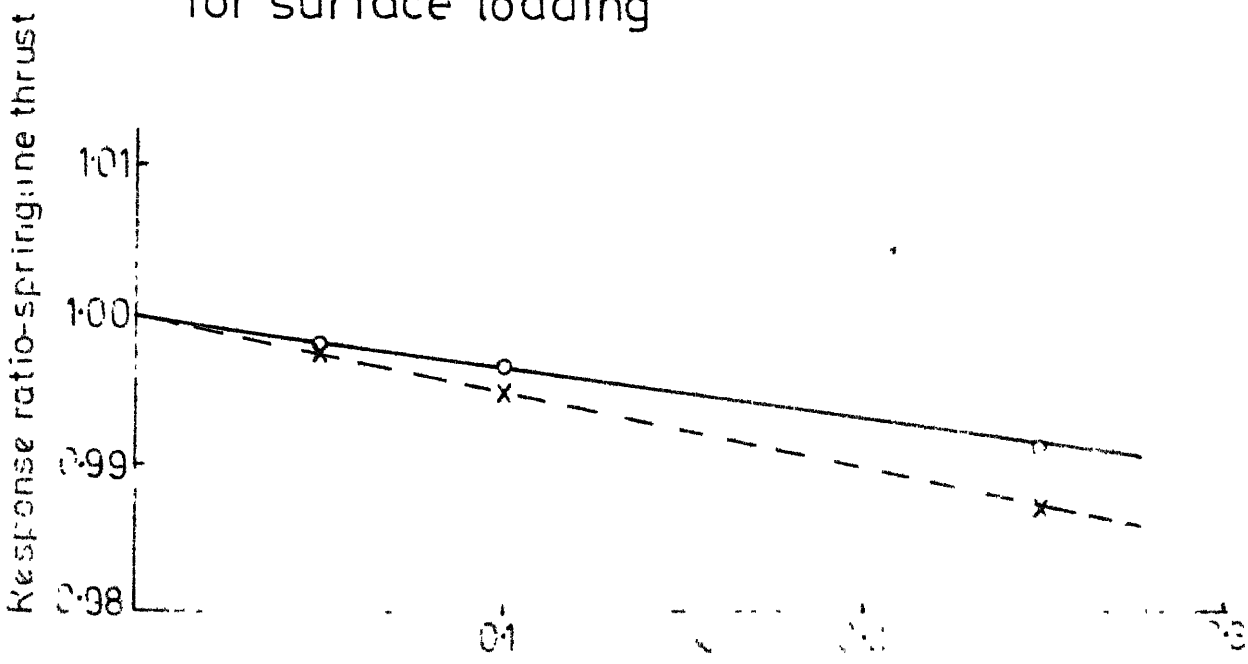

Fig. 3-37 Response ratio of springline thrust versus α for surface loading

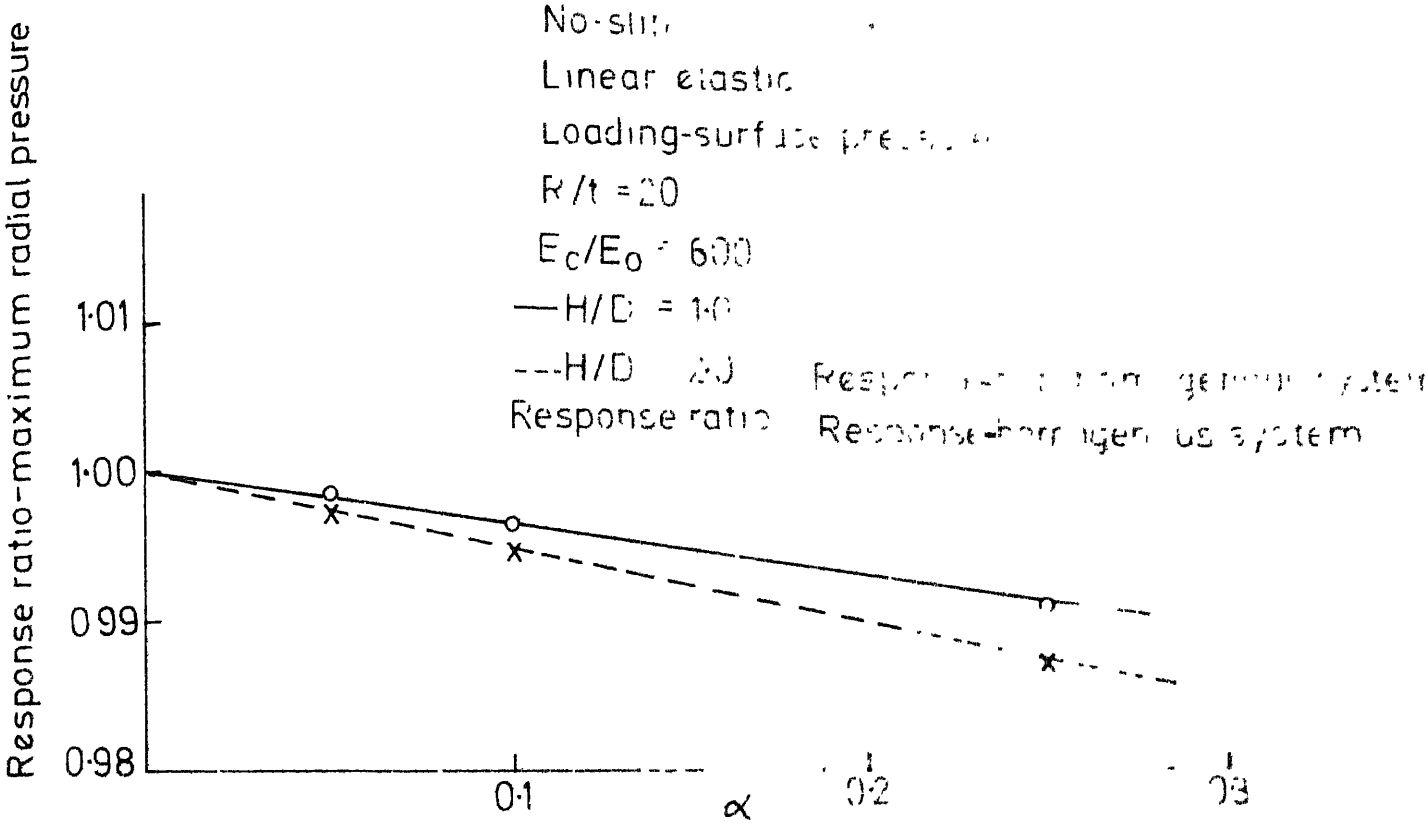

Fig. 3-38 Response ratio of maximum radial pressure versus α for surface loading

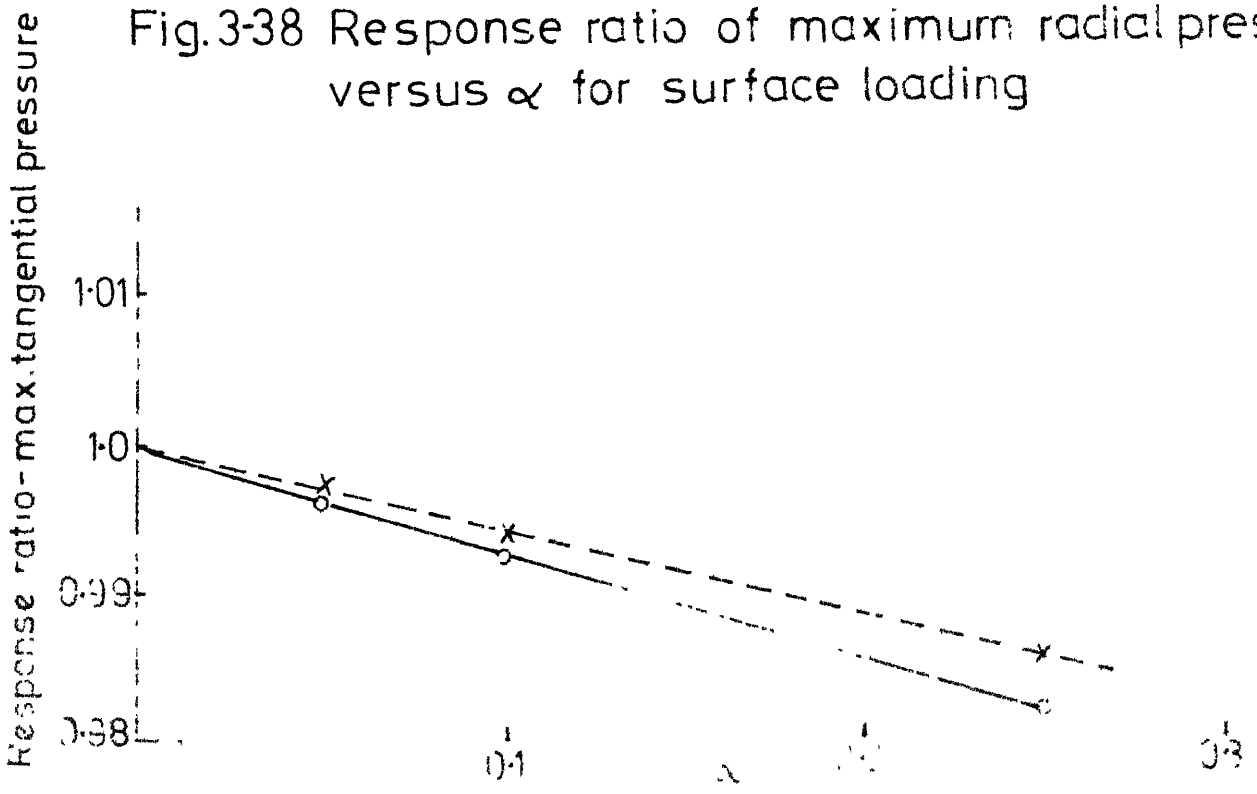

Fig 3-39 Response ratio of maximum tangential pressure versus α for surface loading

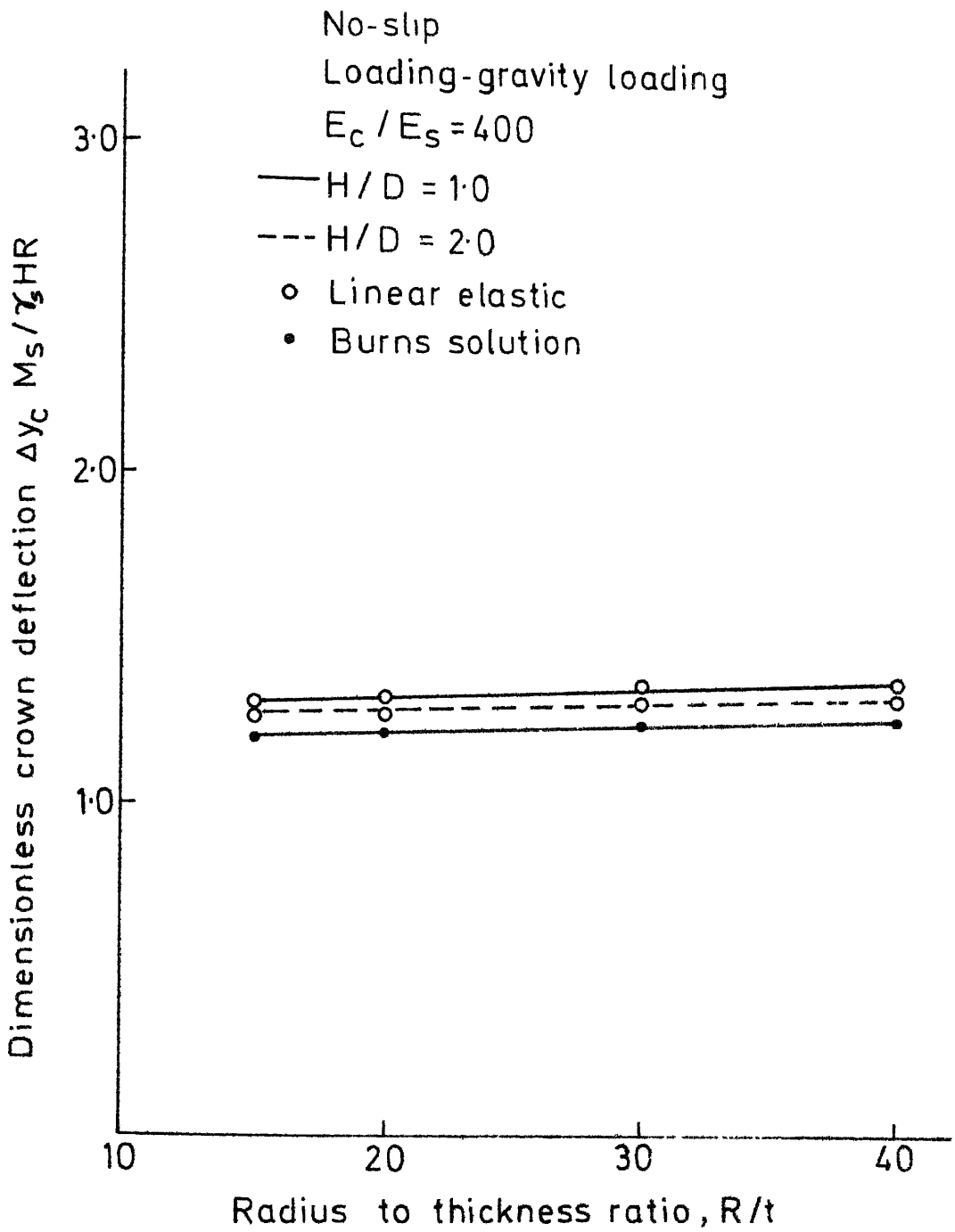

Fig. 3-40 Dimensionless crown deflection versus radius-to-thickness ratio for gravity loading

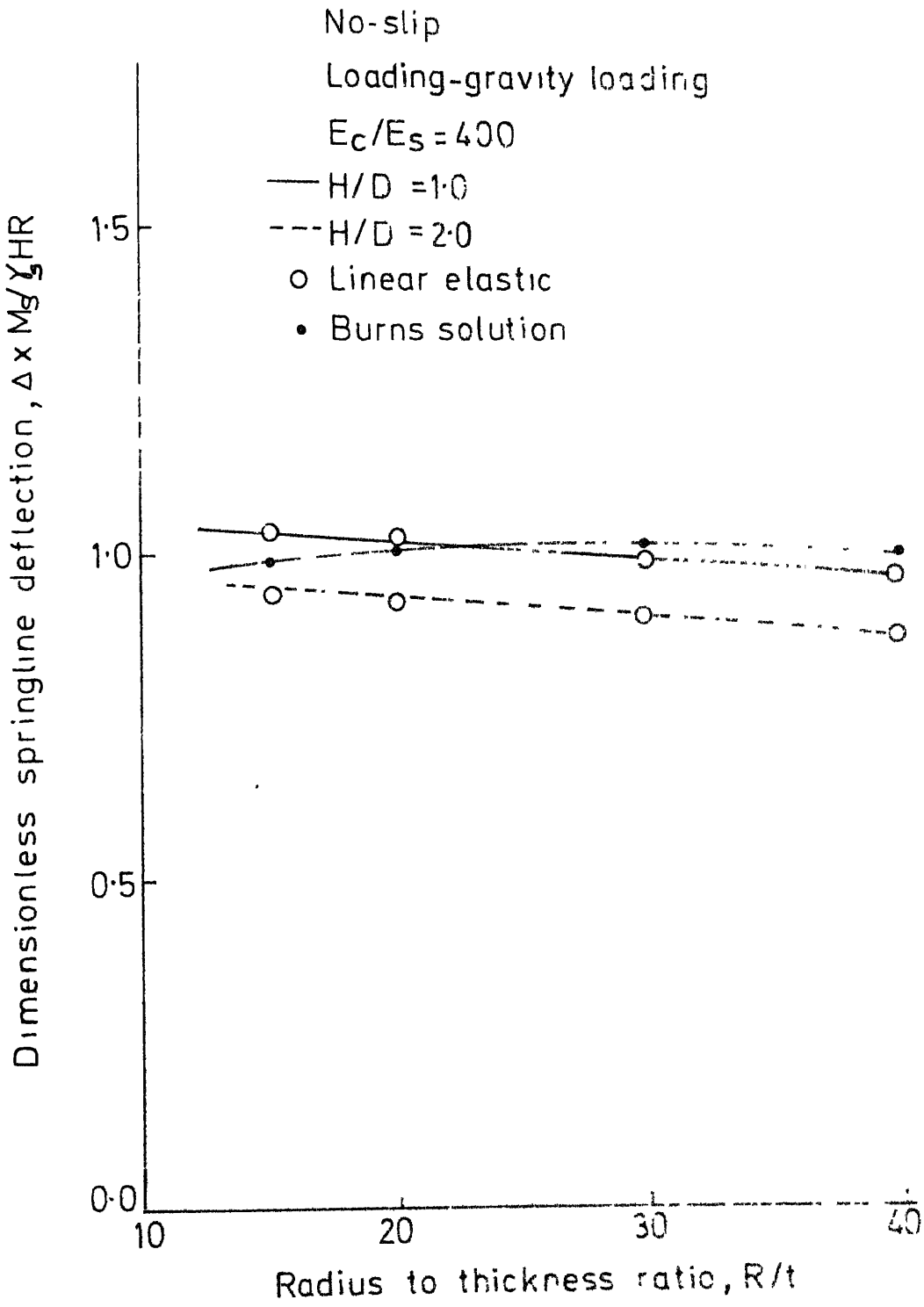

Fig. 3-41 Dimensionless springline deflection versus radius-to-thickness ratio for gravity loading

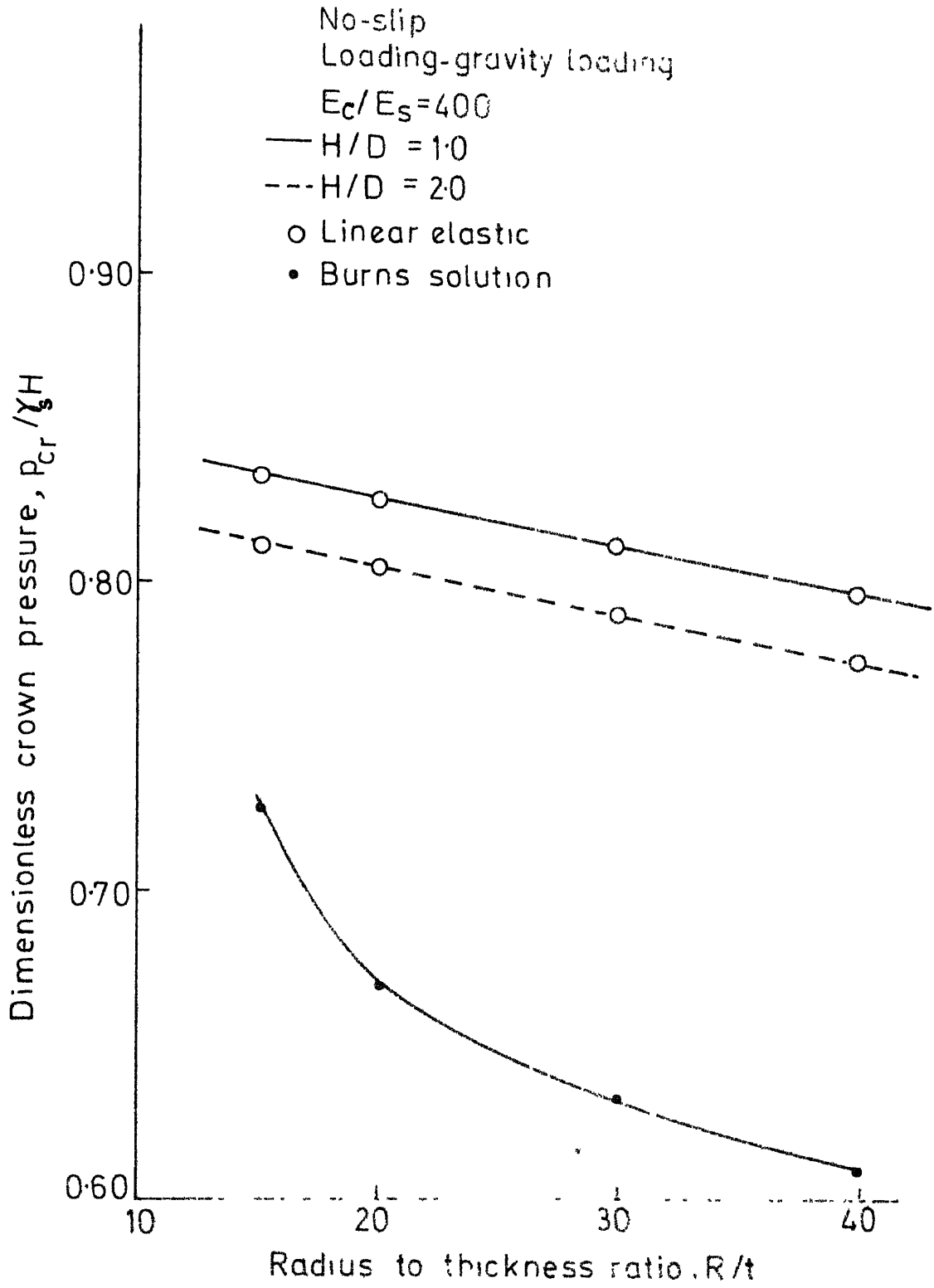

Fig. 3-42 Dimensionless crown pressure versus radius -to- thickness ratio for gravity loading

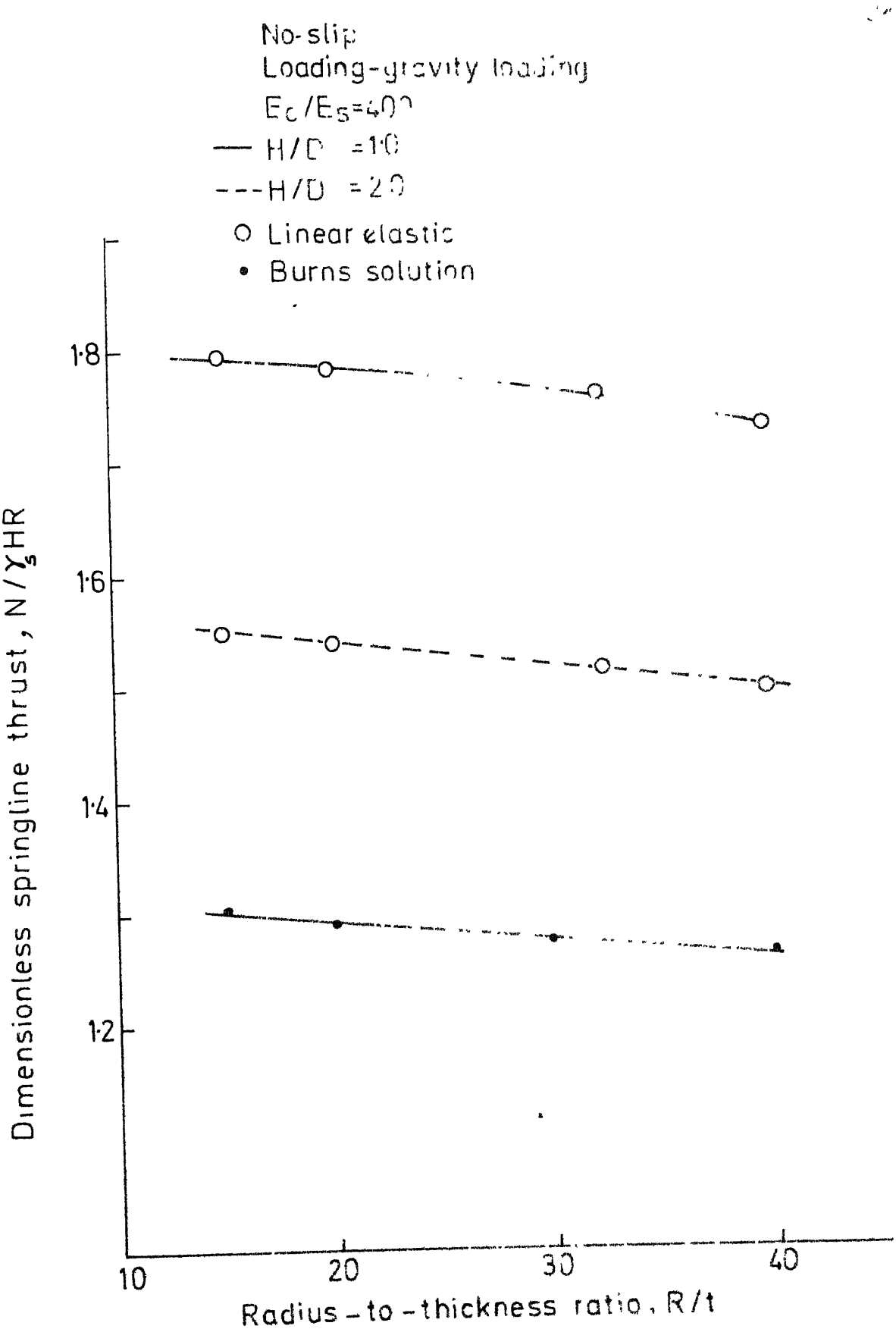

Fig.3·43 Dimensionless springline thrust versus radius-to-thickness ratio for gravity loading

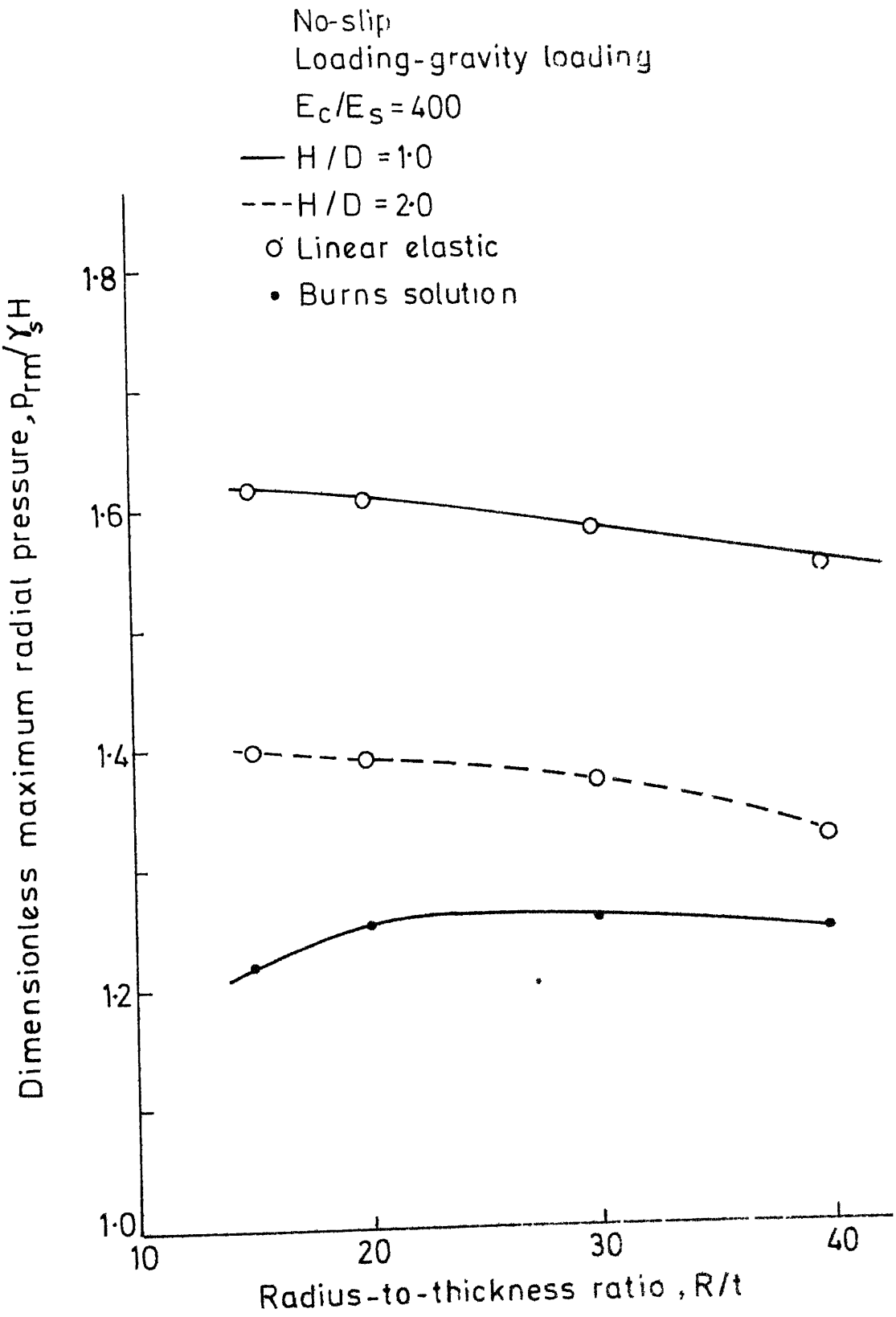

Fig.3·44 Dimensionless maximum radial pressure versus radial-to-thickness ratio for gravity loading

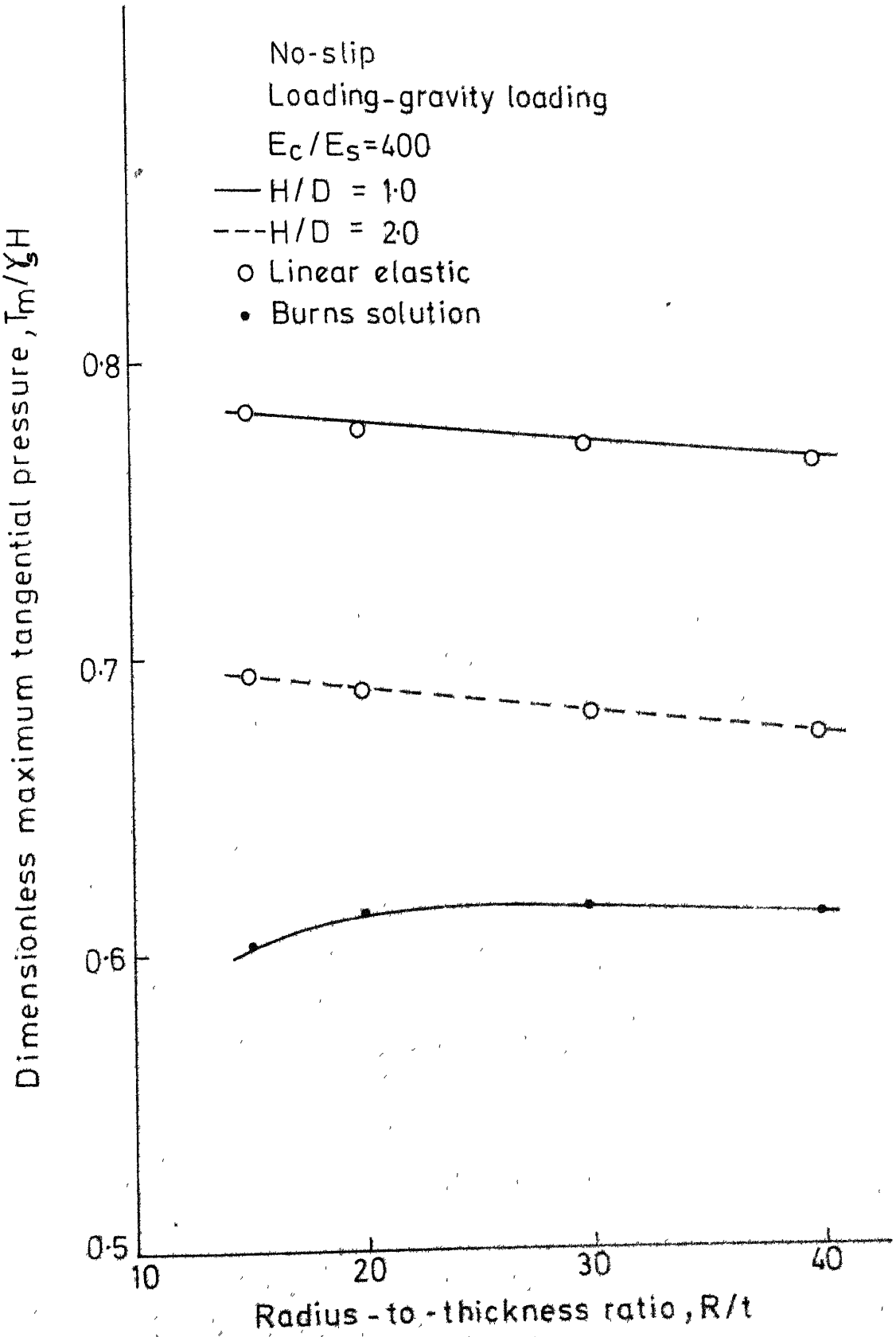

Fig. 3-45 Dimensionless maximum tangential pressure versus radius-to-thickness ratio for gravity loading

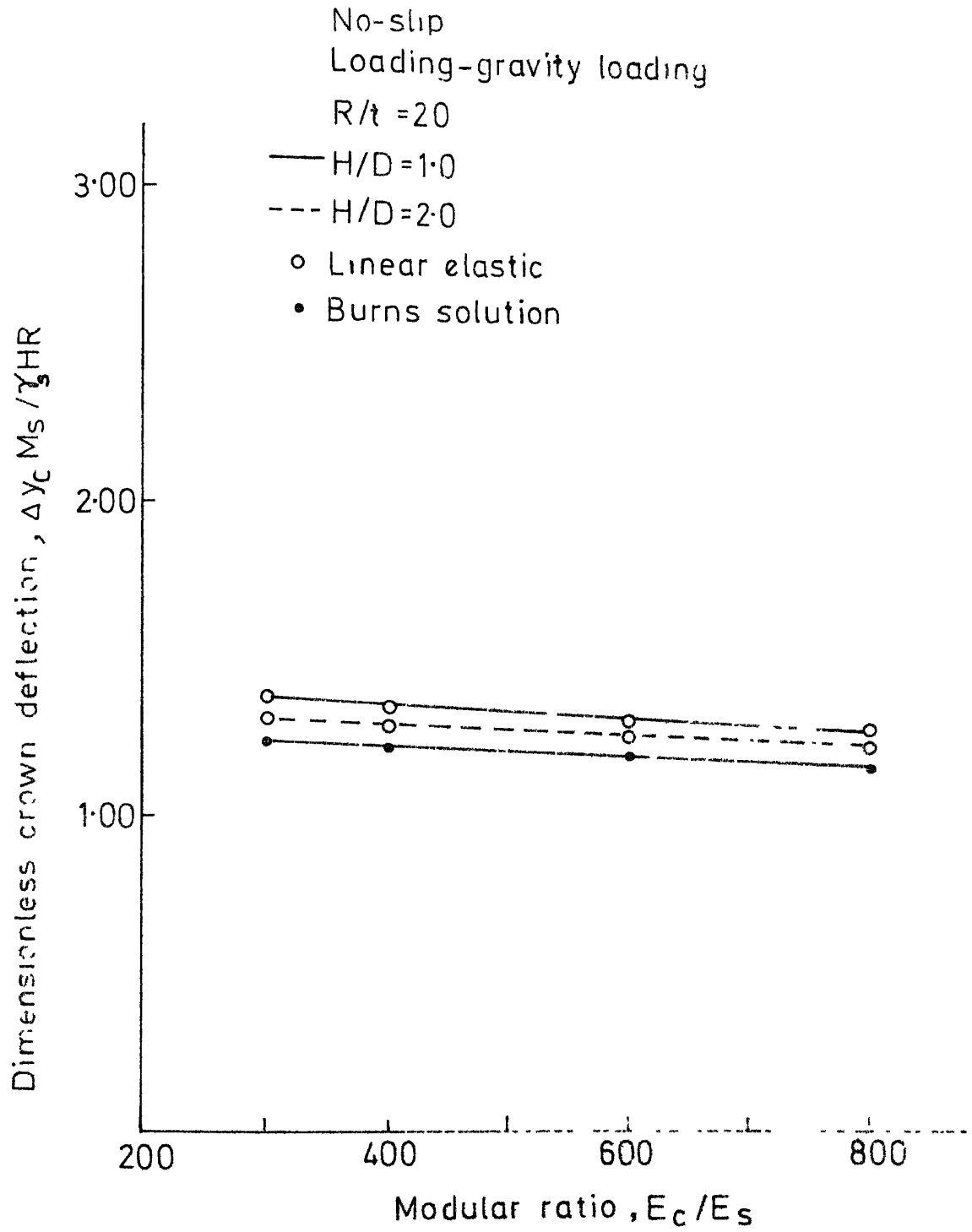

Fig. 3-46 Dimensionless crown deflection vs modular ratio for gravity loading

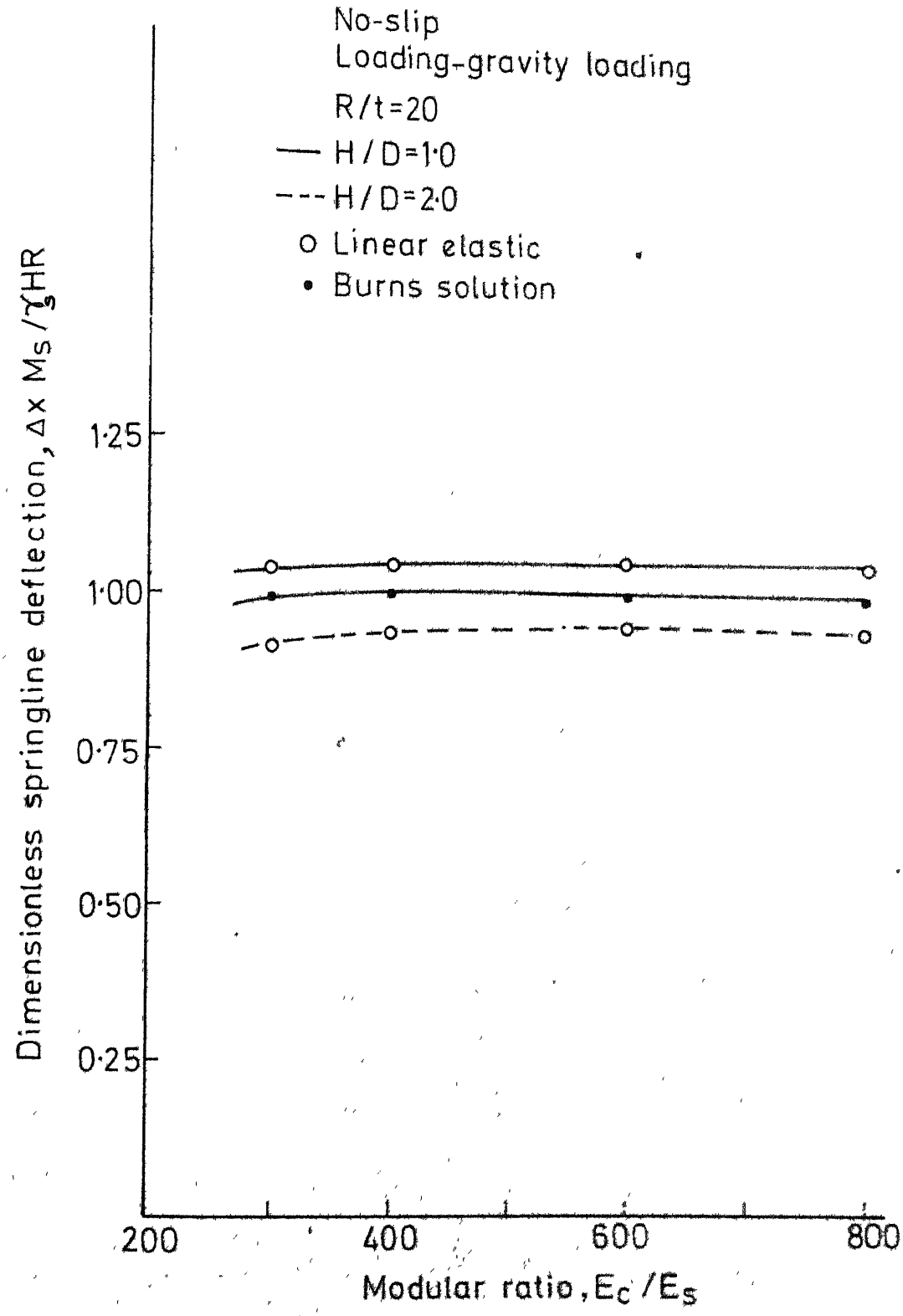

Fig. 3-47 Dimensionless springline deflection versus modular ratio for gravity loading

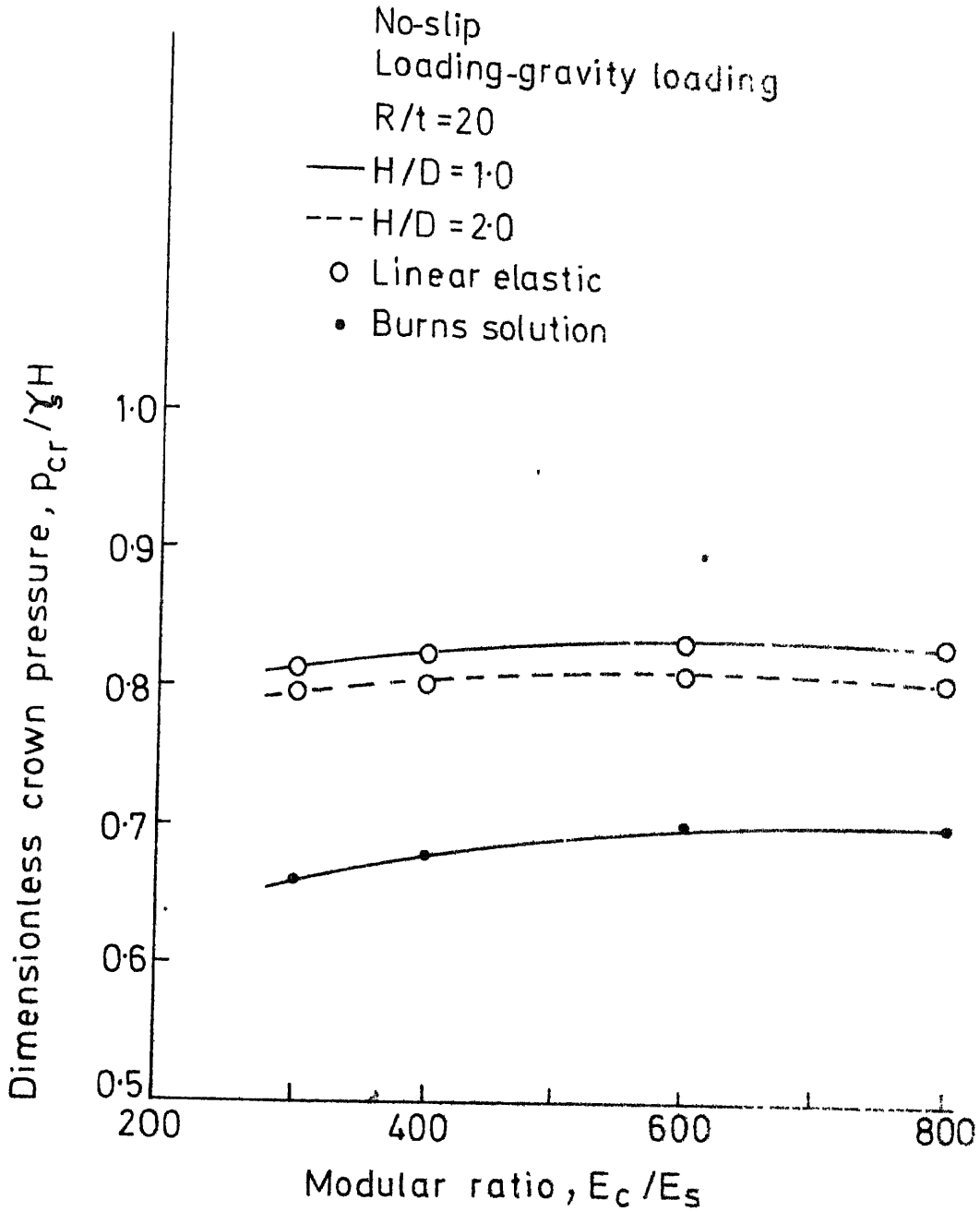

Fig. 3-48 Dimensionless crown pressure versus modular ratio for gravity loading

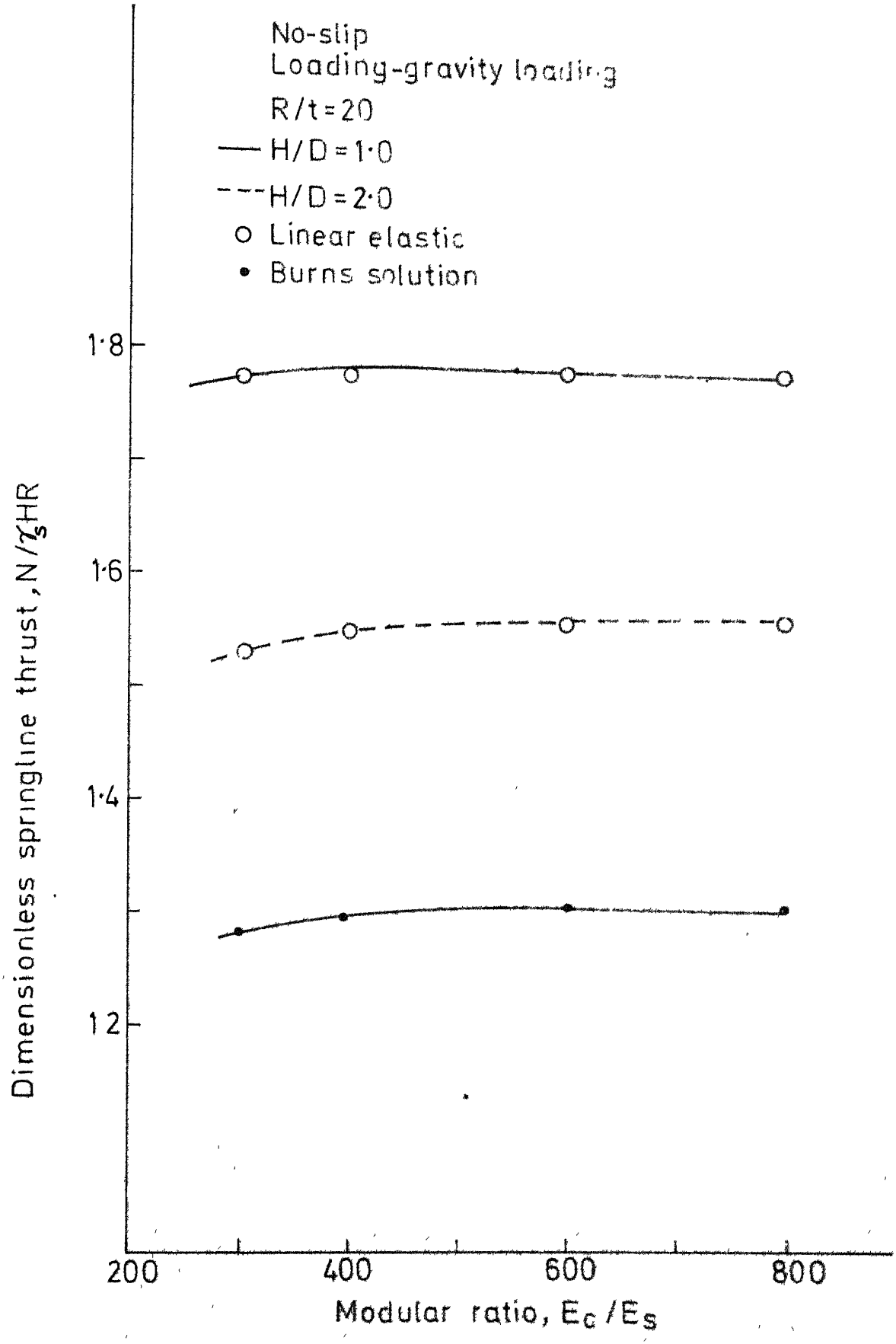

Fig 3 49 Dimensionless springline thrust versus modular ratio for gravity loading

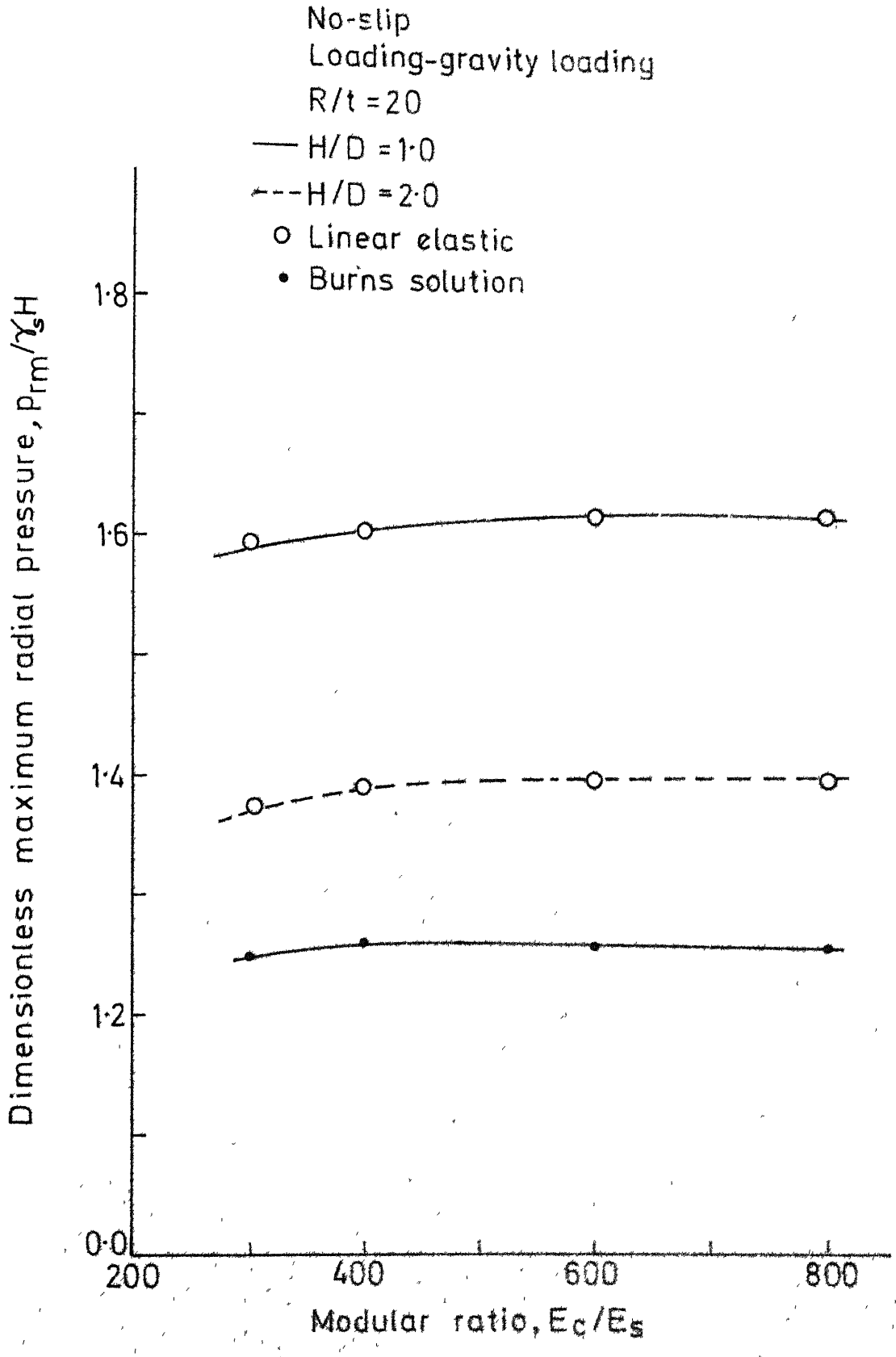

Fig. 3-50 Dimensionless maximum radial pressure versus modular ratio for gravity loading

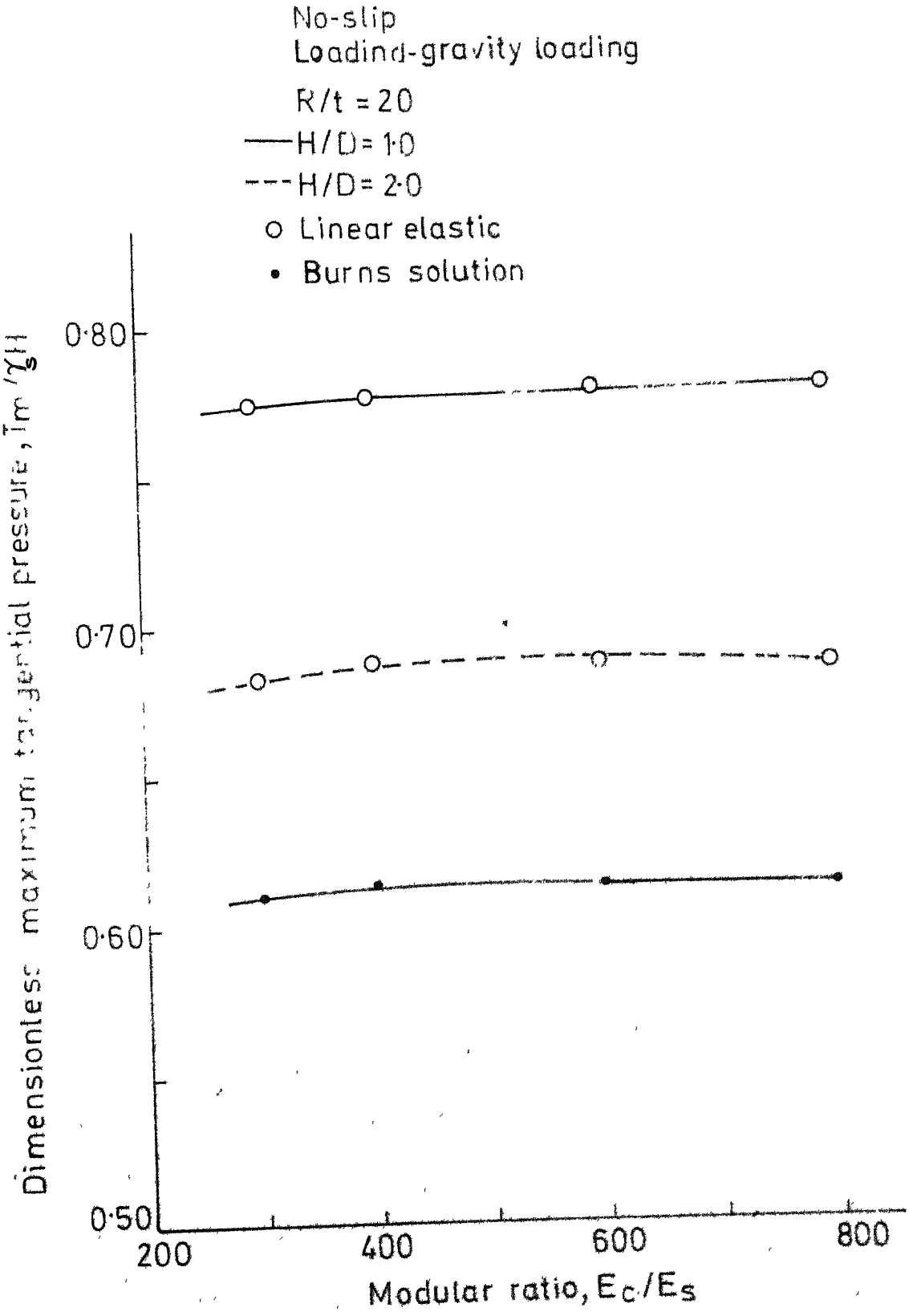

Fig. 3-51 Dimensionless maximum tangential press vs modular ratio for gravity loading

CHAPTER 4

CONCLUSIONS AND RECOMMENDATIONS

4.1 Conclusions

The pipe-soil interaction problem has been studied by using finite element method for a pipe buried in a medium. The effect of full-slip and no-slip has been studied by using interface elements. Linear analysis, and non-linear analysis with the same initial tangent modulus of linear analysis have been carried out. The non-linear interface behaviour has also been incorporated in the finite element analysis. Incremental procedure has been used to carry out the non-linear analysis of interface and material. The influences of the modular ratio of buried pipe and the surrounding medium, radius-to-thickness ratio of pipe and different surface load widths have been investigated. The pipe response for gravity loads has also been analysed. The effects of soft material above the crown and linearly varying modulus of elasticity of soil with depth for full width of surface pressure have been investigated. The following general conclusions can be drawn from these studies.

1) Slip between pipe and surrounding soil does not seem to influence the responses.

2) For full load width, Burns solution and linear elastic finite element solution are in good agreement in predicting the displacements. Crown deflections decrease with increasing modular ratio and increases with increasing radius-to-thickness ratio in all the analyses. Non-linear analysis gives higher values of displacements. Radius-to-thickness and modulus ratios are not highly sensitive in predicting displacements.

3) Crown pressure is less than the surface pressure for full load width. But the springline thrust is more than the load above the pipe, ie, pxR for full load width. R/t is more sensitive in predicting the crown pressure in Burns solution than the finite element solution within the practical range of this parameter . R/t and E_c/E_s are not highly sensitive in predicting the springline thrust.

4) The design parameters such as thickness of the pipe, springline thrust etc. are not affected in linear analysis increasing H/D ratios for full load width but the design parameters get affected in non-linear analysis.

5) Crown deflection and spring line deflection increase with increasing load with. They start decreasing beyond b/R=4. The design parameters get affected in linear analysis for increasing H/D ratio for all $b/R < 8$.

6) Crown pressure increases with increasing b/R in both linear and non-linear analyses. The crown pressure gets affected with increasing H/D ratio for all b/R < 8 . The crown pressure predicted by finite element method is smaller than the traditional Boussinesq prediction (Fig.3.23). The crown pressure predicted by finite element method tends to coincide with Boussinesq's value at higher b/R ratios.

7) Spring line thrust increases with increasing b/R. The spring line thrust gets affected with increasing H/D ratio for b/R < 8 in both the analyses. Beyond b/R=4, the dimensionless value is greater than 1 in all the analyses;i.e. the pipe starts drawing load beyond b/R=4.

8) In gravity load studies, all the responses decrease with increasing H/D ratio for all values of modular ratio and radius-to-thickness ratio in linear elastic analysis which was not seen in the case when only surface pressures are considered.

9) In gravity loads study, Burns solution gives lower pressure value than finite element solution. The crown pressure is 20 percent less than the free field stress at R/t =20.

10) R/t is a sensitive parameter but E_c/E_s is an insensitive parameter in predicting responses due to gravity loads.

11) Provision of soft material around the pipe improves the structural capacity of the pipe. The optimum width, height and modulus of trench material are R, 0.9R and 1/10 of soil modulus respectively.

12) Non-homogeneous analysis taking linearly increasing elastic modulus for the soil with depth gives lower response values than the ones predicted by homogeneous analysis. The decreases is linearly proportional to α, the slope angle . The responses decrease with increasing H/D ratio for all values of α.

4.2 Recommendations for Future Work

The present work has shown the application of finite element method to study the responses of a pipe buried in soil by considering soil behaviour as linearily elastic and non-linearly elastic. Several topics for further research in this area are suggested below.

The non-linear elastic property used in the work does not predict the failure of the soil. So, soil modelling can be improved by using better constitutive laws.

The flexural stiffness of the pipe is not considered in this work. This is one of the important design parameters particularly for flexible culverts. This can be studied by simulating pipe by beam-column elements or shell elements.

The constant-strain triangle elements have been used here. Higher order elements like LST, isoparametric elements may improve the accuracy of the responses.

While the programs developed are quite general for application to buried pipes of different shapes and sizes. Computations have only been carried out for buried circular pipes in this investigation. The studied can easily be extended to other commonly used pipe shapes.

REFERENCES

1. Abel, J.F., Mark, R., and Richards, R., 'Stresses Around Flexible Elliptic Pipes', Journal of the Soil Mechanics and Foundations Division, Proc. ASCE, Vol.99, No.SM 7, July, 1973, pp.509-526.
2. Anand, S.C., 'Stress Distribution Around Shallow Buried Rigid Pipes', Journal of the Structural Division, Proc. ASCE, Vol.100, No.ST1, Jan.,1974, pp. 161-174.
3. Brown, C.B., 'Forces on Rigid Culverts Under High Fills', Journal of the Structural Division, Proc. ASCE, Vol.93, No.ST5, Oct., 1967, pp.195-215.
4. Brown, C.B., Green, D.R., and Pawsey, 'Flexible Culverts Under High Fills', Journal of the Structural Division, Proc. ASCE, Vol.94, No.ST4, April, 1968, pp.905-917.
5. Burns, J.Q., and Richard, R.M., 'Attenuation of Stresses for Buried Cylinders', Proceedings, Symposium on Soil-Structure Interaction, University of Arizona, Tuscon, Arizona, 1964, pp. 378-392.
6. Clough, G.W., and Duncan, J.M., 'Finite Element Analysis of Retaining Wall Behaviour,' Journal of the Soil Mechanics and Foundations Division, Proc.ASCE, Vol.97, No.SM12, Dec., 1971, pp.1657-1673.

7. Dar, S.M., and Bates, R.C., 'Stress Analysis of Hollow Cylindrical Inclusions', Journal of the Geotechnical Engineering Division, Proc. ASCE, Vol.100, No.GT2, Feb., 1974, pp.123-138.

8. Desai, C.S., and Abel, J.F., 'Introduction to Finite Element Method, Affiliated East-West Press (Pvt) Ltd, New Delhi, 1972.

9. Duncan, J.M., and Chang, C.Y., 'Nonlinear Analysis of Stress and Strain in Soils', Journal of the Soil Mechanics and Foundations Division, Proc. ASCE, Vol.56, No.SM5, Sept., 1970, pp.1625-1653.

10. Duncan, J.M., 'Behaviour and Design of Long Span Metal Culverts', Journal of the Geotechnical Engineering Division, Proc. ASCE, Vol.105, No. GT3, Mar., 1979, pp.399-418.

11. Goodman, R.E., Taylor, R.L., and Brekke, T.L., 'A Model for the Mechanics of Jointed Rocks', Journal of the Soil Mechanics and Foundations Division, Proc. ASCE, Vol.94, No.SM3, May, 1968, pp.637-659.

12. Hoeg, K., 'Stresses Against Underground Structural Cylinders', Journal of the Soil Mechanics and Foundations Division, Proc. ASCE, Vol.94, No.SM4, July,1968, pp. 844-858.

13. Katona, M.G., 'CANDE- A Modern Approach for the Structural Design and Analysis of Buried Culverts', Report No.FHWA-RD-77-5, Oct., 1976.

14. Kay, J.N., and Krizek, R.J., 'Adaptation of Elastic Theory to the Design of Circular Conduits', Institution of Engineers, Australia, Civil Engineering Transactions, April, 1970, pp. 85-90.

15. Kondner, R.L., and Zelasko, J.S., 'A Hyperbolic Stress-Strain Formulation for Sands', Proceedings, 2nd Pan-American Conference on Soil Mechanics and Foundation Engineering, Brazil, Vol.1, 1963, pp. 289-324.

16. Kondner, R.L., 'Hyperbolic Stress-Train Response: Cohesive Soils', Journal of the Soil Mechanics and Foundations Division, Proc. ASCE, Vol.89, No.SM1, Jan., 1963, pp.115-143.

17. Lew, T.K., 'Soil/Structure Interaction: Horizontal Cylinders', TR-816, Civil Engineering Laboratory, Naval Construction Battallion Centre, Port Hueneme, California, Oct., 1974.

18. Luscher, U., and Hoeg, K., 'The Action of Soil Around Buried Tubes,' Proceedings, 6th International Conference on Soil Mechanics and Foundation Engineering, Montreal, Canada, Vol.2, 1965, pp. 396-400.

19. Prakash, S., Nayak, G.C., and Gupta, R., 'Analysis of Buried Pipe Under Embankment', ASCE, Numerical Methods in Geomechanics, Vol.2, 1976, pp. 886-900.

20. Spangler, M.G., Soil Engineering, International Text Book Company, Scanton, Pa., 1960, pp. 431-437.

21. Valliappan, S., Matsuzaki, K., and Rajasekar, H.L., 'Non-linear Stress Analysis of Buried Pipes', Proceedings, International Symposium on Soil-Structure Interaction, University of Roorkee, Roorkee, 1977, pp.1-8.

22. Watkins, R.K., Buried Structures, Ch.23, Foundation Engineering Handbook, Ed: Winterkorn, H.F., and Fang,H., Van Nostrand Reinhold Co., N.Y.,1975.

23. Zienkiewicz, O.C., The Finite Element Method , McGraw-Hill Publishing Company Ltd., London, England, 1977.